universität wien

DISSERTATION

Titel der Dissertation

„Radon Exposure and the Influence of Aerosol Dust Concentration and Ventilation Conditions“

verfasst von

Mag. rer. nat. Claudia Landstetter

angestrebter akademischer Grad

Doktorin der Naturwissenschaften (Dr. rer. nat.)

Wien, 2013

Studienkennzahl lt. Studienblatt:	A 091 419
Dissertationsgebiet lt. Studienblatt:	Dr.-Studium der Naturwissenschaften Chemie
Betreuerin / Betreuer:	Ao. Univ.-Prof. Mag. Dr. Gabriele Wallner

Contents

Abstract ... 3

1. Introduction ... 5

1.1. Objective ... 5
1.2. Radon and its progeny ... 6
1.3. Unattached and attached radionuclides ... 7
1.4. Radiotoxicity ... 7

2. Measuring methods ... 8

2.1. Attached radon daughters ... 8
2.2. Unattached radon daughters ... 10
2.3. Long-lived radon daughters ... 10

3. Results and discussion ... 11

3.1. Measurements in the radon gallery Bad Gastein ... 12
3.1.1. Short-lived radon daughters, July 2003 ... 12
3.1.1.1. Attached short-lived radon daughters, July 2003 ... 13
3.1.2. Short-lived radon daughters, January 2004 ... 16
3.1.2.1. Attached short-lived radon daughters, January 2004 ... 16
3.1.2.3. Unattached Short-Lived Radon Daughters January 2004 ... 21
3.1.3. Long-lived radon daughters ... 27
3.1.3.1. Long-lived radon daughters, July 2003 ... 28
3.1.3.2. Long-lived radon daughters, January 2004 ... 29
3.1.3.3. Long-lived radon daughters, October 2004 ... 30
3.2. Measurements in the therapy centre building ... 35
3.2.1. Short-lived radon daughters in the foyer ... 36
3.2.1.1. Attached short-lived radon daughters in the foyer ... 36
3.2.2. Short-lived radon daughters in the gym ... 39
3.2.2.1. Attached short-lived radon daughters in the gym ... 39
3.2.2.2. Unattached short-lived radon daughters in the gym ... 41
3.2.3. Short-lived radon daughters in the doctor's office 5 ... 46
3.2.3.1. Attached short-lived radon daughters in the doctor's office 5 ... 46
3.2.3.2. Unattached short-lived radon daughters in the doctor's office 5 ... 48
3.3. Influence of the aerosol particle concentration ... 55
3.4. Calculation of the effective dose ... 62
3.4.1. Radon gallery Bad Gastein ... 66
3.4.2. Therapy centre building ... 70
3.4.2.1. Foyer Bad Gastein, October 2004 ... 70
3.4.2.2. Gym Bad Gastein, October 2004 ... 70
3.4.2.3. Doctor's office 5 Bad Gastein, October 2004 ... 73
3.4.3. Dose contribution of the long-lived radionuclides ... 75

4. Conclusion ... 76

5. Appendix 1 ... 79

5.1. References ... 79
5.2. List of figures ... 83
5.3. List of tables ... 86
5.4. Data tables ... 90

6. Appendix 2 ... 97

Zusammenfassung ... 108

Acknowledgements

I would like to express my thankfulness to:

Karl Irlweck and Gabriele Wallner, for their supervision, great support and useful critiques of this research work.

Axel Berner for providing and operating the cascade impactors and the technical support.

Austrian Social Insurance for Occupational Risks (AUVA) for providing the LCD-BWLM-PLUS (LCD-Battery operating Working-Level-Monitor) and making measurements possible.

Tracer Lab for providing the BWLM-PLUS Free fraction measurement system and for the technical support.

The staff of the Gasteiner Heilstollen for their help during the on site measurements.

Austrian Central Institute for Meteorology and Geodynamics (ZAMG) for providing the data of the atmospheric pressure.

Shahram Ayromlou for his useful recommendations.

My fellow students for valuable discussion.

My colleagues at work for their constructive recommendations and patients during my absence.

My parents and my sisters for their encouragement, constructive questions, for backing me up which helped to stay the course and for their financial support.

All of my friends for their encouragement and constructive questions.

Abstract

In the frame of this thesis, measurements of the radon daughter activity concentrations in the radon gallery and its adjacent therapy centre in Böckstein near Bad Gastein, Austria were performed. The three measuring sites in the therapy centre (foyer, gym and doctor's office 5) as well as the measuring site in the radon gallery were proposed by the Austrian Social Insurance for Occupational Risks (AUVA) control surveys. For these measurements, three Instruments were purchased and provided by the AUVA.

The attached and the unattached short-lived radon daughters were measured and the potential alpha energy concentration was calculated. Consequently, the attached and the unattached fraction were calculated from these results. In addition, aerosols were collected on aluminium foils with a cascade impactor. ^{210}Pb, ^{210}Bi and ^{210}Po were leached from this aluminium foils and measured by liquid scintillation counting. The aerosol particle concentration was calculated.

The equilibrium equivalent radon activity concentration and the potential alpha energy concentration can be reduced through sufficient ventilation. This can be observed in the radon gallery during daytime, when the ventilation is turned on, or in the gym, where the equilibrium equivalent radon concentration increases during the night. However, in the gallery, atmospheric pressure has a higher influence to the equilibrium equivalent radon concentration as well as the PAEC than the ventilation. Additionally, in October, an increase of the equilibrium equivalent radon concentration with decreasing atmospheric pressure could be seen during the measurements in the foyer, the gym, and doctor's office 5.

This thesis shows the strong influence of the aerosol particle concentration on both the unattached fraction as well as the equilibrium factor and calculates the attachment rate.

Due to the higher dose conversion factors of the short-lived unattached radionuclides, high unattached fractions play an important role in the calculation of the effective dose. Different methods exist for the calculation of the effective dose, some of which simply ignore the different values of dose conversion factors for the attached and unattached radionuclides. In this thesis, different types of model

calculations for the effective dose are compared and the contributions of the effective dose resulting from the unattached fraction to the total dose are calculated.
The effective dose from the long-lived radionuclides is negligible. The activity size distributions of the long-lived radon daughters are analysed. The activity median aerodynamic diameter (AMAD) of ^{210}Po is shifted to smaller particle sizes compared to the AMAD of ^{210}Pb and ^{210}Bi. This effect was observed before by Wallner et al. during previous measurements and published in 2002.

1. Introduction

1.1. Objective

Measurements were performed on behalf of the Austrian Social Insurance for Occupational Risks (AUVA) in order to assess the effective dose on workers and employees caused by radon progenies in the radon gallery and its adjacent therapy centre in Böckstein near Bad Gastein, Austria. The dose conversion factor which is nowadays recommended by the ICRP 65 and adopted by the European commission in the Council Directive 96/29/Euratom of 13 May 1996 as well as the Austrian Standards ÖNORM S5223-2 (“Abschätzung der effektiven Dosis bei Arbeiten mit natürlichen radioaktiven Stoffen”), is derived from epidemiological studies. As these studies were mainly conducted with underground miners, using this DCF to calculate the dose indoors, can lead to uncertainties. In some studies workers inhaled other cancer causing substances such as arsenic. Additionally inhaled radioactive dust and gamma radiation can cause lung cancer. These circumstances can not be found in houses. The uncertainties of these studies are pointed out extensively in a paper by Puskin and James [1].

Another way to calculate the effective dose is to use DCFs derived from model calculations that are either based on the human respiratory tract model (HRTM) of the ICRP 66 [2] or on airway generation dosimetry models [3]. In its recent ICRP Publication the Commission recommends using the ICRP biokinetic and dosimetric models, including the HRTM and the ICRP systemic models [4]. However, the recommendation by the ICRP of the dose conversion factors to be used is still pending.

For this thesis, the effective dose was calculated by using the DCFs of the ICRP 65 and the DCFs derived from model calculations. One parameter, which has an important influence on the DCF, is the unattached fraction. In order to get an overview of the amount of the unattached and the attached radionuclides they were measured separately. The parameters that influence the unattached fraction, like the aerosol particle concentration in the air and the attachment rate, were either determined or calculated. Additionally the long-lived radon daughter products ^{210}Pb, ^{210}Bi, ^{210}Po were measured and the effective dose was calculated. The activity size distribution of the long-lived radon daughters was analysed.

1.2. Radon and its progeny

Radon and its progeny provide the dominating radiation risk for the population of Austria. The average effective dose for the population of Austria is 4.3 mSv/a [5]. About 1.6 mSv/a are caused by inhalation of Radon and its progeny. The radon concentration shows high variations in different regions of Austria. In some regions, the effective dose caused by radon can therefore exceed the average value by a multiple. About 1.3 mSv/a are caused by medical treatment. This is the mean value for the whole Austrian population. Again, variations exist due to different treatments and frequencies of the treatment. About 1 mSv/a are caused by the external exposition to natural radionuclides.

Radon is generated from the three natural decay series of ^{238}U, ^{235}U and ^{232}Th. It emanates from building materials, basement and rocks. Because of the half-life of ^{222}Rn and ^{220}Rn with 3.8 days and 55 s, respectively, and the ratio of $^{235}U/^{238}U$ in natural uranium of 0.00725, they are more important than ^{219}Rn with its short half-life of 3.9 s. So ^{219}Rn is hence negligible in radiation protection considerations.

If the mass percentage of uranium and thorium in rock is about the same, then ^{222}Rn plays the major role in generating radiation dose. The exposure to ^{220}Rn is only higher in mines with a higher thorium concentration. Moreover, the exposure to ^{220}Rn is also elevated in regions with high concentrations of monazite. Monazite is contained in both igneous rock and metamorphic rock. In Kerala (India), the population is exposed to ^{220}Rn due to the monazite sands of Karunagappally's coastal strip..

When ^{226}Ra decays, the daughter product, ^{222}Rn, receives recoil from the alpha particle ejected. This allows the radon isotopes to escape the solid matter and reach the free space in between, which is filled with air or water. If the atom can release the recoil energy before it is caught in another solid grain, it can diffuse to the soil or rock surface and mix with the air. This is even more likely if the free space is filled with water because the collision rate with the water molecules is higher. For that reason, wet soil emanates more radon than dry soil. The probability of the radon atom to be stopped in a free space decreases rapidly especially in soils with moisture contents lower than 5 % (per weight). Hongbing et al. calculated the radon emanation at different moisture contents of porous media and concluded that the radon emanation increases steadily with increasing moisture content. However, when the moisture content reaches 30 % to 40 %, the radon emanation reaches it's maximum because then diffusion of radon takes place mostly in water instead of air and due to lower diffusion velocity part of the radon decays before reaching the atmosphere [6]. Radon is transported to the surface of the soil or building material by diffusion and convection and is finally exhaled into the atmosphere.

1.3. Unattached and attached radionuclides

After radon decay, a fraction of 88 % of the formed ^{218}Po is positively charged [7]. The ^{218}Po reacts with trace gases and vapours within one second. These particles have a diameter of 0.5 nm to 5 nm and are called cluster or unattached radionuclides. Furthermore, the neutralisation of the ^{218}Po ions occurs through recombination with negative air ions as well as charge transfer processes in connection with NO, NO_2, H_2O vapours and other air impurities.

The cluster then gets attached to aerosols and forms the attached radionuclides. They can be discriminated into the fine particle fraction with particles smaller than 1 µm, and the coarse particle fraction with particles bigger than 1 µm. The fine particle fraction consists of the nucleation mode with particles smaller than 0.1 µm and the accumulation mode with particles between 0.1 µm and 1 µm.

Those unattached and attached particles in the air can either be washed out by precipitation (rain or snow), or removed from the air by plate-out on surfaces. The plate-out on walls and furniture in buildings is an important factor for the radon daughter concentration in indoor air.

1.4. Radiotoxicity

In Europe [8], North America [9] and Asia [10],numerous studies linking indoor radon with lung cancer have been conducted in recent years. They have provided evidence that a substantial number of lung cancers in the general population is caused by radon. According to the WHO, between 3 % and 14 % of all lung cancers are linked to radon, depending on the average radon concentration in a country as well as on the calculation method. Radon is the primary cause of lung cancer among people who have never smoked [11].

Radon is an inert gas with low chemical reactivity and low solubility in body tissues. Because of the long half-life of 3.8 days, compared to the duration of a breath, the radiotoxicity of ^{222}Rn is negligible.

For radiation protection considerations, mainly the short-lived α-emitting radon daughters have to be taken into account to calculate the effective dose. The unattached and attached radionuclides are inhaled and deposit in the airway generations of the respiratory tract. These airway generations can be divided into the bronchial region (airway generation 0 to 8), the bronchiolar region (airway generation 9 to 15), and the alveolar interstitial region (airway generations > 15) as carried out in the ICRP 66 [2]. The bronchial region consists of the trachea, the primary bronchi and the bronchi. The bronchiolar region consists of bronchioles, the alveolar interstitial region of alveoli. After deposition, the attached and the unattached radionuclides can be removed from the lung by lung clearance. Such clearance includes the absorption into the blood and transport of particles into the gastrointestinal tract or the lymph nodes. With their short half-lives being shorter than one second to 26.8 min, some radionuclides either completely decay in the lung before they are removed or get bound to the lung tissue. Their whole alpha energy is delivered to the lung tissues. The basal cells and the secretory cells in the epithelium are assumed to be the critical target cells which can mutate to cancer cells.

Further explanations about the differences between the unattached and the attached fraction as well as other biological and aerosol particle parameters, which have to be considered, are given in the section “3.4. Calculation of the effective dose”.

2. Measuring methods

The attached and the unattached short-lived radon daughters as well as the long-lived Radon daughters on aerosols of different particle size have been measured to gain an overview of the radiation dose in the radon gallery and its adjacent therapy centre in Böckstein.

2.1. Attached radon daughters

Two portable LCD-BWLM-PLUS (LCD-Battery operating Working-Level-Monitor) from TRACERLAB have been used to measure the activity concentration of the

attached radionuclides and to estimate the Radon activity concentration in air. This equipment has been provided by the AUVA (Austrian Social Insurance for Occupational Risks). One working-level-monitor consists of a microcomputer, a multi-channel-analyser, a pump and a measuring device with a silicon surface barrier detector as well as a filter holder. At the measuring site, the LCD-BWLM-PLUS was operated over night or for a few days. The pump drew air through the membrane filter with a pore size of 0.8 µm for about 26 minutes. The attached radionuclides were collected on the filter and, directly after collection, the alpha particles were measured for 4 minutes. Then the pump was restarted and the measuring cycle repeated.
With this method the alpha particles of ^{218}Po and ^{214}Po can be measured directly. Due to the very short half-life of ^{214}Po, of 164 µs, it can be assumed that ^{214}Po is in equilibrium with ^{214}Bi. The working level monitor uses an iterative method to calculate the activity concentration of the short-lived radon nuclides. The equilibrium factor F and the ^{222}Rn concentration in air are estimated from the measurements of the attached or unattached daughters.
The equilibrium factor F is the ratio of the ^{222}Rn equilibrium equivalent concentration to the existing activity concentration of ^{222}Rn in air. It characterises the disequilibrium of the mixture of the short-lived decay products in air and the mother nuclide in air.

$$F = \frac{C_{eq}}{C_0} \qquad \text{Equation 1}$$

F = equilibrium factor
C_{eq} = equilibrium equivalent activity concentration of ^{222}Rn in air [Bq/m³]
C_0 = activity concentration of ^{222}Rn in air [Bq/m³]
The equilibrium equivalent activity concentration of ^{222}Rn is a calculated activity concentration of ^{222}Rn in radioactive equilibrium with its daughter products that has the same potential alpha energy as the actually measured mixture of the short-lived daughter radionuclides in air.

$$C_{eq} = 0.105 \cdot C_{Po-218} + 0.516 \cdot C_{Pb-214} + 0.379 \cdot C_{Bi-214} + 6 \cdot 10^{-8} \cdot C_{Po-214} \qquad \text{Equation 2}$$

C_j =activity concentration of the radionuclide j [Bq/m³]
The potential alpha energy concentration (PAEC) is the entire alpha energy that is emitted by a mixture of short-lived daughter radionuclides in air during their decay to ^{210}Pb. Within this decay chain, one atom ^{214}Po emits an alpha particle with an energy of 7.69 MeV ($1.23 \cdot 10^{-12}$ J), and one atom ^{218}Po emits an alpha particle with 6.00 MeV ($9.62 \cdot 10^{-13}$)[12]. The potential alpha energy of one atom ^{214}Po and one atom ^{218}Po is

7.69 MeV and 13.69 MeV ($2.19 \cdot 10^{-12}$ J), respectively. The dimension of the PAEC is J/m³ or the old unit Working Level (WL).

$$C_p\,[WL] = \frac{C_{eq}}{3700} \qquad \text{Equation 3}$$

C_p = potential alpha energy concentration [WL]
C_{eq} = equilibrium equivalent activity concentration of ^{222}Rn [Bq/m³]
The PAEC is 1 WL ($2.08 \cdot 10^{-5}$ J/m³)[2] if the equilibrium equivalent activity concentration is 3700 Bq/m³.

2.2. Unattached radon daughters

For the determination of the unattached fraction, TRACERLAB provided the portable "BWLM-PLUS Free fraction" measurement system. It consists of a microcomputer, a multi-channel-analyser and a copper wire screen with 200 mesh. The ^{218}Po and ^{214}Po atoms deposit spontaneously on the wire screen. After a 26-minutes sampling period, the silicium surface barrier detector measures the alpha particles. The instrument was calibrated at the Federal Office for Radiation Protection (BfS) in Berlin.

2.3. Long-lived radon daughters

The long lived radon daughters ^{210}Pb, ^{210}Bi and ^{210}Po were collected with an 8-stage cascade impactor for about 24 hours. The aerosols of particle sizes between 0.05 µm to 16 µm were collected.
The cut off diameters and the mean diameters are listed in Table 1.

Stage Number	Cut off diameter [µm]	Average aerosol diameter [µm]
1	0.05	0.088
2	0.12	0.175
3	0.25	0.35
4	0.5	0.71
5	1.0	1.4
6	2.0	2.8
7	4.0	5.6
8	8.0	11

Table 1: Cut off and average aerosol diameter of the collected particles on the aluminium foils of the cascade impactor

The aluminium foils for aerosol deposition were placed in the stages and the cascade impactor was connected to a pump. Air was sucked through the impactor for about 24 hours to collect the aerosols from ~ 50 m³ of air. The aluminium foils were cut in small pieces and the aerosols washed off with concentrated HNO_3. This solution was evaporated to dryness and fumed with concentrated HNO_3. Then the residue was dissolved in 4 ml 7 M H_3PO_4. Afterwards, 0.66 ml 1 M HCl and 1 ml of the extractive scintillation cocktail Polex™ from Etrac Laboratories Inc. were added to the solution and the ^{210}Po as well as ^{210}Bi were extracted. 0.7 ml aliquots of Polex were measured with the Quantulus 1220 at a PSA of 130 [13,14,15]. Using pulse shape analysis, the signals produced by alpha radiation and the signals produced by beta radiation could be distinguished, therefore creating an alpha spectrum and a beta spectrum. ^{210}Po and the ^{210}Bi could be evaluated separately in the respective spectrum. For the measurement of ^{210}Pb, two different methods were used. For the small particle sizes, were a high ^{210}Pb activity is assumed 4 ml of the H_3PO_4 / HCl solution were taken after bismuth and polonium extraction, mixed with 16 ml of Hisafe 3™ and measured by LSC. Due to the relatively high background of this method (2.5 cpm) and thus a high lower limit of detection (LLD) of 0.09 mBq/m³, this method could not be used for the larger particle sizes. In this case, the sample was stored until the ^{210}Bi was in equilibrium with the ^{210}Pb and then the ^{210}Bi was extracted again with Polex™. Here, ^{210}Pb was measured via ^{210}Bi. The LLD of this method varies between 0.02 mBq/m³ and 0.05 mBq/m³, depending on the time gap between sampling and extraction.

3. Results and discussion

Measurements were performed during three sampling periods in July 2003, in January 2004 and in October 2004. Station 1 of the radon gallery and its nearby therapy centre were chosen as sampling sites. This figure shows the radon gallery with the stations I, Ia, II, III and IV and the therapy centre building at the entrance.

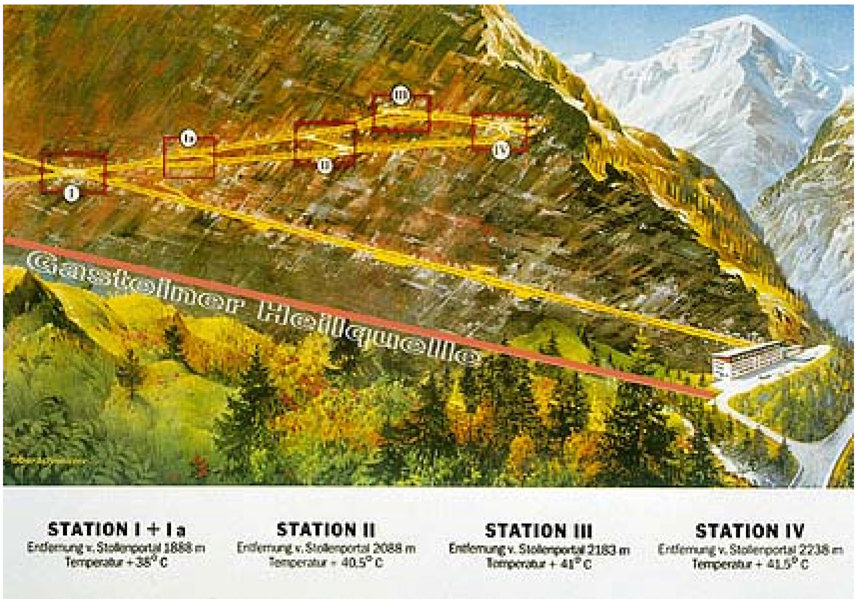

Source: http://www.gasteiner-heilstollen.com/heilstollentherapie.html

The attached and unattached short-lived radon daughters as well as the long-lived radon daughters were measured. In October 2004, also the aerosol particle concentration in the radon gallery was determined. Table 2 shows the measurements that were performed at the different sampling sites during the aforementioned periods.

Period	Site	Measurements			
July 2003	radon gallery	attached short-lived Rn daughters		long-lived Rn daughters	
January 2004	radon gallery	attached short-lived Rn daughters	unattached short-lived Rn daughters	long-lived Rn daughters	
October 2004	radon gallery			long-lived Rn daughters	aerosol particle concentration
October 2004	therapy centre foyer	attached short-lived Rn daughters			
October 2004	therapy centre gym	attached short-lived Rn daughters	unattached short-lived Rn daughters		
October 2004	therapy centre doctor's office 5	attached short-lived Rn daughters	unattached short-lived Rn daughters		

Table 2: List of measurements which were performed at different periods and sites.

3.1. Measurements in the radon gallery Bad Gastein

3.1.1. Short-lived radon daughters, July 2003

The first sampling period was set between noon of 7 July and 11:30 on 10 July. During this time, the attached short-lived radon daughters were measured. The instrument was placed in station 1 of the radon gallery. There, the temperature is between 37°C and 39°C, with a relative air humidity between 75 % and 80 %. Patients are driven to the therapy stations with a battery-operated train at 8, 10, 12, 14, and 16 o'clock. During this sampling period, the ventilation system operated with 110 m³/min. The therapeutic section is provided with 10% of this volume, whereas the remaining 90 % are used for the ventilation of a tunnel outside the therapeutic section, where the workers and employees can rest during their stay in the gallery. The air volume in the therapeutic section is 7,680 m³ and the air change rate with this ventilation is 0.086/h.

3.1.1.1. Attached short-lived radon daughters, July 2003

The measurement results from the LCD-BWLM-PLUS are detailed in Appendix 2. Figure 1 shows the activity concentration in Bq/m³ of the short-lived daughter products ^{218}Po, ^{214}Pb and $^{214}Bi/^{214}Po$, of the equilibrium equivalent radon and the estimated radon between 7 July at noon and 10 July at 11:30. The two radionuclides ^{214}Bi and ^{214}Po are in equilibrium, due to the short half-life time of ^{214}Po with 162 µsec. Hence, the results for these two radionuclides will be combined and defined as the activity concentration $^{214}Bi/^{214}Po$ or Bi-214/Po-214. Figure 2 shows the PAEC in WL and J/m³. Tables 3 to 6 in Appendix 1 summarise the daily results.

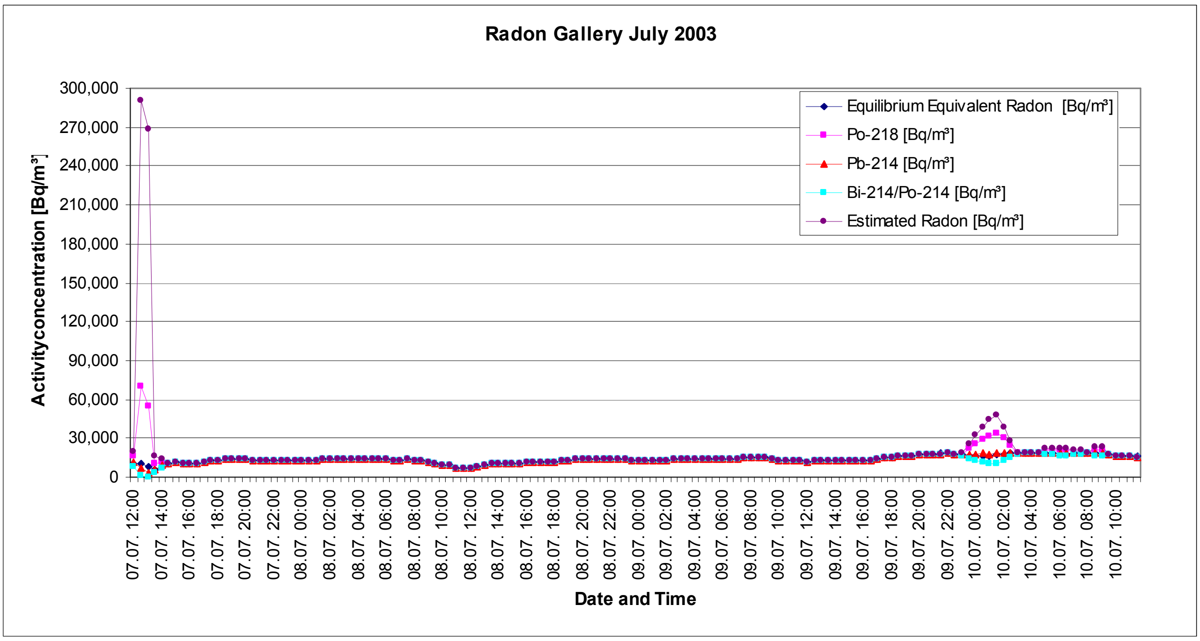

Figure 1: Radon gallery measurement results from July 2003. The activity concentrations of the short lived radon daughter products, the equilibrium equivalent radon and the estimated radon are illustrated.

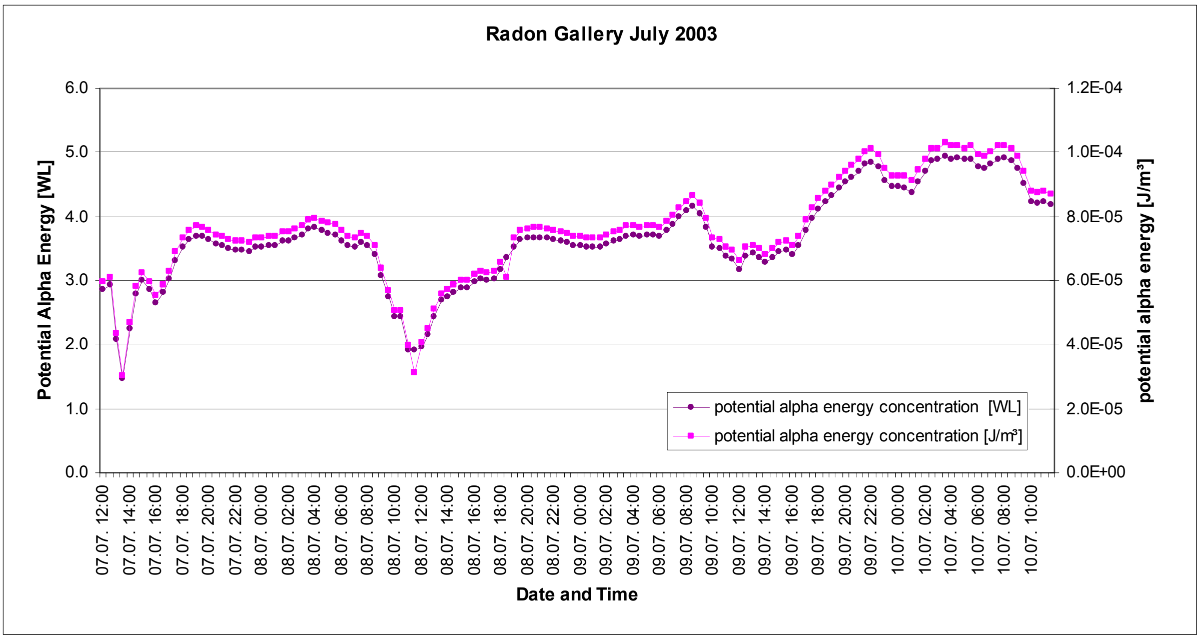

Figure 2: The potential alpha energy in WL and J/m³ during the radon gallery measurements in July 2003.

The maximum value of the radon activity concentration in air estimated from the measurements of the attached short-lived daughters was between noon and 13:30 on the 7 July. This maximum value was 291,000 Bq/m³. However, the radon was not in equilibrium with its short-lived daughter products. Therefore, although the radon activity concentration was high, the PAEC reached the minimum value at 13:30 with 1.5 ± 0.1 WL. An explanation for the maximum radon value of 300 kBq/m³ at 12:30 on the 7 July could not be found. It could have occurred due to the installation of the measuring instruments and thus a repeated opening and closing of the door to the climate room. This, however, would not explain the second maximum radon value of 50 kBq/m³ at 01:30 on 10 July. Radon measurements in the Bozkov Cave also showed short and very high peaks of radon [16]. The authors have no explanation either, but suggest that these maximum values could be due to a sudden release related to slight earthquakes.

Low activity concentrations were measured during daytime, whereas the activity concentrations increased during night (see figure 1 and 2). Therefore, the mean value for the PAEC was 3.32 ± 0.03 WL during daytime (from 7:00 to 18:00) and 3.97 ± 0.03 WL during night. This can be explained through operating the ventilation system, which is turned on at 8:00 and turned off at 17:30.

Figure 3 shows the daily mean activity concentration values of the short-lived daughter products, the equilibrium equivalent radon as well as the estimated radon. The daily mean values of the PAEC are shown in figure 4.

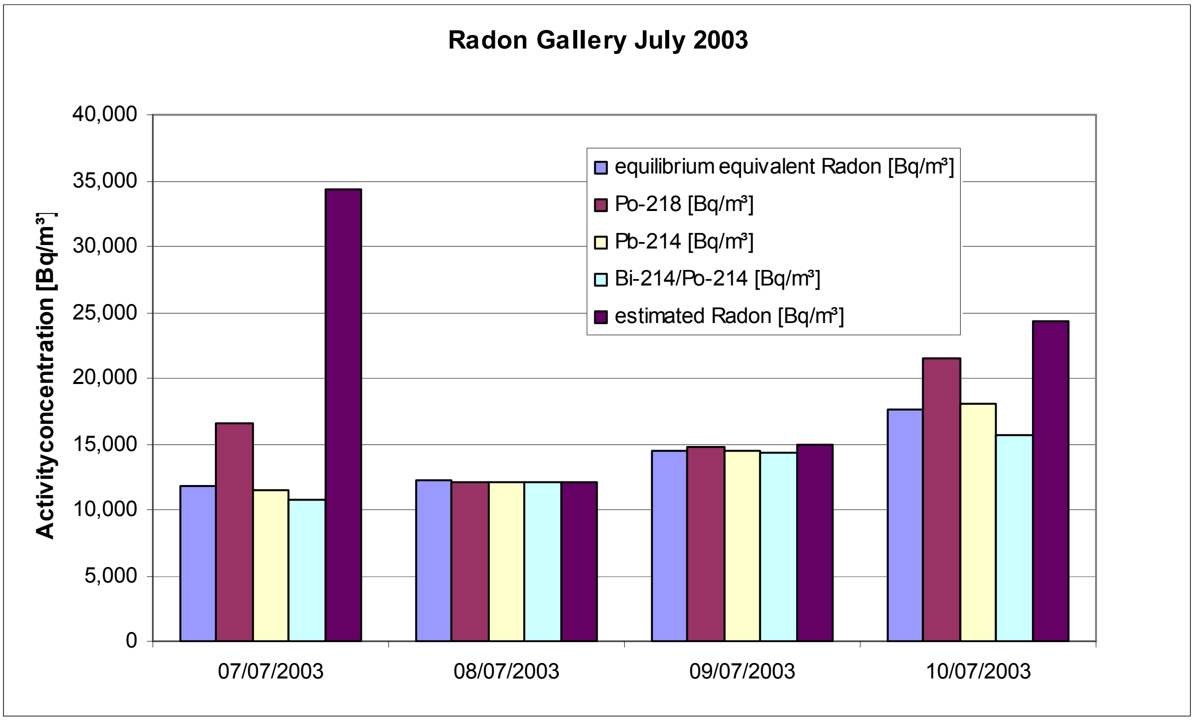

Figure 3: Mean values of the attached short-lived radon daughter products, the equilibrium equivalent radon and the estimated radon.

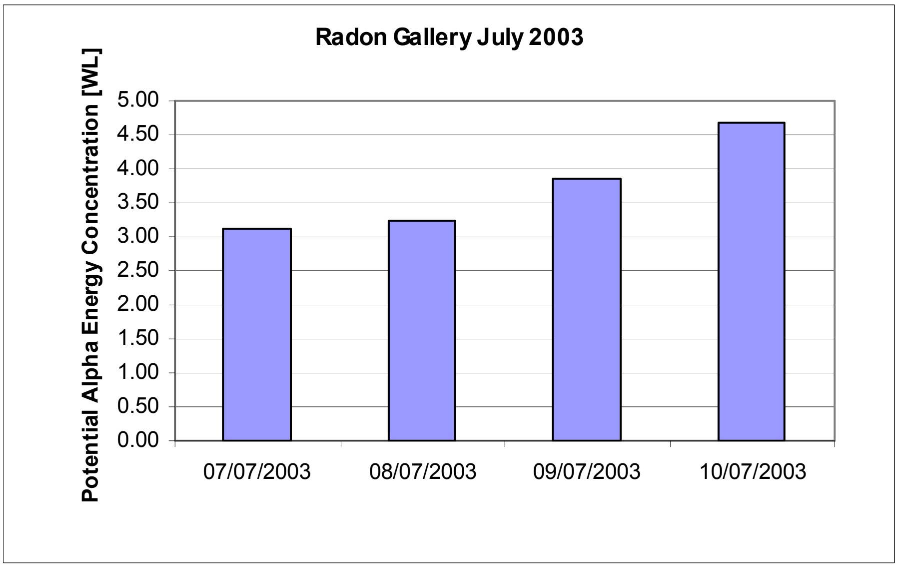

Figure 4: Mean values of the PAEC during the sampling period 7 July to 10 July, 2003.

During the entire measurement period, the mean value of the PAEC increased from 3.13 ± 0.04 WL on 7 July to 4.66 ± 0.06 WL on 10 July.

This increase was caused by an elevated emanation of radon from the mountain. Comparable situations had been measured before by Pohl-Rühling [17] and had been caused by a decrease in atmospheric pressure. Figure 5 illustrates the atmospheric pressure measured in Rauris, showing a decrease in atmospheric pressure and an increase in the PAEC over time The data was provided by the Austrian Central Institute for Meteorology and Geodynamics (ZAMG).

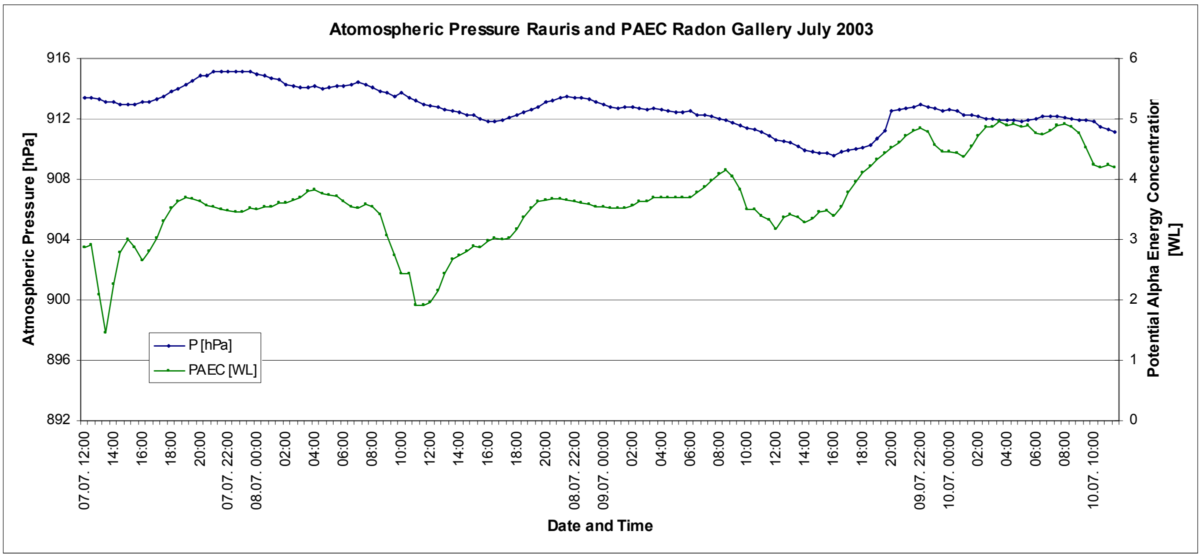

Figure 5: The atmospheric pressure in Rauris and the PAEC in the radon gallery in July 2003

3.1.2. Short-lived radon daughters, January 2004

The second sampling period started on 7 January and ended on 9 January. During this period, the attached and unattached radon daughters were measured. The therapy period, when patients are treated in the radon gallery, starts in mid-January and ends in mid-November. The remaining time of the year is used for repair works, cleaning and reconstruction. During this sampling period reconstruction work was carried out in the so-called climate room, a tunnel outside the therapeutic section, which is used by the workers and employees during their stay in the gallery. Therefore, the ventilation system was still running at 110 m³/min, with just 10% of the air provided for the therapeutic section, the door to the therapeutic section was closed. Also in this case, station 1 was used as sampling point.

3.1.2.1. Attached short-lived radon daughters, January 2004

The results of the measurements are detailed in Appendix 2.

Figure 6 shows the activity concentration in Bq/m³ of the short-lived daughter products ^{218}Po, ^{214}Pb and ^{214}Bi/^{214}Po, of the equilibrium equivalent radon and estimated radon between 11:30 on 7 January and 10:30 on 9 January. Figure 7 shows the change of the potential alpha energy in WL and J/m³ during this time. Tables 7 to 9 in appendix 1 summarise the daily results.

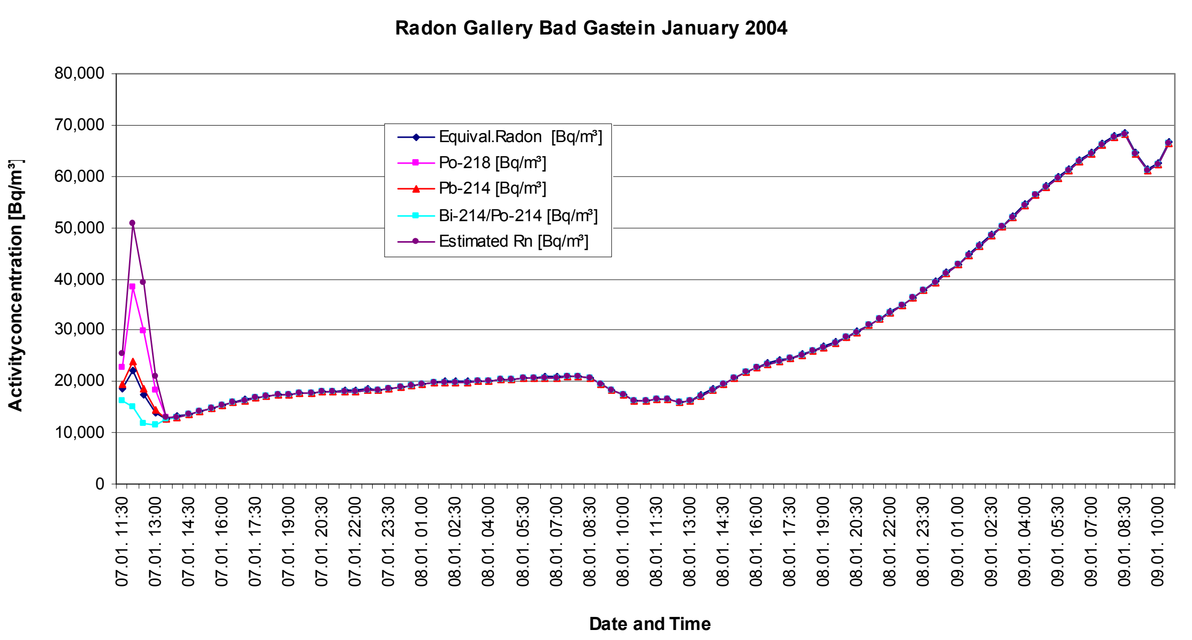

Figure 6: Activity concentration of the attached short lived radon daughter products, the equilibrium equivalent radon and the estimated radon in the radon gallery in January 2004.

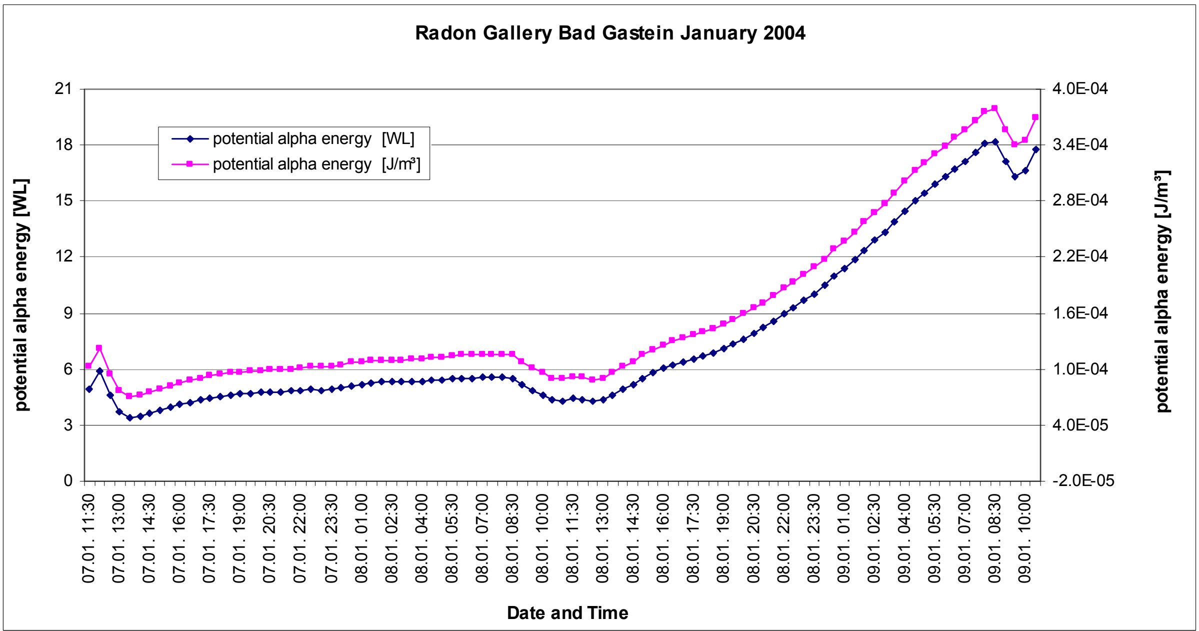

Figure 7: Potential alpha energy concentration calculated from the attached radionuclides.

During these three days, the mean values of the activity concentrations of radon and its progeny increased continuously on 8 January and 9 January. Each day, with the start of the ventilation, a decline of the activity concentrations can be observed. The

mean values of the PAEC increased from 4.5 ± 0.1 WL on the 7 January to 15.0 ± 0.2 WL on the 9 January. These values exceeded the values of July (the maximum value measured in July was 5.0 ± 0.3 WL).
During working hours (assumption 7:00 to 18:00) the average PAEC was 4.2 ± 0.1 WL on 7 January, 5.3 ± 0.1 WL on 8 January and 17.4 ± 0.4 WL on 9 January. Contrary to what is expected, the average PAEC during working hours with additional artificial ventilation on 9 January was higher than the average PAEC during the hours without artificial ventilation (measurements were performed between midnight and 10:30). The reason for this is the elevated emanation of radon due to the decrease in atmospheric pressure. Figure 8 shows the atmospheric pressure measured in Rauris and the PAEC measured in the radon gallery.
These results assess that ventilation only has a minor influence on the PAEC. The PAEC is mainly influenced by the atmospheric pressure.

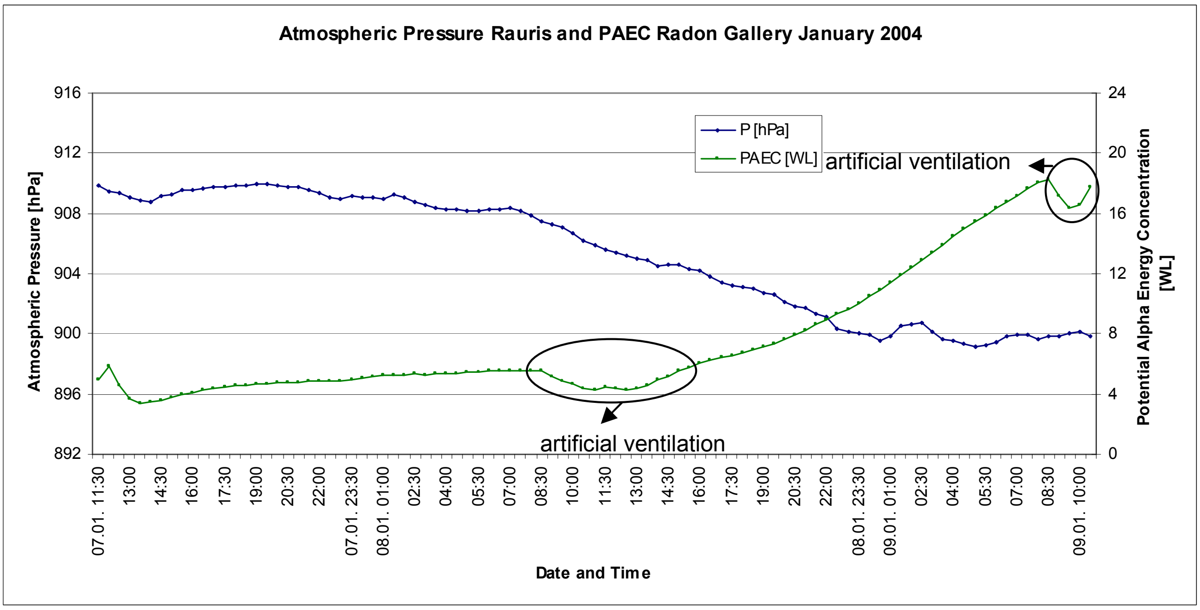

Figure 8: The atmospheric pressure measured in Rauris and the PAEC measured in the radon gallery.

Figure 9 shows the daily mean activity concentration values of the short-lived daughter products, the equilibrium equivalent radon and the estimated radon. The daily mean values of the PAEC are shown in Figure 10.

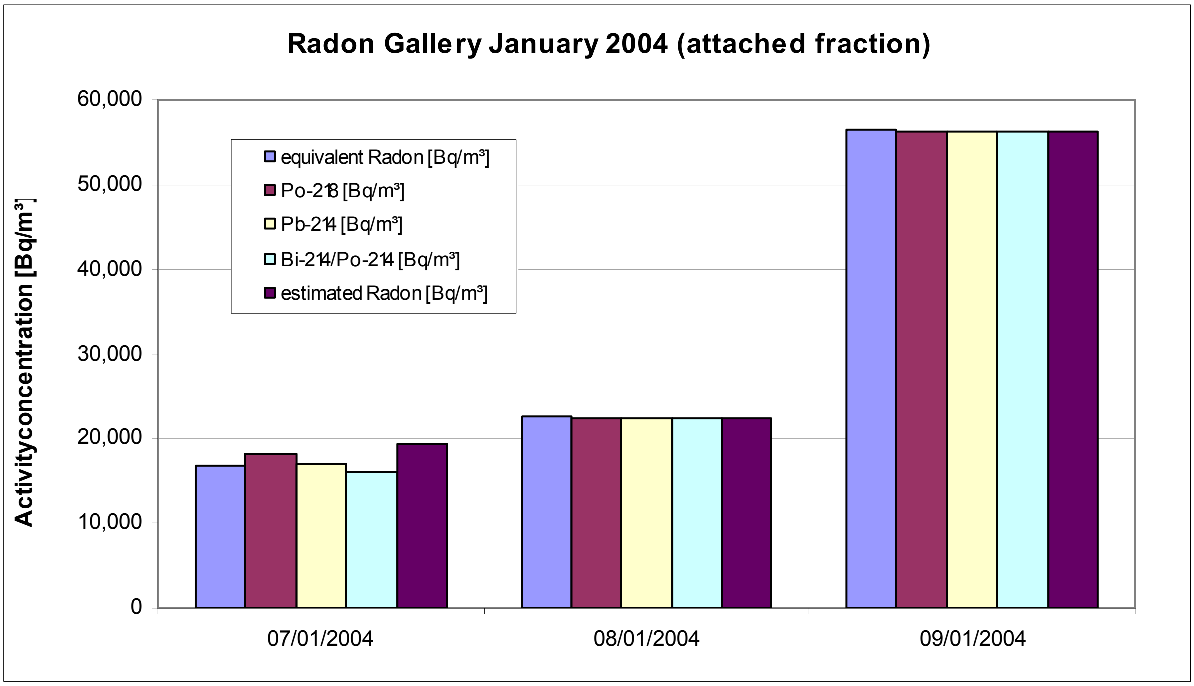

Figure 9: Mean values of the activity concentrations of the attached short lived radon daughter products, the equilibrium equivalent radon and the estimated radon.

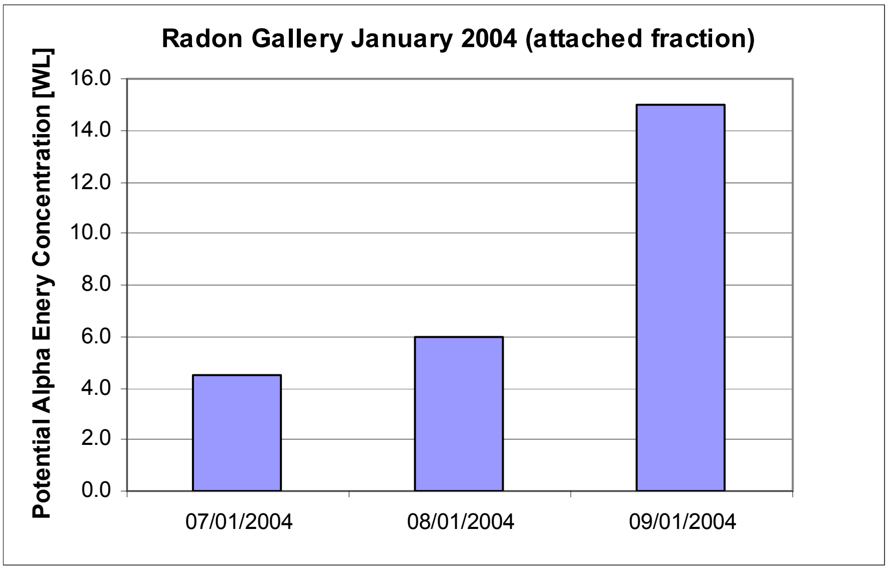

Figure 10: Daily mean values of the PAEC in the radon gallery, January 2004

During the measurement period in July, the average activity concentration for ^{218}Po was about 16,000 Bq/m³, for ^{214}Pb about 14,000 Bq/m³ and for ^{214}Bi/^{214}Po about 13,000 Bq/m³. The equilibrium equivalent radon concentration was about 14,000 Bq/m³.

During the measurement period in January, the average equilibrium equivalent radon activity concentration was about 32,000 Bq/m³. The average activity concentrations for ^{218}Po, ^{214}Pb and ^{214}Bi/^{214}Po were about 32,000 Bq/m³. These values are about twice as high as the values in July. Whereas on 7 January the average activity concentration for ^{218}Po was about 18,000 Bq/m³, for ^{214}Pb about 17,000 Bq/m³, for ^{214}Bi/^{214}Po about 16,000 Bq/m³ and for the equilibrium equivalent radon it was 17,000 Bq/m³. These values are similar to the values in July. The value of atmospheric pressure was 913 hPa in July and 910 hPa on 7 January, with atmospheric pressure dropping to 900 hPa on 9 January.

In order to decrease the activity concentration and the PAEC, the normal ventilation of 110 m³/min during daytime is not sufficient. For example, the equilibrium equivalent radon concentration decreased from 21,100 ± 1,300 Bq/m³ to 16,100 ± 1,000 Bq/m³ during normal ventilation conditions on 8 January 2004. On 9 January, it decreased from 68,600 ± 4,200 Bq/m³ to 61,500 ± 3,800 Bq/m³.

During full ventilation, the ventilation system operates with 180 m³/min. The volume of the entire gallery is 18,860 m³. The air change rate under these conditions is 0.573/h. Measurements under these conditions had been performed in a previous measuring campaign in 1999 [18], with the results showing a decrease in activity concentrations due to full ventilation conditions. The atmospheric pressure was not taken into consideration. The equilibrium equivalent radon concentration fell from about 10,000 Bq/m³ to about 1,000 Bq/m³. Data of the atmospheric pressure between 11 January till the 13 January were available from the Central Institute for Meteorology and Geodynamics (ZAMG). In the morning of 11 January the atmospheric pressure was 891 hPa and increased to 904 hPa until the 12 January in the evening. The full ventilation conditions as well as the decrease of the equilibrium equivalent concentration and an increase in atmospheric pressure happened simultaneously. However, at about 1 o'clock on 13 January 1999, the equilibrium equivalent concentration started to increase again, in spite of the full ventilation conditions. During this time, it increased from 1 kBq/m³ to about 2 kBq/m³, while atmospheric pressure dropped from 904 hPa on 12 January in the night to 894 hPa at about 5 o'clock the next morning.

These new results show that normal ventilation conditions merely have a minor influence, whereas full ventilation conditions, with an open door to the therapy sections, have a big influence that still has to compete with the atmospheric pressure. It could hence be useful to increase the ventilation rate when a drop in atmospheric pressure occurs.

3.1.2.3. Unattached Short-Lived Radon Daughters January 2004

The measurement results of the portable BWLM-PLUS Free fraction measurement system are detailed in Appendix 2.

Figure 11 shows the activity concentration in Bq/m³ of the short-lived daughter products ^{218}Po, ^{214}Pb and ^{214}Bi/^{214}Po, the equilibrium equivalent radon and the estimated radon between 11:30 on 7 January and 10:00 on 9 January. Figure 12 shows the PAEC in WL and J/m³ during this time. Tables 10 to 12 in Appendix 1 summarise the results of the respective day.

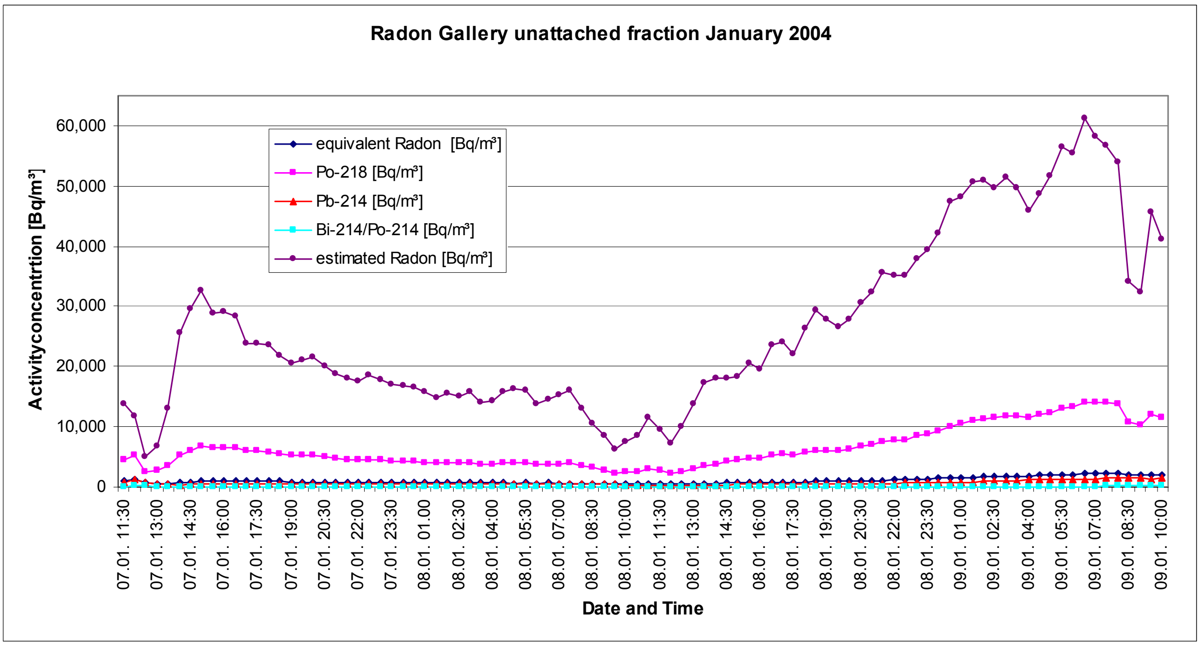

Figure 11: Activity concentrations of the unattached short-lived radon daughter products, the equilibrium equivalent radon and the estimated radon in the radon gallery in January 2004

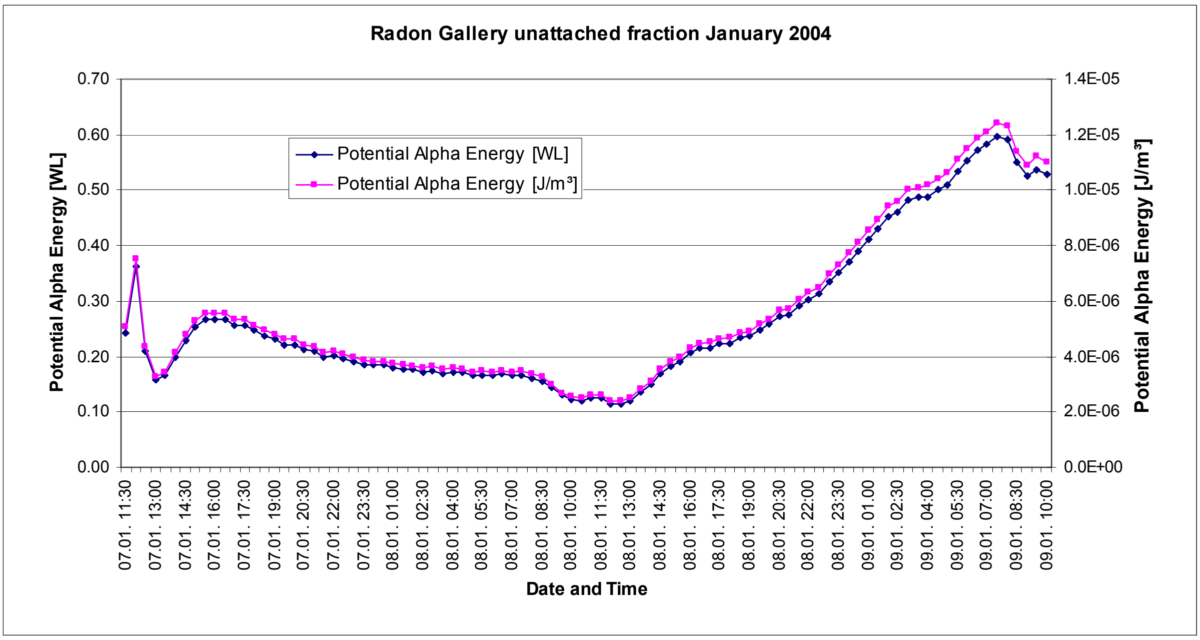

Figure 12: The potential alpha energy concentration in January in the radon gallery

Due to the lower activity concentrations of the unattached radon daughters compared to the attached ones the PAEC was between 0.11 ± 0.01 WL and 0.60 ± 0.04 WL. During working hours (assumption 7:00 – 18:00) the average PAEC was 0.24 ± 0.01 WL on 7January, 0.16 ± 0.01 WL on 8 January and 0.56 ± 0.01 WL on 9 January.

Figure 13 shows the daily mean activity concentrations of the short-lived daughter products, the equilibrium equivalent and estimated radon. The daily mean values of the PAEC are shown in figure 14.

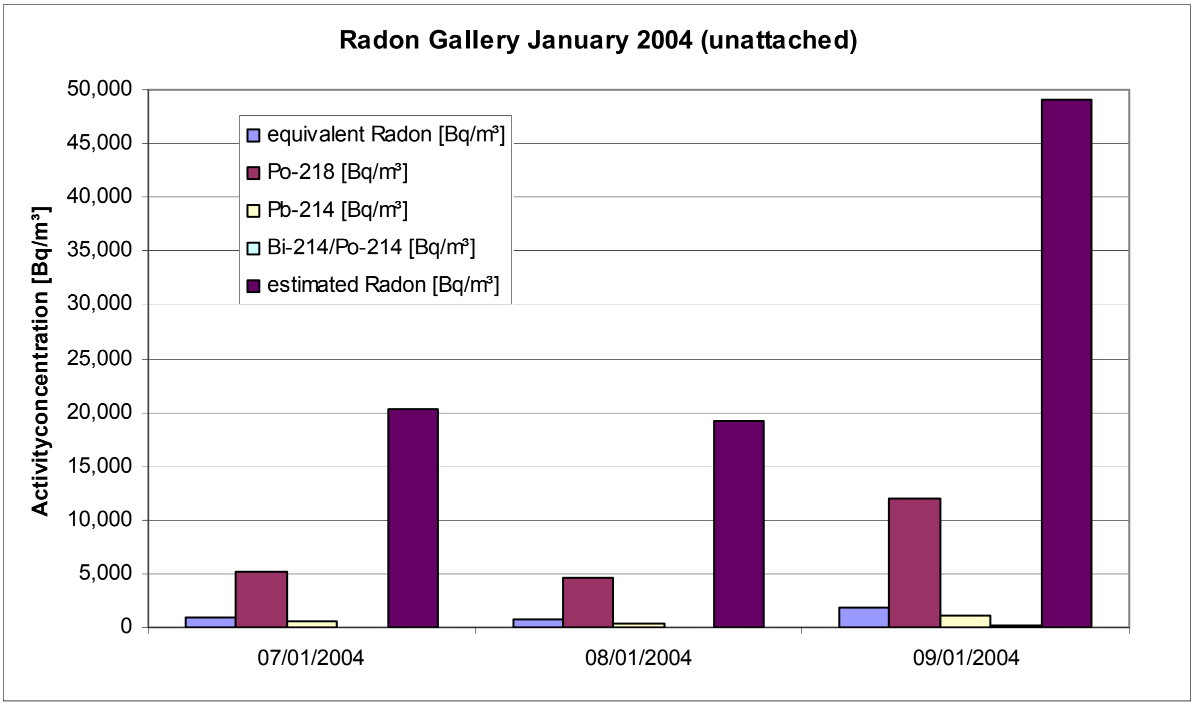

Figure 13: Mean values of the activity concentrations of the unattached short lived radon daughter products, the equilibrium equivalent radon and the estimated radon.

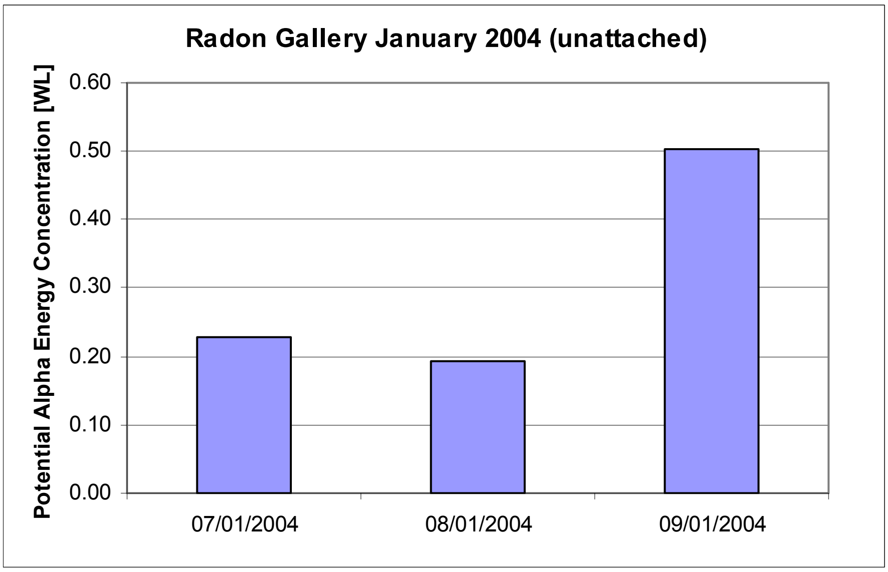

Figure 14: Daily mean values of the PAEC of the unattached radionuclides.

The activity concentration of the unattached and the attached ^{218}Po, ^{214}Pb and ^{214}Bi/^{214}Po and the unattached fraction of each nuclide are shown in Figure 15 to 17. The fraction of each unattached radon daughter f_j or the whole unattached fraction f_p can be calculated as follows

$$f_j = \frac{C_j^f}{C_j} \qquad \text{Equation 4}$$

C^f_j = activity concentration of an unattached radon daughter nuclide j in air [Bq/m³]

C_j = total activity concentration (attached and unattached) of a radon daughter nuclide j in air [Bq/m³]

f_j = unattached fraction of a radon daughter nuclide j [19].

$$f_p = \frac{C^f_{eq}}{C_{eq}} \qquad \text{Equation 5}$$

C^f_{eq} = equilibrium equivalent activity concentration of ^{222}Rn of the unattached radionuclides in air [Bq/m³]

C_{eq} = total equilibrium equivalent activity concentration (attached and unattached) of ^{222}Rn in air [Bq/m³]

f_p = unattached fraction

Figure 18 shows the calculated equilibrium equivalent radon activity concentration of the attached and unattached measurements and the unattached fraction.

Tables 13 to 15 in Appendix 1 summarise the results of the respective day.

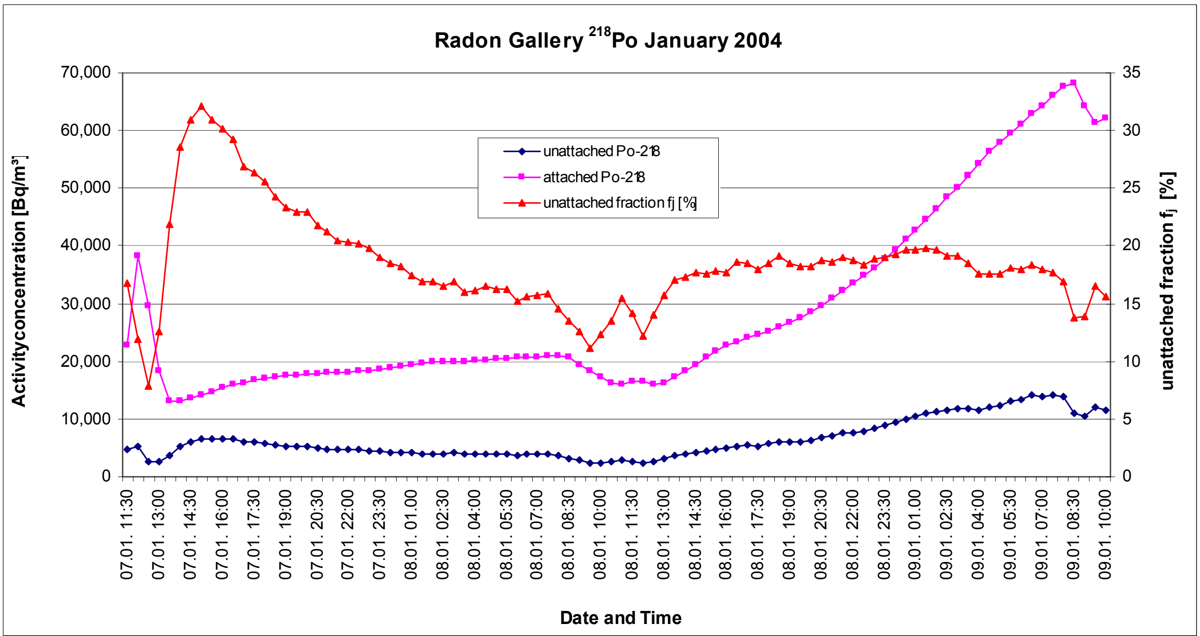

Figure 15: Activity concentrations of the attached and unattached ^{218}Po and the fraction of the unattached ^{218}Po to the total ^{218}Po.

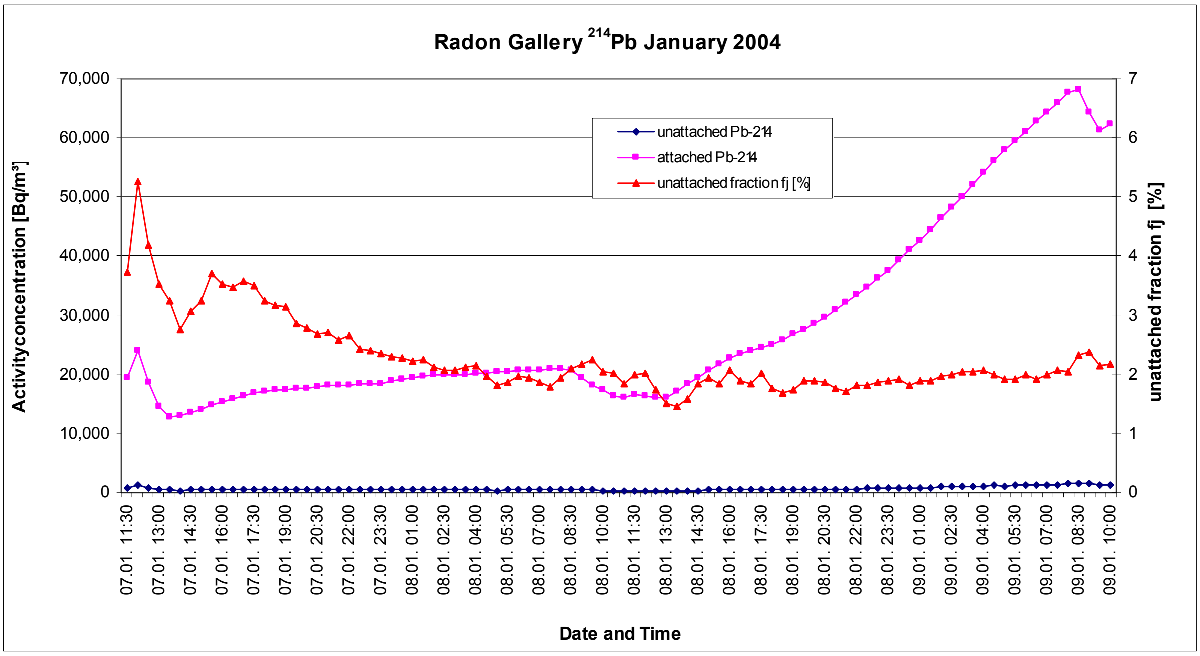

Figure 16: Activity concentrations of the attached and unattached ^{214}Pb and the fraction of the unattached ^{214}Pb to the total ^{214}Pb.

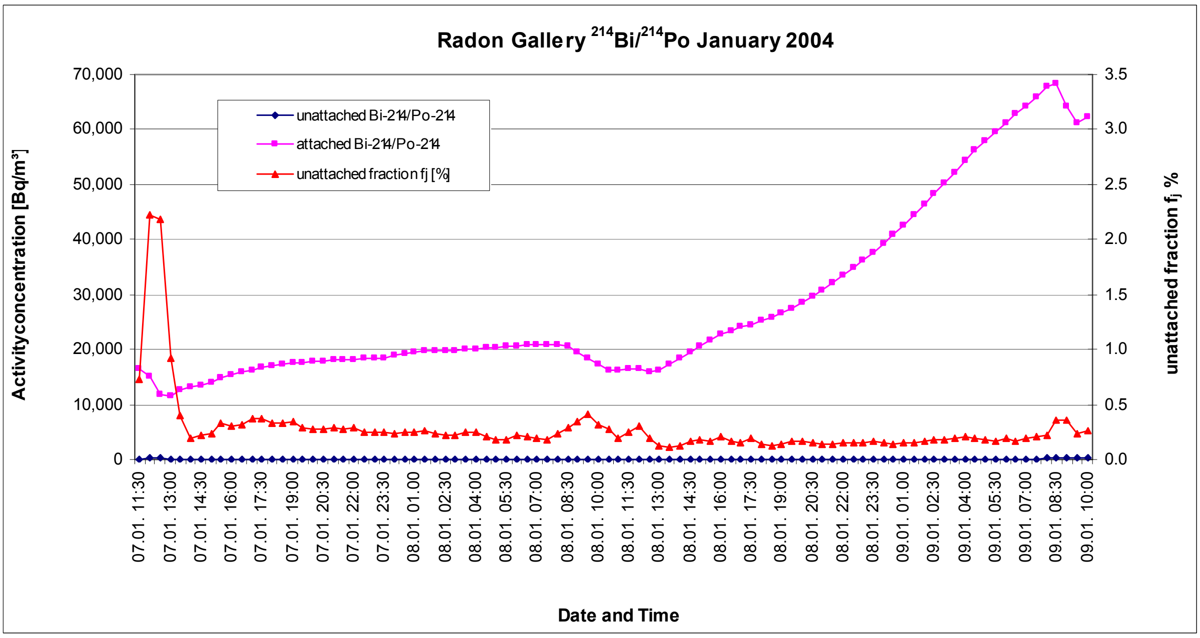

Figure 17: Activity concentrations of the attached and unattached $^{214}Bi/^{214}Po$ and the fraction of the unattached $^{214}Bi/^{214}Po$ to the total $^{214}Bi/^{214}Po$.

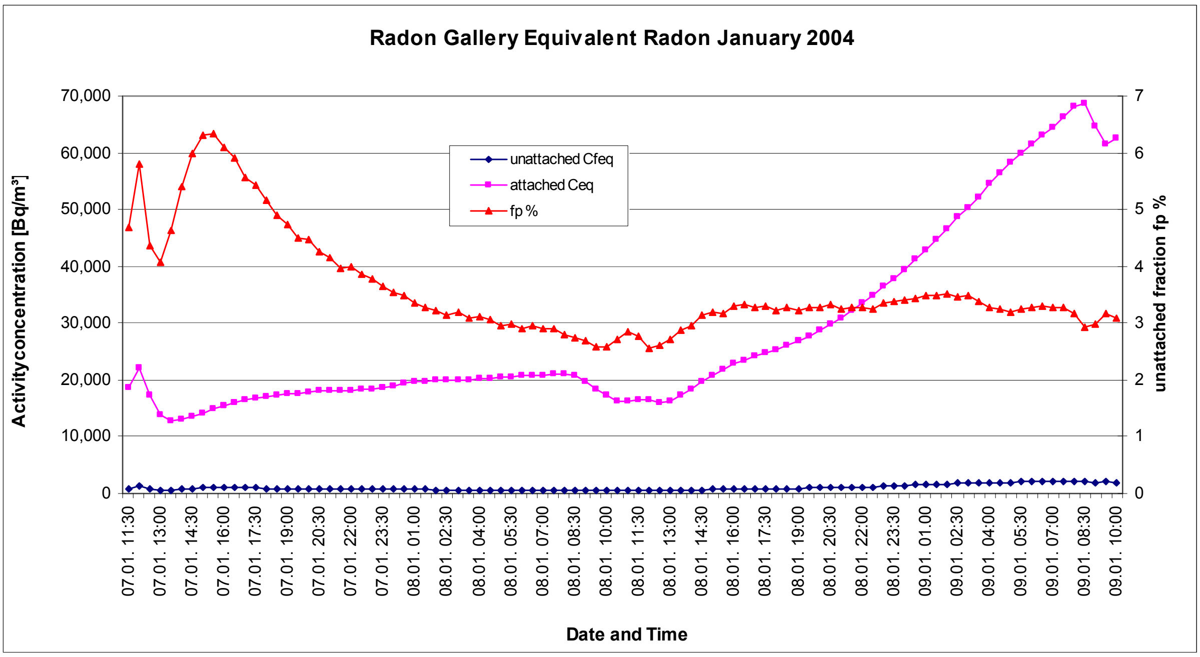

Figure 18: Activity concentrations of the attached and unattached equilibrium equivalent radon concentration and the unattached fraction.

Figure 19 shows the daily mean values of the unattached fraction and the unattached fraction of each radon daughter.

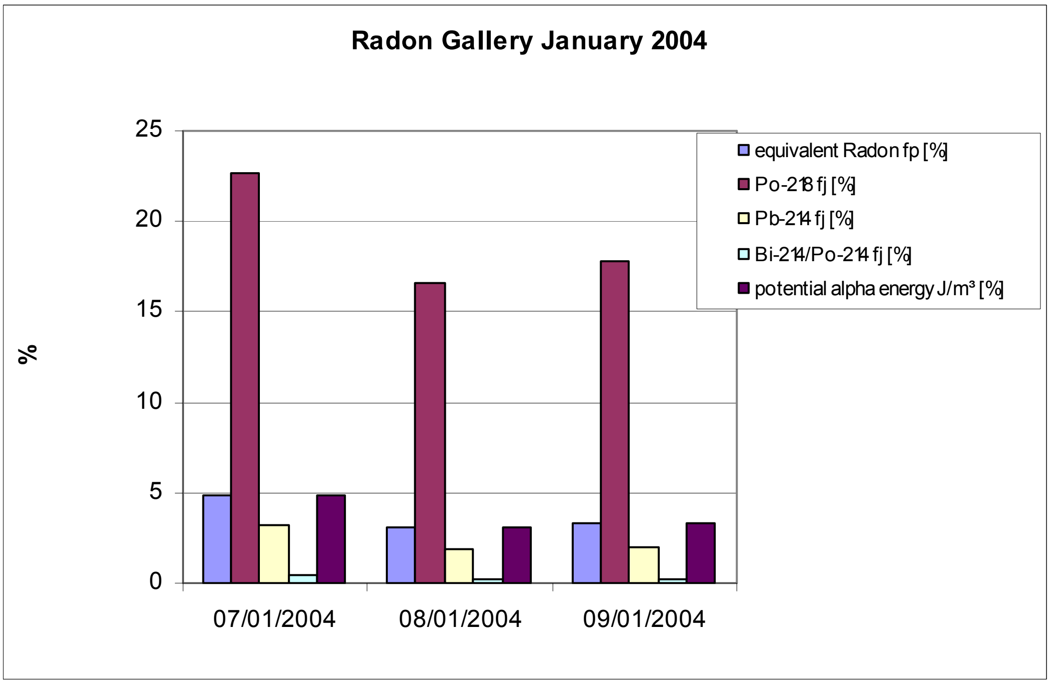

Figure 19: Mean values of the unattached fraction, the fraction of each unattached daughter product and the contributions of the unattached radionuclides to the total PAEC.

It can be clearly seen that the highest contribution to the unattached fraction results from ^{218}Po. An explanation for this is that due to its gaseous precursor ^{222}Rn and its short half-life of 3.05 min the ^{218}Po is generated in the air and reacts with trace gases and vapours to build the unattached clusters. Afterwards these clusters attach to aerosols. The lowest contribution results from ^{214}Bi and ^{214}Po. The contribution of the different unattached daughter products to the unattached fraction is calculated as follows:

The unattached fraction is:

$$f_p = \frac{C_{eq}^f}{C_{eq}} \qquad \text{Equation 5}$$

C^f_{eq} = equilibrium equivalent activity concentration of ^{222}Rn of the unattached radionuclides in air [Bq/m³]

C_{eq} = total equilibrium equivalent activity concentration (attached and unattached) of ^{222}Rn in air [Bq/m³]

Using the following equation 2

$$C_{eq} = 0.105 \cdot C_{Po-218} + 0.516 \cdot C_{Pb-214} + 0.379 \cdot C_{Bi-214} + 6 \cdot 10^{-8} \cdot C_{Po-214} \qquad \text{Equation 2}$$

the unattached fraction can be written as:

$$f_p = \frac{C_{eq}^f}{C_{eq}} = \frac{0.105 \cdot C_{Po-218}^f + 0.516 \cdot C_{Pb-214}^f + 0.379 \cdot C_{Bi-214}^f}{0.105 \cdot C_{Po-218} + 0.516 \cdot C_{Pb-214} + 0.379 \cdot C_{Bi-214}} \qquad \text{Equation 6}$$

The contribution of the unattached radionuclide j to the unattached fraction is:

$$Contribution_{Po-218} = \frac{0.105 \cdot C_{Po-218}^f}{C_{eq}^f} \qquad \text{Equation 7}$$

$$Contribution_{Pb-214} = \frac{0.516 \cdot C_{Pb-214}^f}{C_{eq}^f} \qquad \text{Equation 8}$$

$$Contribution_{Bi-214} = \frac{0.379 \cdot C_{Bi-214}^f}{C_{eq}^f} \qquad \text{Equation 9}$$

During the whole measurement period the mean contribution to the unattached fraction from ^{218}Po was 65% and from ^{214}Bi just 2.6%. The relatively high contribution from ^{214}Pb with 32% results from the recoil of the ^{214}Pb after α-emission of ^{218}Po. The contribution from ^{214}Po can be neglected

3.1.3. Long-lived radon daughters

For the determination of the long-lived radon daughters ^{210}Pb, ^{210}Bi and ^{210}Po, the aerosols were collected with a cascade impactor with 8 stages.

The aerosol particles can be classified into three size categories: the nucleation mode with a particle diameter smaller than 0.1 µm, the accumulation mode with particle diameters between 0.1 µm and 1 µm, and the coarse mode with a particle diameter larger than 1 µm.

According to this classification, the first 4 stages of the cascade impactor comprise the accumulation mode aerosols, while stages 5 to 8 comprise the coarse mode aerosols. Some nucleation mode particles can also be collected on the filter in stage 1.

3.1.3.1. Long-lived radon daughters, July 2003

During the first sampling period in July 2003 two sets (8 to 9 July and 9 to 10 July) of aluminium foils were collected with the cascade impactor. Tables 16 and 17 show the respective results of the measurements. The sampling started at 11:00 on 8 July and ended at 16:30 on 8 July (because of malfunction of the pump). The sampled air volume was 9.3 m³. The sampling of the second set of aluminium foils started at 12:45 on 9 July and ended at 11:15 on 10th of July. The volume of the air sampled was 41.86 m³

08.07.2003	Pb-210	Bi-210	Po-210
Aerosol Diameter	mBq/m³	mBq/m³	mBq/m³
0.05 -0.12 µm	81.6 ± 4.3	14.3 ± 1.2	34.8 ± 1.8
0.12 – 0.25 µm	160.7 ± 7.9	29.1 ± 2.4	42.3 ± 2.3
0.25 – 0.5 µm	152 ± 7.5	25.1 ± 2.0	22.0 ± 1.1
0.5 – 1 µm	52 ± 2.4	8.99 ± 0.70	8.36 ± 0.46
1 – 2 µm	8.25 ± 0.41	1.68 ± 0.16	1.59 ± 0.11
2 – 4 µm	1.259 ± 0.066	0.146 ± 0.019	0.672 ± 0.052
4 – 8 µm	0.311 ± 0.017	< 0.75	0.102 ± 0.013
8 – 16 µm	4.13 ± 0.21	< 2.5	3.42 ± 0.19
Total activity concentration	460 ± 12	79.3 ± 3.4	113.2 ± 3.2

Table 16: Activity concentration of ^{210}Pb, ^{210}Bi and ^{210}Po in mBq/m³ collected in the radon gallery with the cascade impactor.

09.07.2003	Pb-210	Bi-210	Po-210
Aerosol Diameter	mBq/m³	mBq/m³	mBq/m³
0.05 -0.12 µm	43.4 ± 2.1	6.03 ± 0.50	12.19 ± 0.64
0.12 – 0.25 µm	130.8 ± 6.1	20.2 ± 1.6	26.0 ± 1.4
0.25 – 0.5 µm	123.7 ± 5.8	19.5 ± 1.6	21.0 ± 1.1
0.5 – 1 µm	35.9 ± 1.8	5.05 ± 0.40	5.20 ± 0.28
1 – 2 µm	5.61 ± 0.30	0.964 ± 0.085	1.665 ± 0.091
2 – 4 µm	1.145 ± 0.060	0.162 ± 0.017	0.293 ± 0.019
4 – 8 µm	0.467 ± 0.024	0.234 ± 0.022	0.253 ± 0.017
8 – 16 µm	0.272 ± 0.014	0.141 ± 0.016	0.0978 ± 0.0086
Total activity concentration	341.3 ± 8.9	52.3 ± 2.4	66.7 ± 1.9

Table 17: Activity concentration of ^{210}Pb, ^{210}Bi and ^{210}Po in mBq/m³ collected in the radon gallery with the cascade impactor.

The highest activity concentrations of all three radionuclides are located in the accumulation mode in the fractions from 120 nm to 250 nm and from 250 nm to 500 nm.

3.1.3.2. Long-lived radon daughters, January 2004

During the second sampling period in January 2004 two sets (7 to 8 January and 8 to 9 January) of aluminium foils were collected with the cascade impactor. The sampling started at 11:30 on 7 January and ended at 11:05 on 8 January. The sampled volume of the air was 45.28 m³. The sampling for the second set of aluminium foils started at 11:45 on 8 January and ended at 10:20 on 9 January. The volume of the air sampled was 43.36 m³

In January the highest activity concentration of all three Radionuclides was located in the fraction from 250 – 500 nm. This can be seen in Tables 18 and 19.

07.01.2004	Pb-210	Bi-210	Po-210
Aerosol Diameter	mBq/m³	mBq/m³	mBq/m³
0.05 -0.12 µm	75.6 ± 3.6	14.1 ± 1.1	18.6 ± 1.0
0.12 – 0.25 µm	397 ± 18	53.7 ± 3.9	33.1 ± 1.7
0.25 – 0.5 µm	733 ± 34	177 ± 13	58.5 ± 2.9
0.5 – 1 µm	227 ± 11	57.9 ± 4.2	14.04 ± 0.73
1 – 2 µm	24.5 ± 1.4	5.37 ± 0.43	1.328 ± 0.071
2 – 4 µm	2.24 ± 0.13	0.598 ± 0.051	0.424 ± 0.025
4 – 8 µm	0.588 ± 0.040	0.124 ± 0.013	0.229 ± 0.015
8 – 16 µm	0.458 ± 0.036	< 0.13	0.257 ± 0.016
Total activity concentration	1460 ± 40	308.5 ± 14	126.5 ± 3.5

Table 18: Activity concentration of ^{210}Pb, ^{210}Bi and ^{210}Po in mBq/m³ collected in the radon gallery with the cascade impactor.

08.01.2004	Pb-210	Bi-210	Po-210
Aerosol Diameter	mBq/m³	mBq/m³	mBq/m³
0.05 -0.12 µm	62.4 ± 2.9	13.4 ± 1.0	17.05 ± 0.89
0.12 – 0.25 µm	495 ± 23	107.2 ± 7.6	53.6 ± 2.6
0.25 – 0.5 µm	919 ± 43	241 ± 17	60.5 ± 3.0
0.5 – 1 µm	136.0 ± 6.3	39.3 ± 2.8	9.67 ± 0.53
1 – 2 µm	2.97 ± 0.17	0.619 ± 0.052	0.345 ± 0.021
2 – 4 µm	1.95 ± 0.12	10.07 ± 0.84	1.327 ± 0.072
4 – 8 µm	1.90 ± 0.12	< 0.74	0.277 ± 0.022
8 – 16 µm	0.668 ± 0.046	< 0.41	0.177 ± 0.017
Total activity concentration	1619 ± 49	411 ± 19	142.9 ± 4.1

Table 19: Activity concentration of ^{210}Pb, ^{210}Bi and ^{210}Po in mBq/m³ collected in the radon gallery with the cascade impactor.

The mean total activity concentration of ^{210}Bi in January was 360 ± 17 mBq/m³. This value is 5.5 times higher than the mean total activity concentration of ^{210}Bi in July with 65.8 ± 2.9 mBq/m³. The ^{210}Pb mean total activity concentration in January (1,540 ± 45 mBq/m³) is 3.8 times higher than in July (401 ± 11 mBq/m³). The smallest increase was observed at the ^{210}Po mean total activity concentration which is 1.5 times higher in January (90.0 ± 2.6 mBq/m³) than in July (134.7 ± 3.8 mBq/m³). The increase was mainly caused by the increase of the activity concentration in the fraction between 250 and 500 nm.

3.1.3.3. Long-lived radon daughters, October 2004

Three sets of aluminium foils were collected with the cascade impactor during the third sampling period in October 2004 (12 to 13 Oct., 13 to 14 Oct. and 14 to 15 Oct.). The sampling started at 13:25 on 12 October and ended at 12:25 on 13 October. The sampled volume of the air was 42.79 m³. The sampling for the second set of aluminium foils started at 12:50 on 13 October and ended at 12:25 on 14 October. The sampled air volume was 43.87 m³. The sampling for the third set of aluminium foils started at 12:50 on 14 October and ended at 12:25 on 15 October. The result of the determinations in October can be seen in the Tables 20 to 22. The highest activity concentration was again located in the fraction from 120 nm to 250 nm. The second highest activity concentrations were located in the fractions from 50 nm to 120 nm and from 250 nm to 500 nm.

12.10.2004	Pb-210	Bi-210	Po-210
Aerosol Diameter	mBq/m³	mBq/m³	mBq/m³
0.05 -0.12 µm	285 ± 14	55.9 ± 4.1	30.3 ± 1.6
0.12 – 0.25 µm	534 ± 25	91.0 ± 6.6	44.8 ± 2.4
0.25 – 0.5 µm	397 ± 20	70.6 ± 5.1	27.2 ± 1.5
0.5 – 1 µm	101.6 ± 4.8	n.d.	13.69 ± 0.68
1 – 2 µm	31.8 ± 1.7	n.d.	4.35 ± 0.21
2 – 4 µm	n.d.	n.d.	n.d.
4 – 8 µm	n.d.	n.d.	n.d.
8 – 16 µm	n.d.	n.d.	n.d.
Total activity concentration	1349 ± 36	217.4 ± 9.3	120.3 ± 3.3

Table 20: Activity concentration of ^{210}Pb, ^{210}Bi and ^{210}Po in mBq/m³ collected in the radon gallery with the cascade impactor.

13.10.2004	Pb-210	Bi-210	Po-210
Aerosol Diameter	mBq/m³	mBq/m³	mBq/m³
0.05 -0.12 µm	611 ± 29	146 ± 11	122.6 ± 6.5
0.12 – 0.25 µm	1178 ± 55	154 ± 11	140.4 ± 7.3
0.25 – 0.5 µm	691 ± 33	160 ± 12	62.1 ± 3.3
0.5 – 1 µm	118.7 ± 6.1	12.22 ± 0.92	8.74 ± 0.47
1 – 2 µm	25.0 ± 1.4	3.19 ± 0.26	2.04 ± 0.12
2 – 4 µm	5.80 ± 0.34	0.424 ± 0.037	0.640 ± 0.040
4 – 8 µm	n.d.	n.d.	n.d.
8 – 16 µm	n.d.	n.d.	n.d.
Total activity concentration	2629 ± 70	475 ± 19	336 ± 10

Table 21: Activity concentration of ^{210}Pb, ^{210}Bi and ^{210}Po in mBq/m³ collected in the radon gallery with the cascade impactor.

14.10.2004	Pb-210	Bi-210	Po-210
Aerosol Diameter	mBq/m³	mBq/m³	mBq/m³
0.05 -0.12 µm	567 ± 27	79.6 ± 5.9	99.2 ± 5.3
0.12 – 0.25 µm	1068 ± 50	141 ± 10	129.5 ± 6.8
0.25 – 0.5 µm	598 ± 28	78.8 ± 5.8	53.4 ± 2.9
0.5 – 1 µm	70.1 ± 4.0	20.6 ± 1.6	6.05 ± 0.32
1 – 2 µm	20.2 ± 1.2	4.88 ± 0.39	1.424 ± 0.078
2 – 4 µm	5.64 ± 0.33	0.775 ± 0.064	0.535 ± 0.031
4 – 8 µm	2.99 ± 0.18	0.685 ± 0.059	0.333 ± 0.021
8 – 16 µm	3.34 ± 0.20	< 0.47	0.297 ± 0.019
Total activity concentration	2335 ± 64	325 ± 13	290.7 ± 9.1

Table 22: Activity concentration of ^{210}Pb, ^{210}Bi and ^{210}Po in mBq/m³ collected in the radon gallery with the cascade impactor.

For ^{210}Bi, the mean total activity concentration was 340 ± 15 mBq/m³ in October. This value is 5.2 times higher than the mean total activity concentration of 65.8 ± 2.9 mBq/m³ in July. For ^{210}Pb, mean total activity concentration was 5.3 times higher in October (2,104 ± 59 mBq/m³) than in July (401 ± 11 mBq/m³). The smallest increase could again be observed in the ^{210}Po activity concentration, which is 2.8

times higher in October (249.2 ± 8.2 mBq/m³) than in July (90.0 ± 2.6 mBq/m³). This time, the increase was mainly caused by the increase of the activity concentration in the fraction between 50 nm and 120 nm.

Measurements of ^{210}Pb, ^{210}Bi and ^{210}Po had been performed in previous measuring campaigns [18]. In May 1999, Wallner et al. performed measurements under standard ventilation during regular therapeutic operation. The mean values are shown in Table 23. The highest activity concentration could again be located in the fraction from 120 nm to 250 nm.

May 1999	Pb-210	Bi-210	Po-210
Aerosol Diameter	mBq/m³	mBq/m³	mBq/m³
0.05 -0.12 µm	97.3 ± 5.8	17.4 ± 1.4	21.5 ± 1.0
0.12 – 0.25 µm	345 ± 21	80.0 ± 6.3	54.0 ± 3.0
0.25 – 0.5 µm	210 ± 13	64 ± 4.8	31.3 ± 2.0
0.5 – 1 µm	66.0 ± 4.0	20 ± 1.5	11.2 ± 0.70
1 – 2 µm	9.9 ± 0.6	3.10 ± 0.40	2.20 ± 0.20
2 – 4 µm	2.0 ± 0.14	1.0 ± 0.2	0.60 ± 0.06
4 – 8 µm	0.68 ± 0.07	0.19 ± 0.060	0.20 ± 0.04
8 – 16 µm	0.54 ± 0.07	0.04 ± 0.02	0.19 ± 0.03
Total activity concentration	731 ± 26	186 ± 8.2	121 ± 3.8

Table 23: Results of the measurements in the radon gallery from Wallner et. al.[18].

Table 24 shows the daily measurements' mean values of the total activity concentrations within a month.

	Pb-210	Bi-210	Po-210
	mBq/m³	mBq/m³	mBq/m³
July 2003	401 ± 11	65.8 ± 2.9	90.0 ± 2.6
January 2004	1,540 ± 45	360 ± 17	134.7 ± 3.8
October 2004	2,104 ± 59	340 ± 15	249.2 ± 8.2
May 1999 [18]	731 ± 26	186 ± 8.2	121 ± 3.8

Table 24: Total activity concentration of ^{210}Pb, ^{210}Bi and ^{210}Po during four different measurement periods collected in the radon gallery with a cascade impactor

The values of May 1999 are within the range of the mean value of those values measured in both July 2003 and January 2004. The highest total activity concentration was measured in October 2004. The values in October 2004 are about twice as high than the values from May 1999. From these four sampling periods, the ranges for ^{210}Pb, ^{210}Bi and ^{210}Po were 400 to 2,100 mBq/m³, 70 to 360 mBq/m³ and 90 to 250 mBq/m³, respectively.

Figures 20 to 23 show the activity size distributions of the long-lived radon daughter products calculated from the mean values of the daily measurements of each month.

The fraction of the activity collected on each stage in relation to the total activity collected by the cascade impactor was calculated as shown in equation 10.

$$y = \frac{A_{Stage_x}}{\sum A_{Stage_x}} \qquad \text{Equation 10}$$

Thus it can bee seen that the fractions of the three radionuclides on the stages are different.

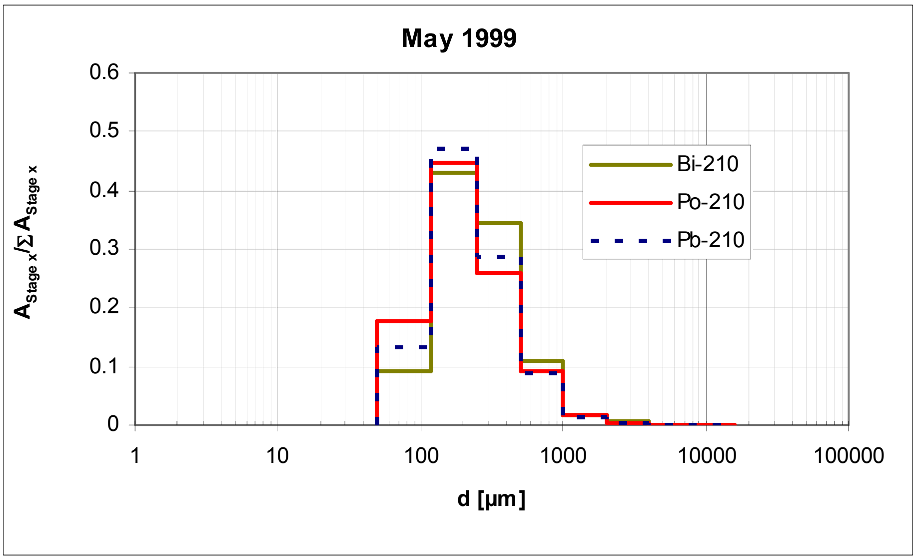

Figure 20: The fraction of the activity of ^{210}Pb, ^{210}Bi and ^{210}Po collected on each stage in relation to the total activity collected by the cascade impactor.

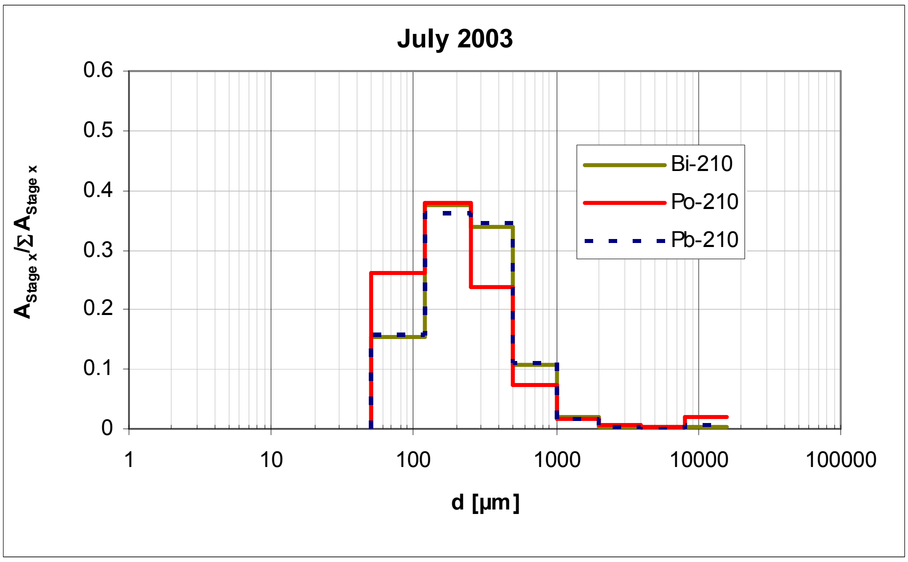

Figure 21: The fraction of the activity of ^{210}Pb, ^{210}Bi and ^{210}Po collected on each stage in relation to the total activity collected by the cascade impactor.

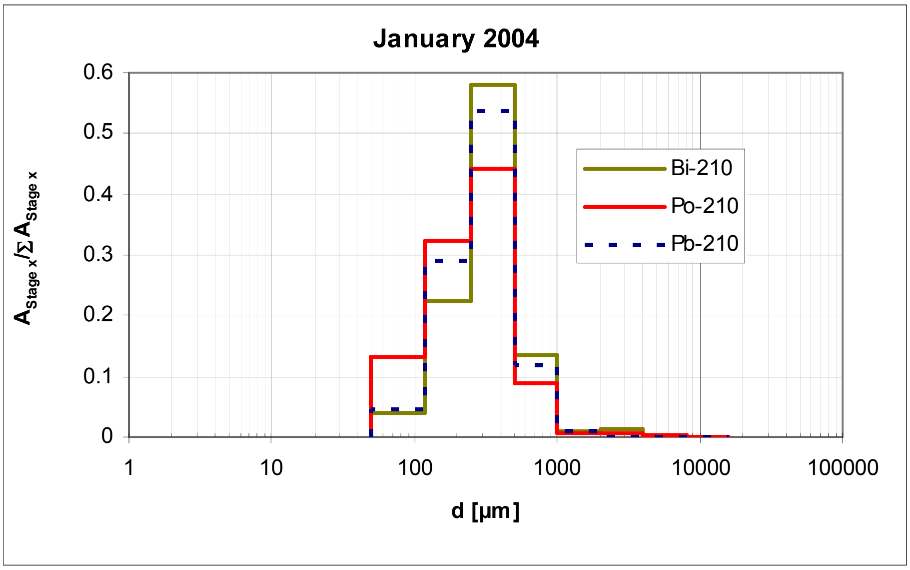

Figure 22: The fraction of the activity of ^{210}Pb, ^{210}Bi and ^{210}Po collected on each stage in relation to the total activity collected by the cascade impactor.

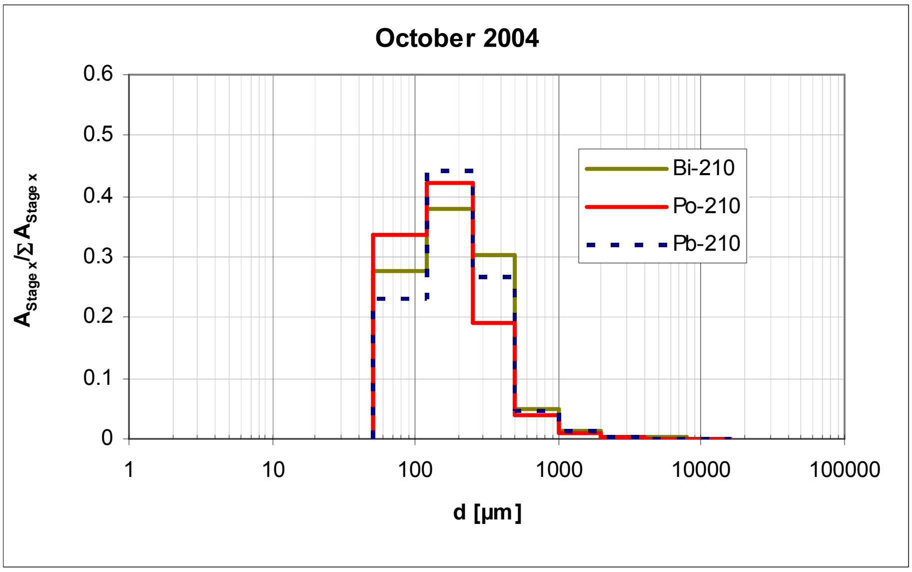

Figure 23: The fraction of the activity of ^{210}Pb, ^{210}Bi and ^{210}Po collected on each stage in relation to the total activity collected by the cascade impactor.

These figures clearly show that—compared to the AMAD of ^{210}Pb and ^{210}Bi—the activity median aerodynamic diameter (AMAD) of ^{210}Po is shifted to smaller particle sizes. This effect was observed before by Wallner et al. published in 2001 [20] and 2002 [18].

Additionally the AMAD in January 2004 shifted to higher particle sizes compared to the AMAD in May 1999, July 2003 and October 2004. The reason for this shift is not yet known.

In some publications, the change of the activity median aerodynamic diameter (AMAD) of the aerosol-attached radionuclides during working conditions is described. Reineking et al. measured average AMAD of 188 – 234 nm in low ventilated rooms without additional aerosol sources [21].

During working hour, a large number of aerosol particles is generated mainly by the diesel engines in mines. The activity size distribution by these particles has smaller median diameters AMAD (200 nm) than the aged aerosol existing in the mine during non-working hours (350 nm) [22].

However, no diesel engines are operated in the radon gallery in Bad Gastein, where a battery-operated train is used instead. The shift of the AMAD can be caused by the mechanical grinding of the gallery train tracks or the corrosion of Fe in the old metal wall brackets. Evidence for that was given by Wallner et al. who published a paper in 2005 in which Fe, Co, Cr were found in the aerosols collected by the cascade impactor. The rust content was between 1,7 % and 5,1 % in the accumulation mode of the aerosol particles [23].

In July and October, the radon gallery was open for the public, with the train driving repeatedly through the therapeutic section. In January, however, there were only reconstruction works in the so-called climate room. The therapeutic section was not in use, nobody was in that section, and the train was not driving through it. The shift of the activity concentration to higher particle diameter which had been observed in January, was due to the same effects, which causes the shift of the AMAD in the investigations described in previous publications: Without additional aerosol sources only the aged aerosols existed and therefore the AMAD was between 250 nm and 500 nm.

3.2. Measurements in the therapy centre building

During the third sampling period (between 12 and 16 October) the therapy centre building was investigated.

The results of a study of radon concentration in workplaces in Italy showed that the radon concentration in the air of different workplaces within the same municipality shows immense variability, which is higher than the variability in dwellings [24]. Even different rooms of the same building can show significant variations. Different radon concentrations in different rooms of a building are not just due to different ventilation conditions, but also due to the location of the room. A further study conducted looked at schools in Canada, where radon concentration was measured in the basement and on the ground floor. The arithmetic mean of 561 measurements of the ground floor was 51 Bq/m³ whereas the arithmetic mean for the basement was 71 Bq/m³ [25].

Consequently, different sampling sites in the therapy centre were chosen for the measurements. Rooms with different air change rates and situated in different parts of the building were selected. First, the attached radon daughters were measured in the foyer on the ground floor, then the attached and the unattached radon daughters were measured in the gym on the second floor as well as in doctor's office 5 on the ground floor.

3.2.1. Short-lived radon daughters in the foyer

3.2.1.1. Attached short-lived radon daughters in the foyer

The results of the measurements are detailed in Appendix 2. Because of the entering of the patents and employees during the whole day this room has a good aeration but no artificial ventilation system.

Figure 24 shows the activity concentration in Bq/m³ of the attached short-lived daughter products ^{218}Po, ^{214}Pb and ^{214}Bi/^{214}Po, the equilibrium equivalent radon and estimated radon between 10:00 on 12 October and 9:30 on 13 October. Figure 25 shows the PAEC in WL and J/m³ during this time. Tables 25 – 26 in Appendix 1 summarise the daily results.

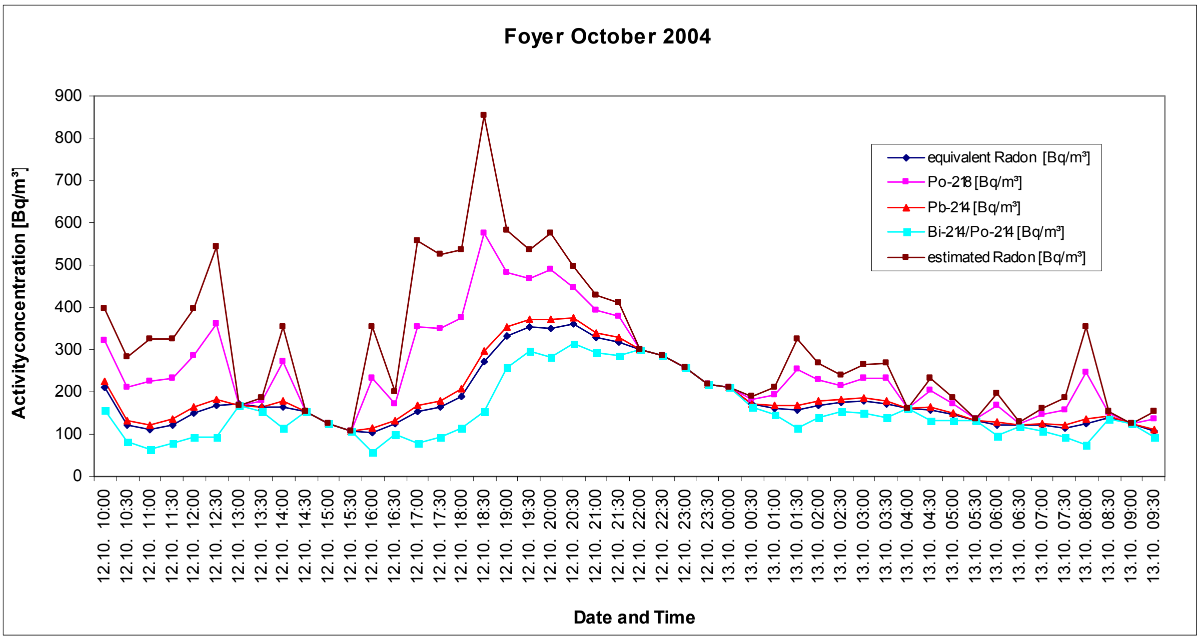

Figure 24: Activity concentrations of the attached short-lived radon daughters, the equilibrium equivalent radon and the estimated radon in the foyer.

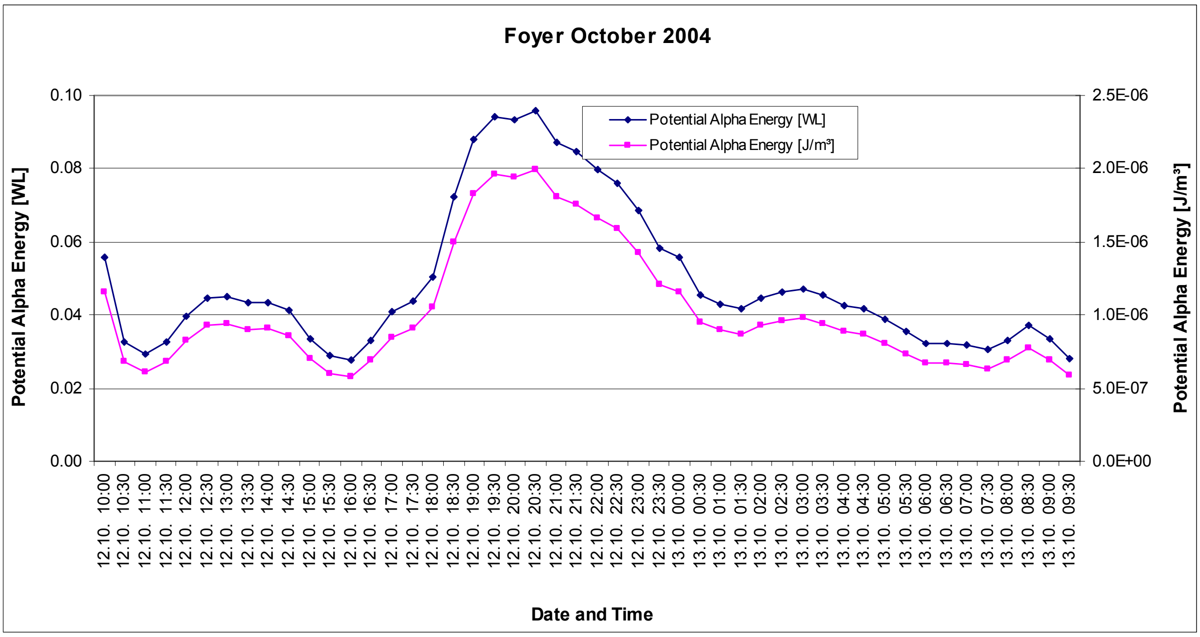

Figure 25: The potential alpha energy concentration in the foyer.

The activity concentration of the equilibrium equivalent radon was between 104 ± 10 Bq/m³ and 361 ± 29 Bq/m³. The PAEC increased after 18:00 and declined after 20:30. The average PAEC during working hours (7:00 – 18:00) was 37.41 ± 0.84 mWL. Whereas the other time of the day the average PAEC was 55.0 ± 1.1 mWL. The foyer is aerated all the time during working hours, because of the entering patients or employees. After 18:00 the doors are closed and the activity concentration of radon and its daughter products can increase. The decrease after

20:30 can be due to an increase of the atmospheric pressure shown in Figure 54. Figure 26 shows the daily mean activity concentrations of the short-lived daughter products, the equilibrium equivalent radon and estimated radon. The daily mean values of the PAEC are shown in Figure 27.

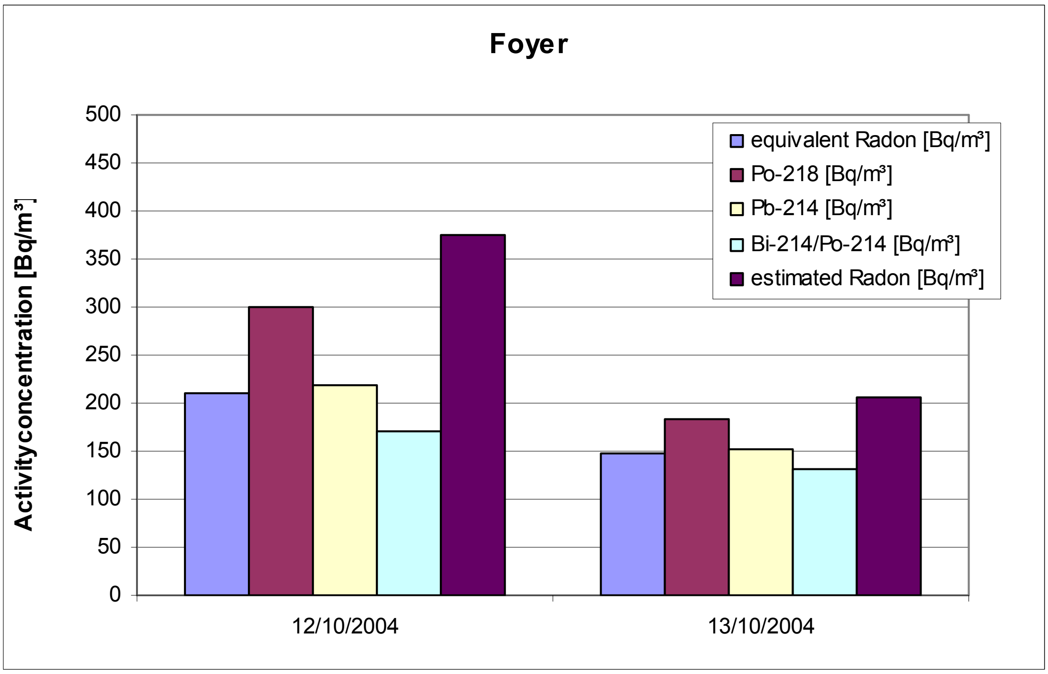

Figure 26: Mean values of the attached short-lived radon daughter products, the equilibrium equivalent radon and the estimated radon.

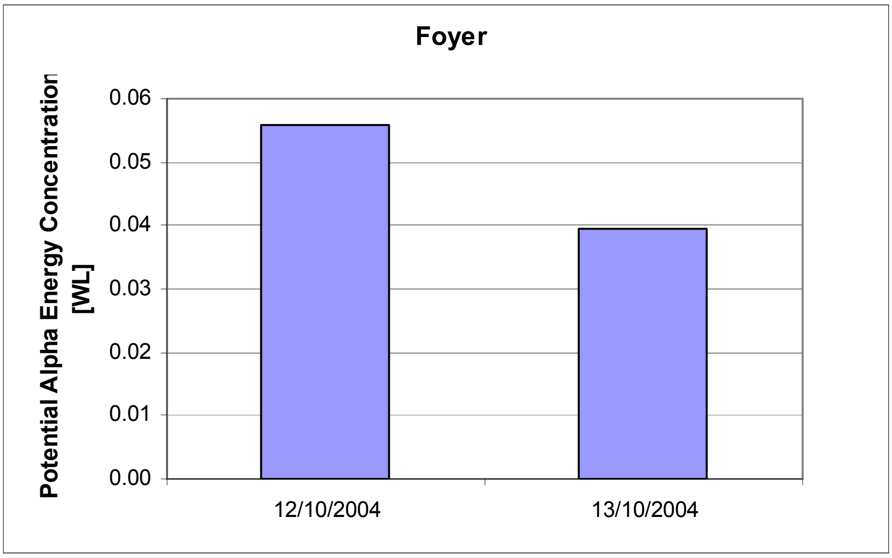

Figure 27: Daily mean values of the PAEC of the attached radionuclides.

3.2.2. Short-lived radon daughters in the gym

3.2.2.1. Attached short-lived radon daughters in the gym

The results of the measurements are detailed in Appendix 2.

Figure 28 shows the activity concentration in Bq/m³ of the short-lived daughter products ^{218}Po, ^{214}Pb and $^{214}Bi/^{214}Po$ and of the equilibrium equivalent radon and estimated radon between 10:00 on 13 October and 9:00 on 14 October. Figure 29 shows the PAEC in WL and J/m³ during this time. Tables 27 to 28 in Appendix 1 summarise the daily results.

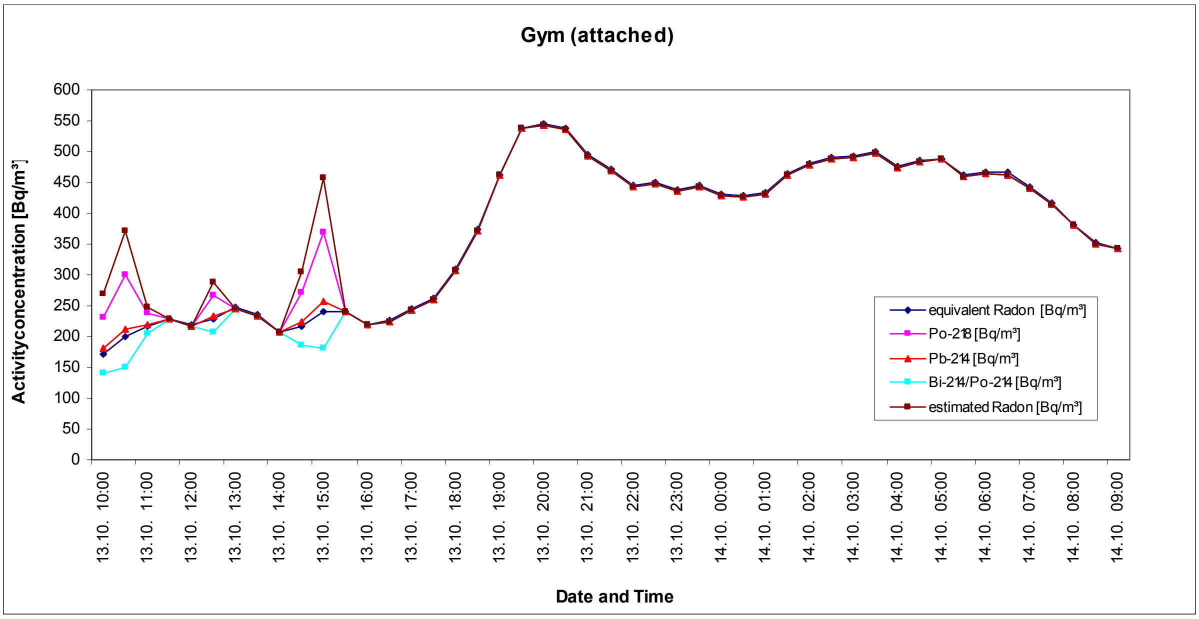

Figure 28: Activity concentrations of the attached short-lived radon daughters, the equilibrium equivalent radon and the estimated radon in the gym in Oct. 2004.

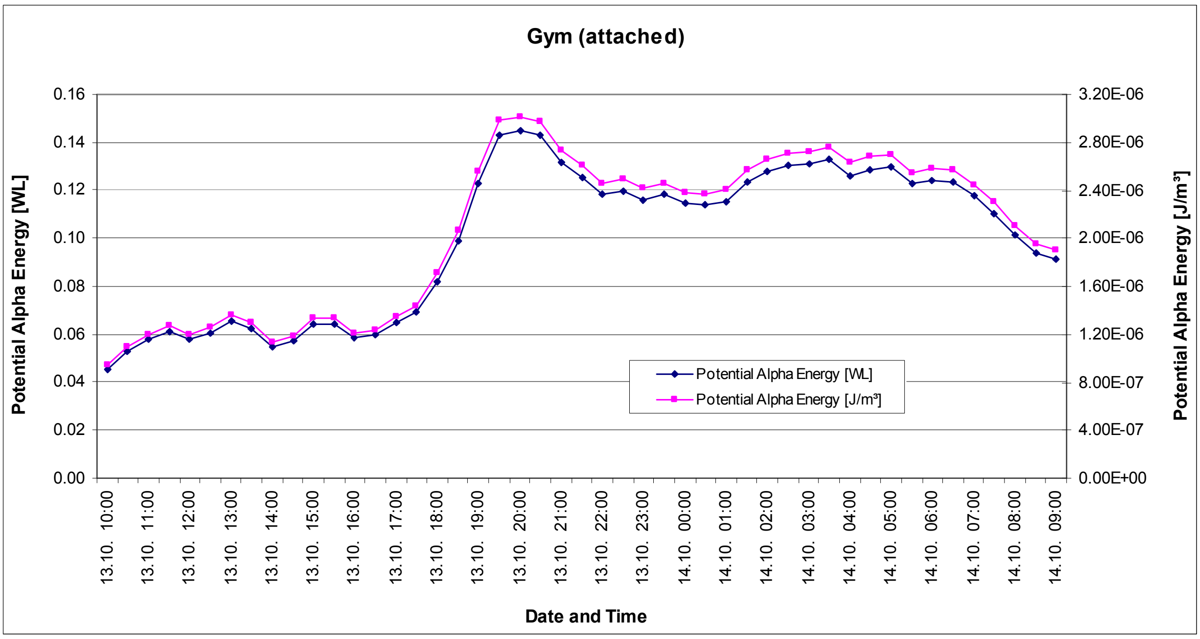

Figure 29: The potential alpha energy concentration of the attached radionuclides in the gym.

The activity concentration of the equilibrium equivalent radon was between 171 ± 26 Bq/m³ and 545 ± 42 Bq/m³. The activity concentrations of Radon and its daughter products increase from 18:00 to 19:00, stay high during the night and decrease at 6:00. The gym was in use during daytime and the windows were frequently opened for aeration. During working hours (assumption 7:00 – 18:00) the average value was 0.071 ± 0.001 WL. The maximum value of the PAEC was measured during night with 0.15 ± 0.01 WL. The average PAEC during night was 0.13 ± 0.02 WL.
Figure 30 shows the daily mean activity concentrations of the short-lived daughter products, the equilibrium equivalent and estimated radon. The daily mean values of the PAEC are shown in Figure 31.

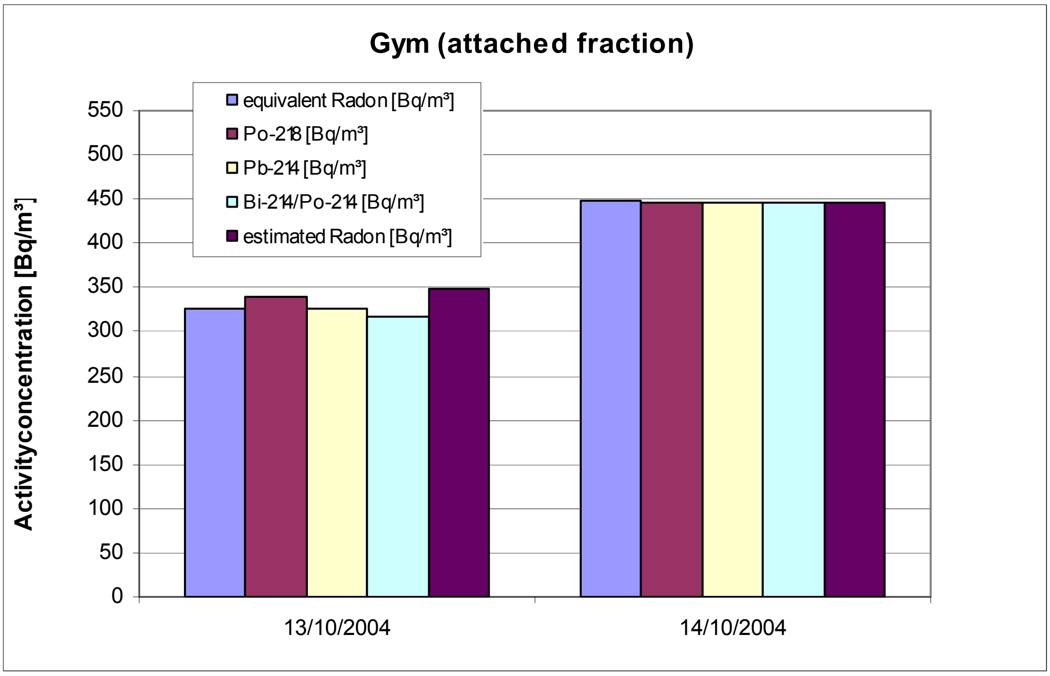

Figure 30: Mean values of the attached short-lived radon daughter products, the equilibrium equivalent radon and the estimated radon.

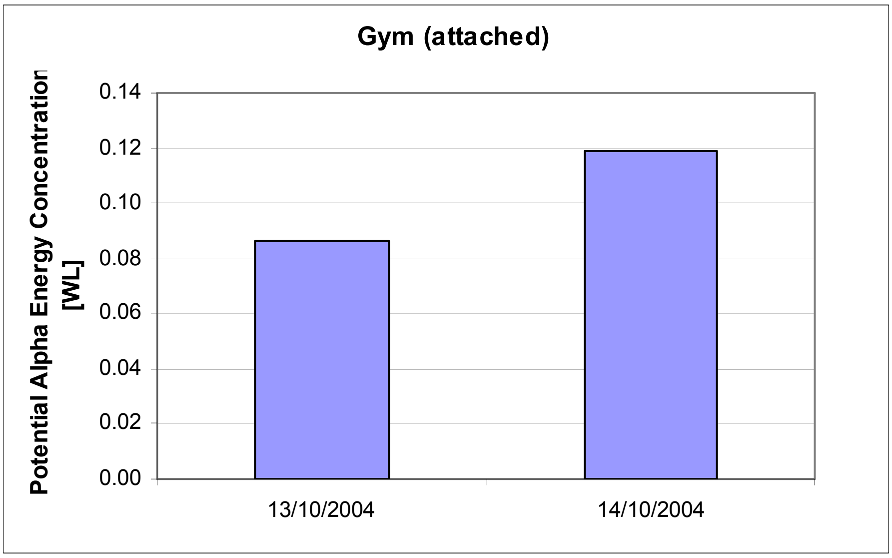

Figure 31: Daily mean values of the PAEC of the attached radionuclides.

3.2.2.2. Unattached short-lived radon daughters in the gym

The measurement results of the portable BWLM-PLUS Free fraction measurement system are detailed in Appendix 2.

Figure 32 shows the activity concentration in Bq/m³ of the unattached short-lived daughter products ^{218}Po, ^{214}Pb and $^{214}Bi/^{214}Po$, the equilibrium equivalent radon and estimated radon between 10:00 on 13 October and 9:00 on 14 October. Figure 33 shows the PAEC in WL and J/m³ during this time. Tables 29 to 30 in Appendix 1 summarise the daily results.

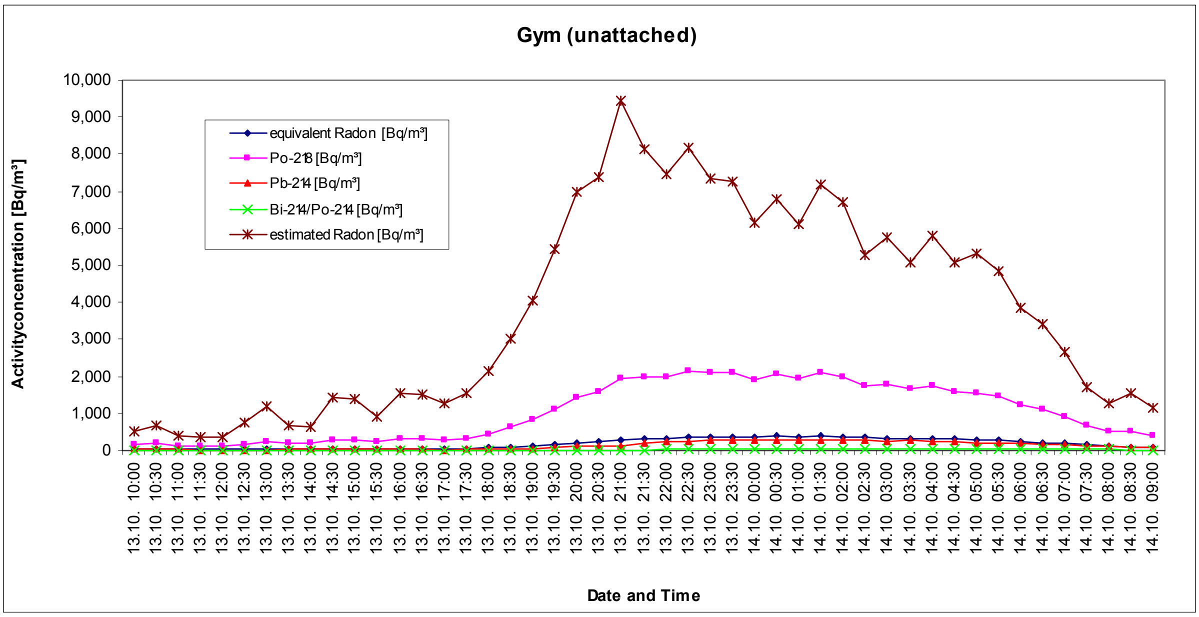

Figure 32: Activity concentrations of the unattached radon daughter products, the equilibrium equivalent radon and the estimated radon in the gym in Oct. 2004

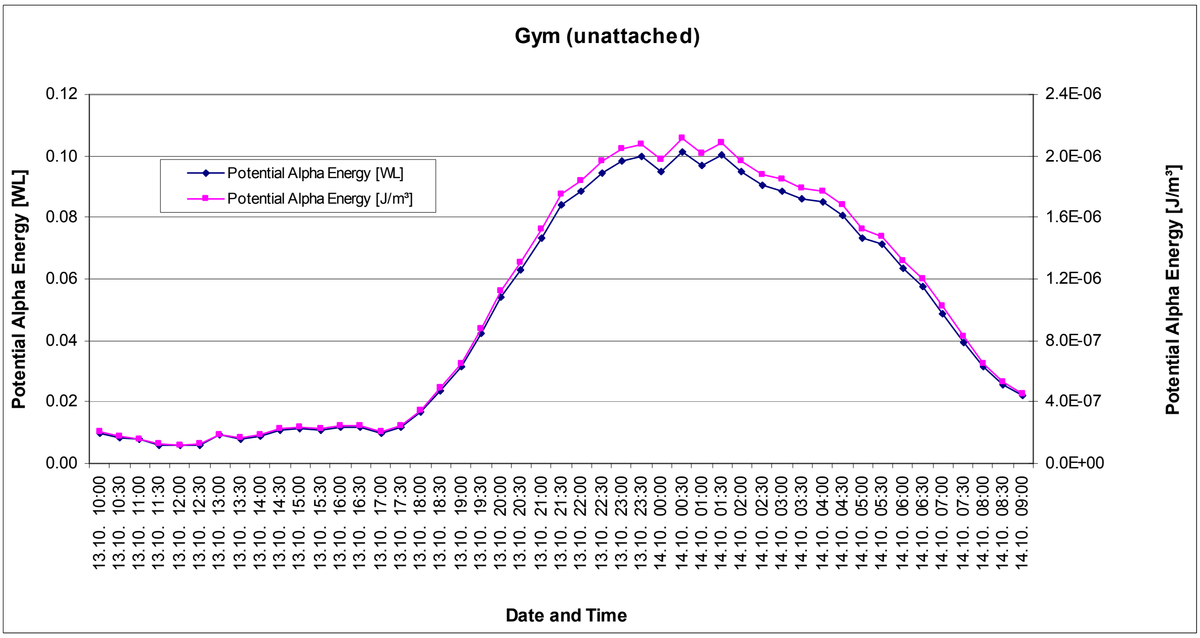

Figure 33: The potential alpha energy concentration of the unattached radionuclides in the gym in October 2004.

During this measuring period the activity concentration of the unattached ^{218}Po exceeded the activity concentration of the attached ^{218}Po. The maximum values for the attached and the unattached ^{218}Po were about 500 Bq/m³ and about 2,200 Bq/m³, respectively. During working hours (assumption 7:00 – 18:00) the average value of the PAEC was 15.1 ± 0.4 mWL. The PAEC reached the maximum value during night with 101.3 ± 7.8 mWL.

Figure 34 shows the daily mean activity concentrations of the unattached short-lived daughter products, the equilibrium equivalent radon and estimated radon. The daily mean values of the PAEC are shown in Figure 35.

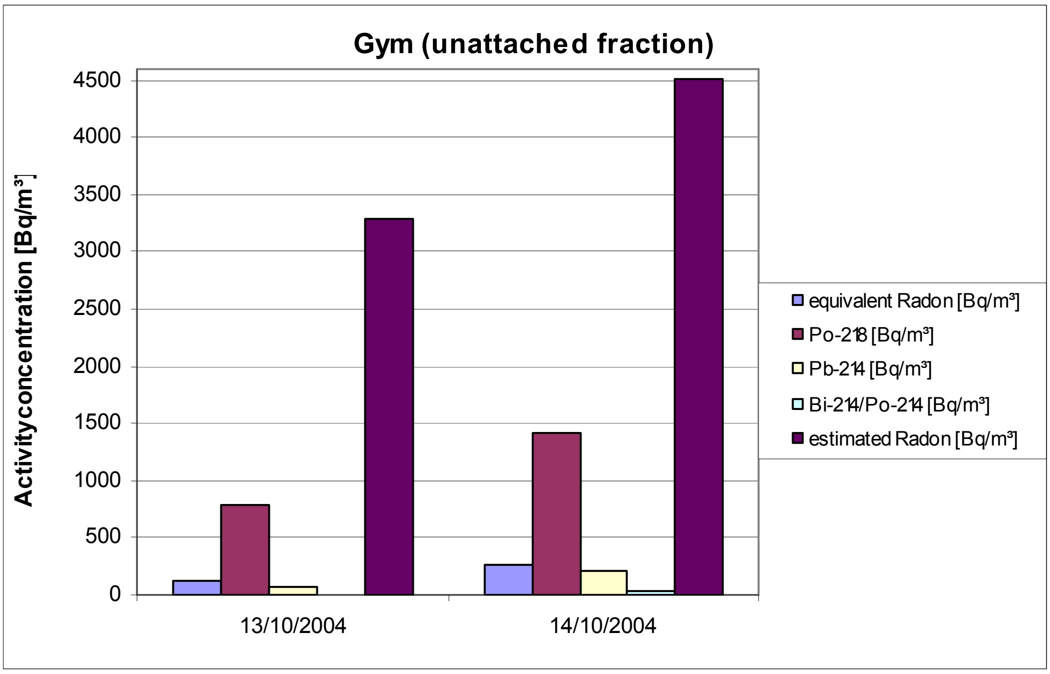

Figure 34: Mean values of the unattached short-lived radon daughter products, the equilibrium equivalent radon and the estimated radon.

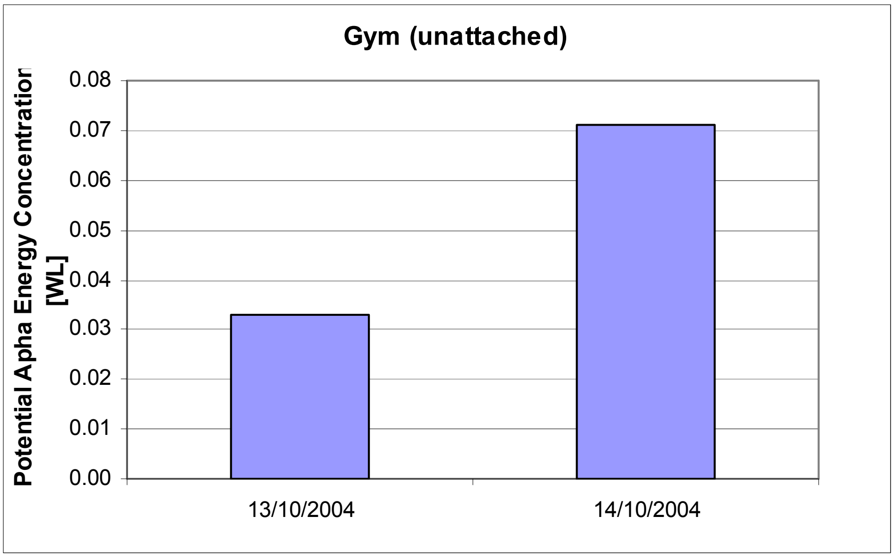

Figure 35: Daily mean values of the PAEC of the unattached radionuclides.

The activity concentrations of the unattached and the attached ^{218}Po, ^{214}Pb and ^{214}Bi/^{214}Po and the unattached fraction of each nuclide are shown in Figures 36 to 38.

Figure 39 shows the calculated equilibrium equivalent Radon activity concentration of the attached and unattached measurements and the unattached fraction.

Tables 31 to 32 in Appendix 1 summarise the daily results.

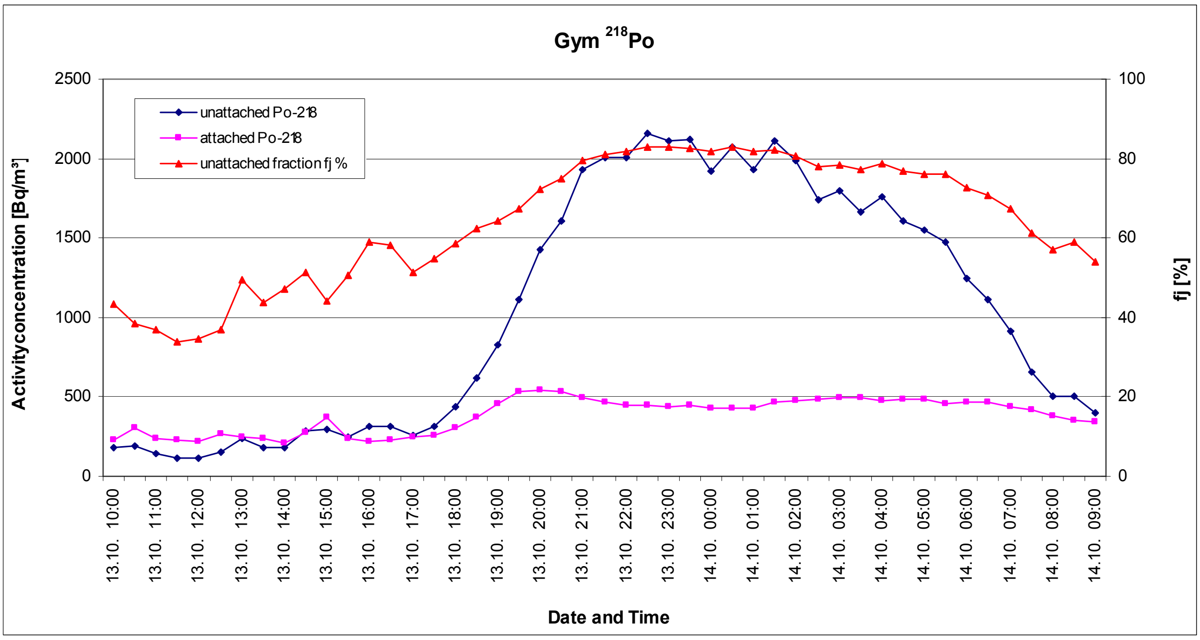

Figure 36: The activity concentrations of the attached and the unattached ^{218}Po and the fraction of the unattached ^{218}Po to the total ^{218}Po

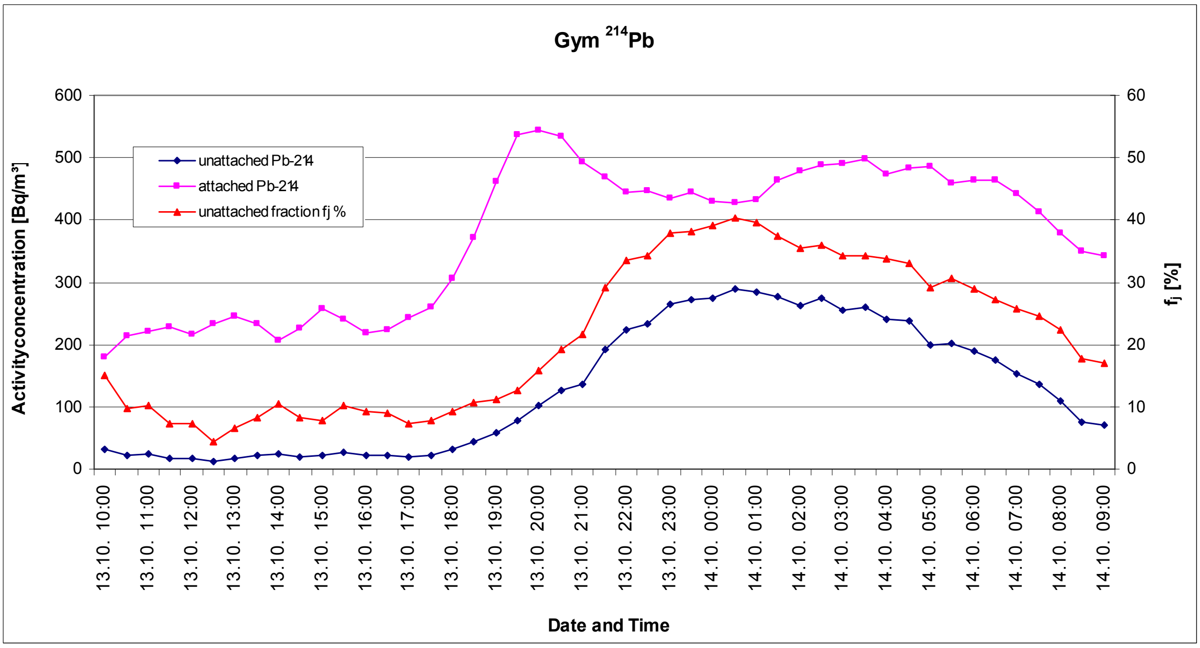

Figure 37: The activity concentrations of the attached and the unattached ^{214}Pb and the fraction of the unattached ^{214}Pb to the total ^{214}Pb.

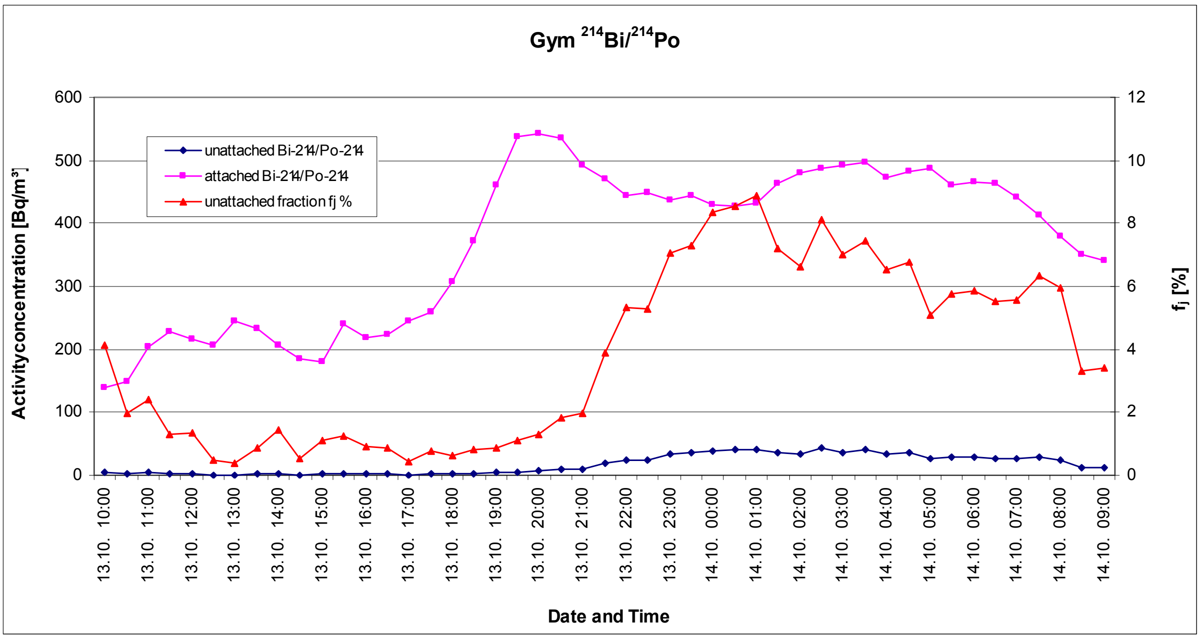

Figure 38: The activity concentrations of the attached and the unattached ^{214}Bi/^{214}Po and the fraction of the unattached ^{214}Bi/^{214}Po to the total ^{214}Bi/^{214}Po.

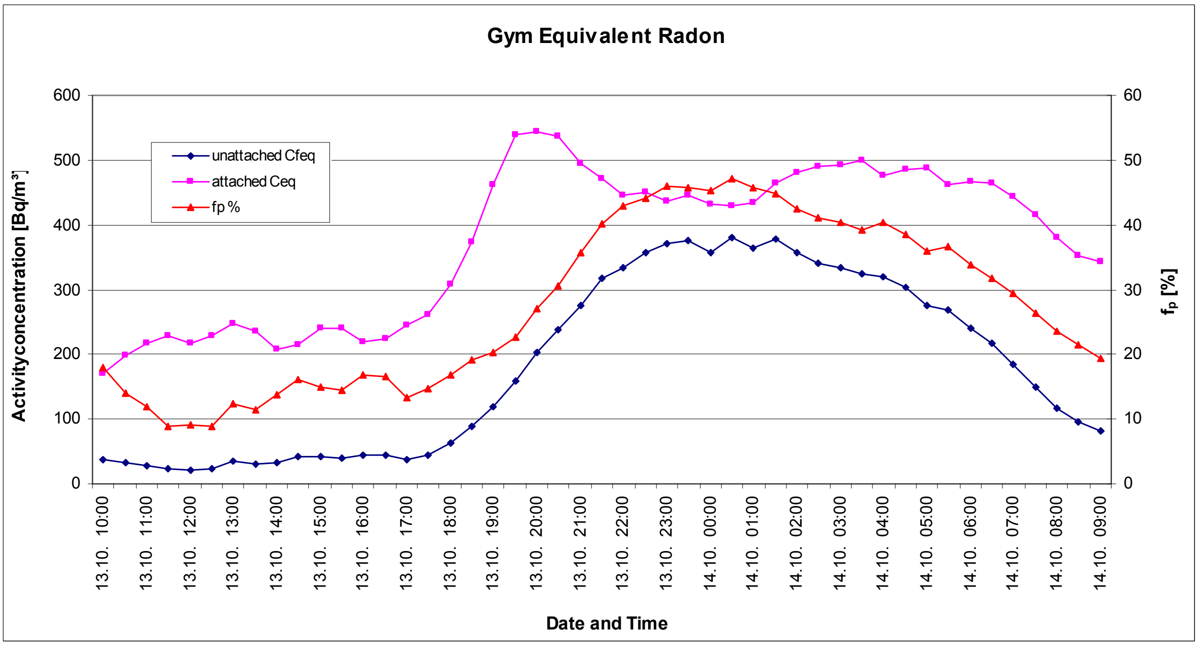

Figure 39: The activity concentrations of the attached and the unattached equilibrium equivalent radon and the unattached fraction.

Figure 40 shows the daily mean values of the unattached fraction and the fraction of the unattached radionuclides of the short-lived daughter products.

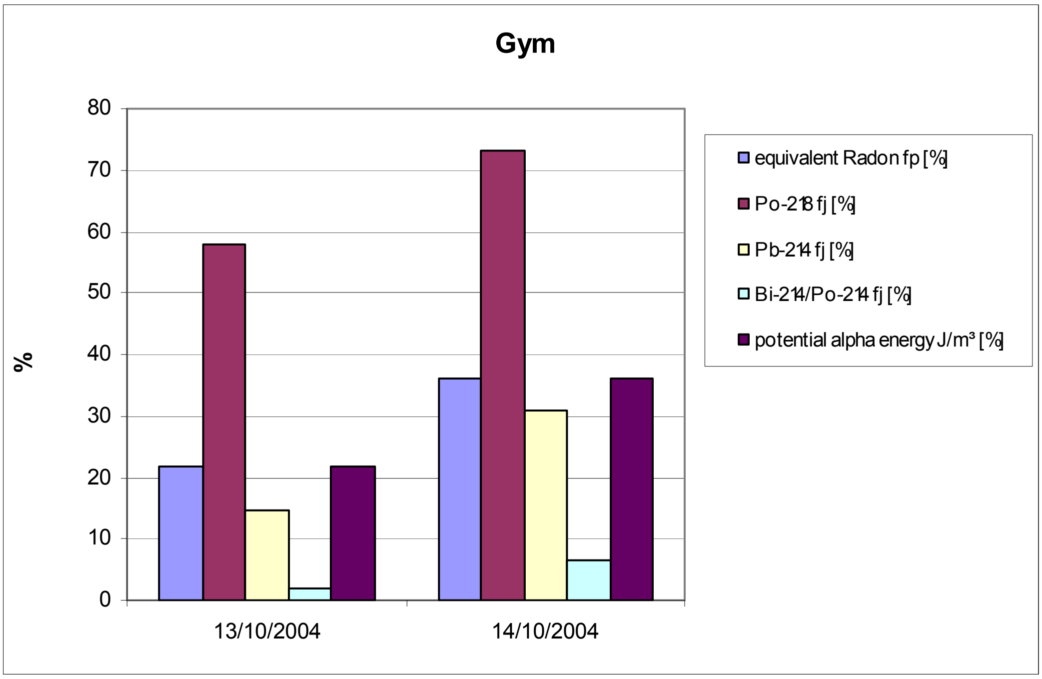

Figure 40: Mean values of the unattached fraction and the fraction of each unattached daughter product and the contribution of the unattached radionuclides to the total PAEC.

The highest contribution to the unattached fraction results from ^{218}Po and the lowest contribution results from ^{214}Bi, like in the radon gallery. During the entire measurement period the mean contribution to the unattached fraction from ^{218}Po was 62% (maximum 74%, minimum 45%) and from ^{214}Bi it was just 3.4% (maximum 7.7%, minimum 0.9%). The contribution from ^{214}Pb was 35% (maximum 48%, minimum 25%). The contribution from ^{214}Po can be neglected. Figure 28 of the gym clearly shows the increase of the equilibrium equivalent radon activity concentration which is 265.7 ± 5.0 Bq/m³ during working time to 470.8 ± 7.3 Bq/m³ in the night. The equilibrium equivalent radon concentration raises about a factor of 1.8. The increase of the unattached fraction is significantly higher. The equilibrium equivalent radon concentration of the unattached fraction raises about a factor of 3.5 from 56.9 ± 1.5 Bq/m³ to 199.4 ± 4.8 Bq/m³. The gym was used during measurements and ventilated during day but not during night. These results show that the equilibrium equivalent radon concentration and therefore the PAEC can be reduced by ventilation.

3.2.3. Short-lived radon daughters in the doctor's office 5

3.2.3.1. Attached short-lived radon daughters in the doctor's office 5

The results of the measurements are detailed in Appendix 2.

Figure 41 shows the activity concentration in Bq/m³ of the attached short-lived daughter products ^{218}Po, ^{214}Pb and $^{214}Bi/^{214}Po$, the equilibrium equivalent radon and estimated radon between 10:30 on 14 October and 15:00 on 16 October. Figure 42 shows the PAEC in WL and J/m³ during this time period. Tables 33 to 35 in Appendix 1 summarise the daily results.

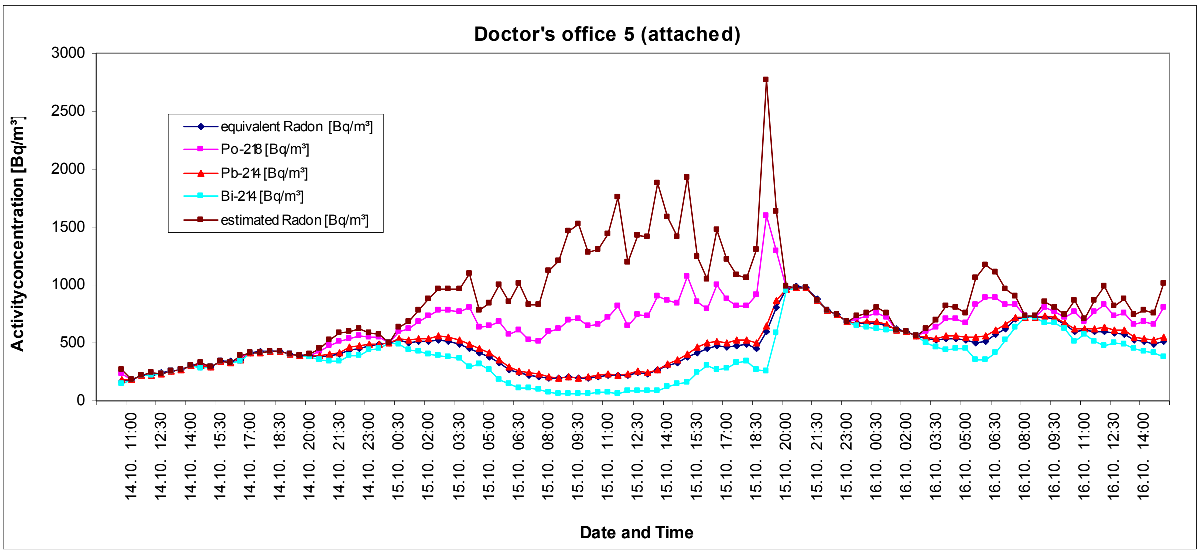

Figure 41: Activity concentrations of the attached radon daughters, the equilibrium equivalent radon and the estimated radon in the doctor's office 5 in October 2004

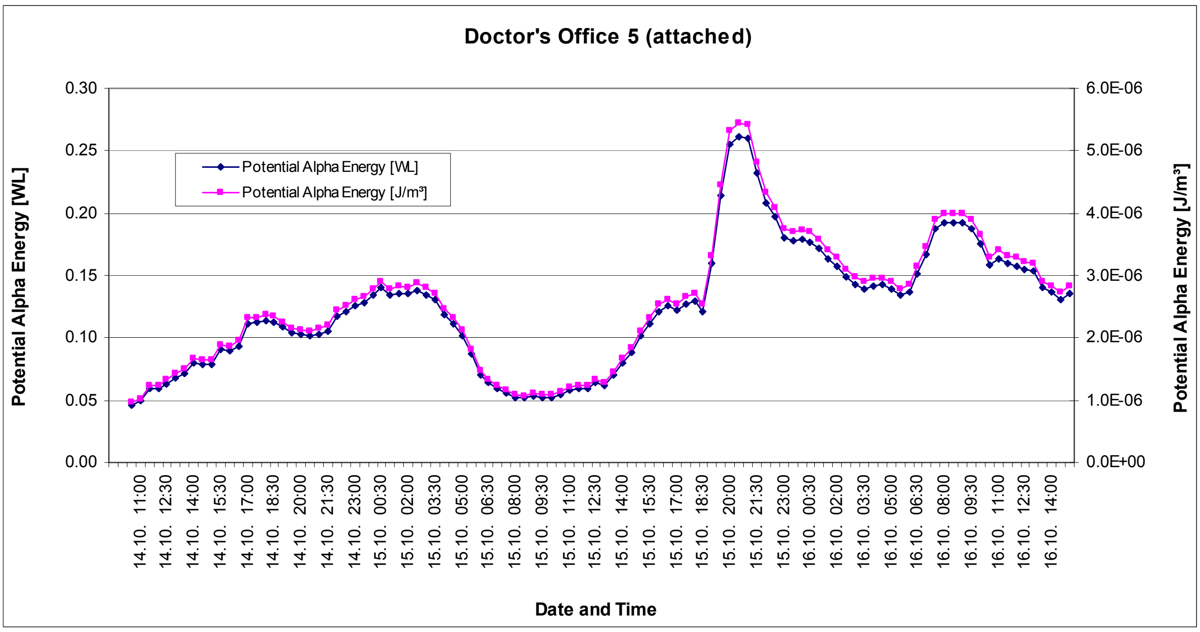

Figure 42: The potential alpha energy concentration of the attached radionuclides in the doctor's office 5 in October 2004. This room was not in use during measurements.

Doctor's office 5 was not in use during the measurements and its windows as well as the door were closed.

Figure 43 shows the daily mean activity concentrations of the short-lived daughter products, the equilibrium equivalent radon and estimated radon. The daily mean values of the PAEC are shown in figure 44.

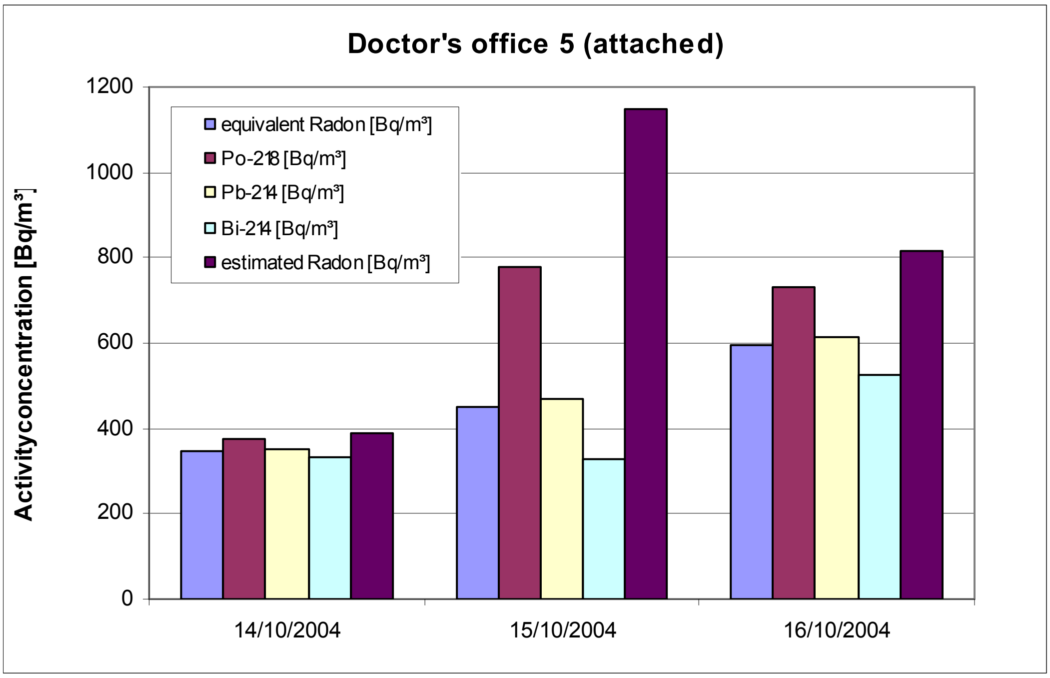

Figure 43: Mean values of the attached short lived radon daughter products, the equilibrium equivalent radon and the estimated radon.

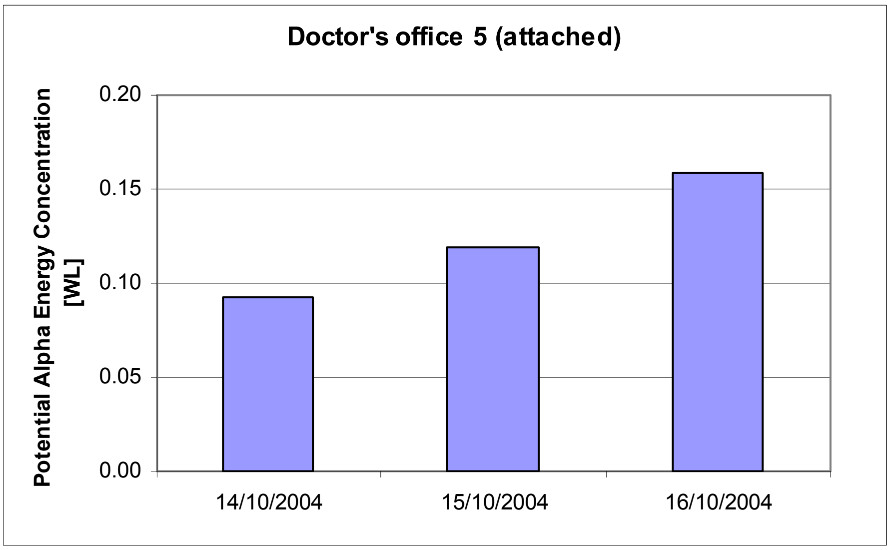

Figure 44: Daily mean values of the PAEC of the attached radionuclides.

3.2.3.2. Unattached short-lived radon daughters in the doctor’s office 5

The results of the measurements are detailed in Appendix 2.

Figure 45 shows the activity concentration in Bq/m³ of the unattached short-lived daughter products ^{218}Po, ^{214}Pb and $^{214}Bi/^{214}Po$, the equilibrium equivalent radon and estimated radon between 10:30 on 14 October and 15:00 on 16 October. Figure 46 shows the PAEC of the unattached radionuclides in WL and J/m³ during this time period. Tables 36 to 38 in Appendix 1 summarise the daily results.

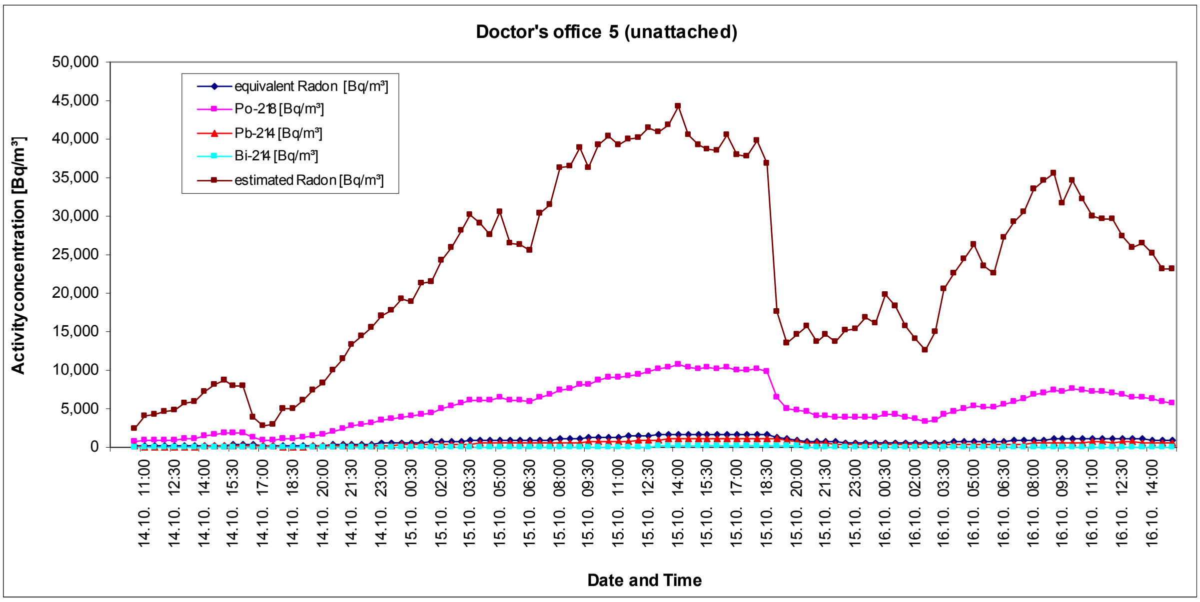

Figure 45: The activity concentrations of the unattached radon daughters, the equilibrium equivalent radon and the estimated radon in the doctor's office 5 in October 2004.

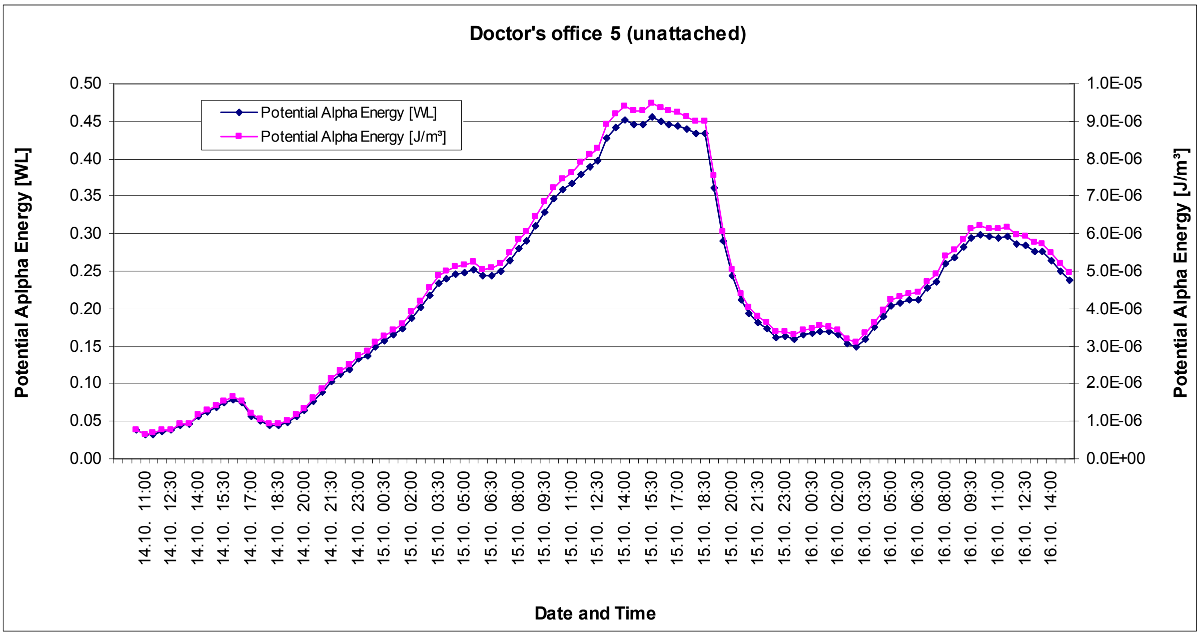

Figure 46: The potential alpha energy concentration in the doctor's office 5 in October 2004.

Figure 47 shows the daily mean activity concentrations of the short-lived daughter products, the equilibrium equivalent radon and estimated radon. The daily mean values of the PAEC are shown in figure 48.

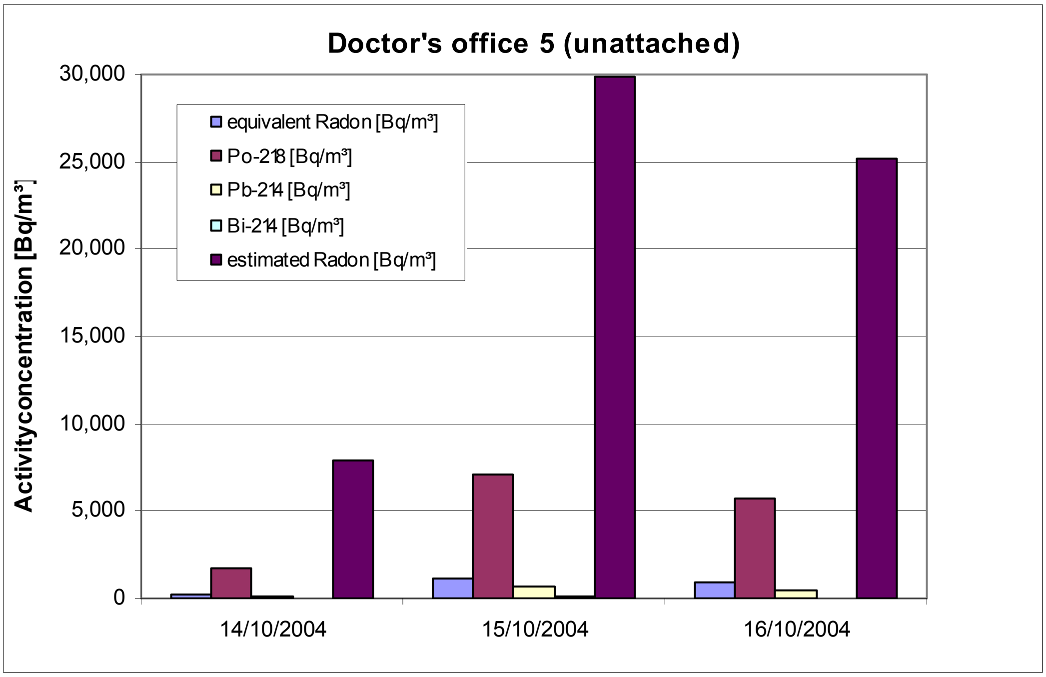

Figure 47: Mean values of the unattached short lived radon daughter products, the equilibrium equivalent radon and the estimated radon.

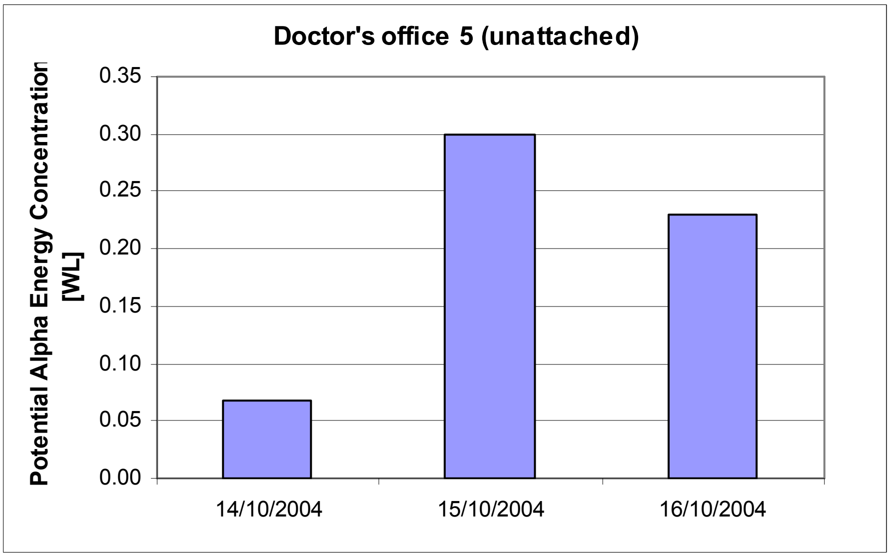

Figure 48: Daily mean values of the PAEC of the unattached radionuclides.

The activity concentration of the unattached and the attached ^{218}Po, ^{214}Pb and ^{214}Bi/^{214}Po and the unattached fraction of each nuclide are shown in Figures 49 to 51. Figure 52 shows the calculated equilibrium equivalent Radon activity concentration of the attached and unattached measurements. Tables 39 to 41 in Appendix 1 summarise the daily results.

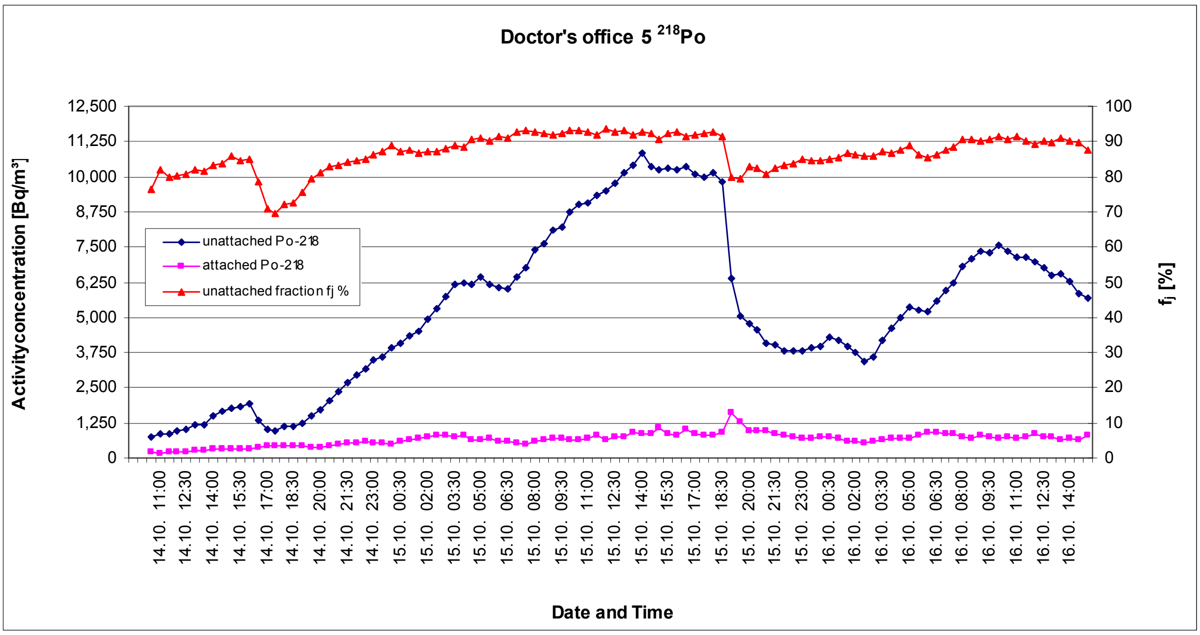

Figure 49: The activity concentrations of the attached and unattached ^{218}Po and the fraction of the unattached ^{218}Po to the total ^{218}Po in the doctor's office 5 in October 2004.

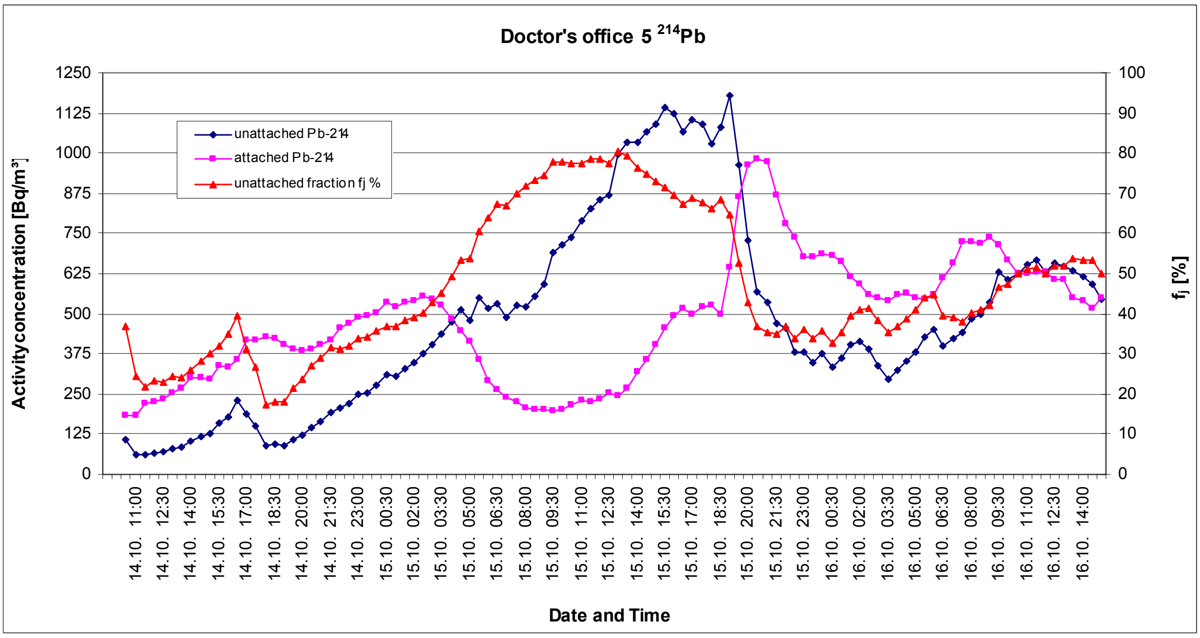

Figure 50: The activity concentrations of the attached and the unattached ^{214}Pb and the fraction of the unattached ^{214}Pb to the total ^{214}Pb in the doctor's office 5 in October 2004.

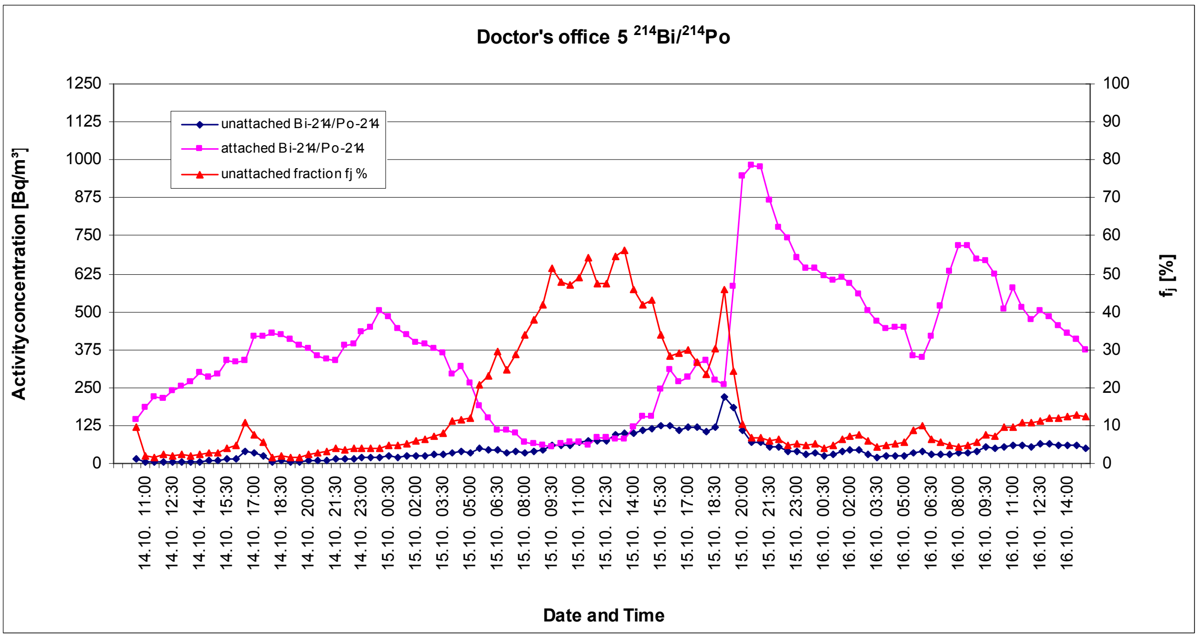

Figure 51: The activity concentrations of the attached and unattached $^{214}Bi/^{214}Po$ and the fraction of the unattached $^{214}Bi/^{214}Po$ to the total $^{214}Bi/^{214}Po$ in the doctor's office 5 in October 2004.

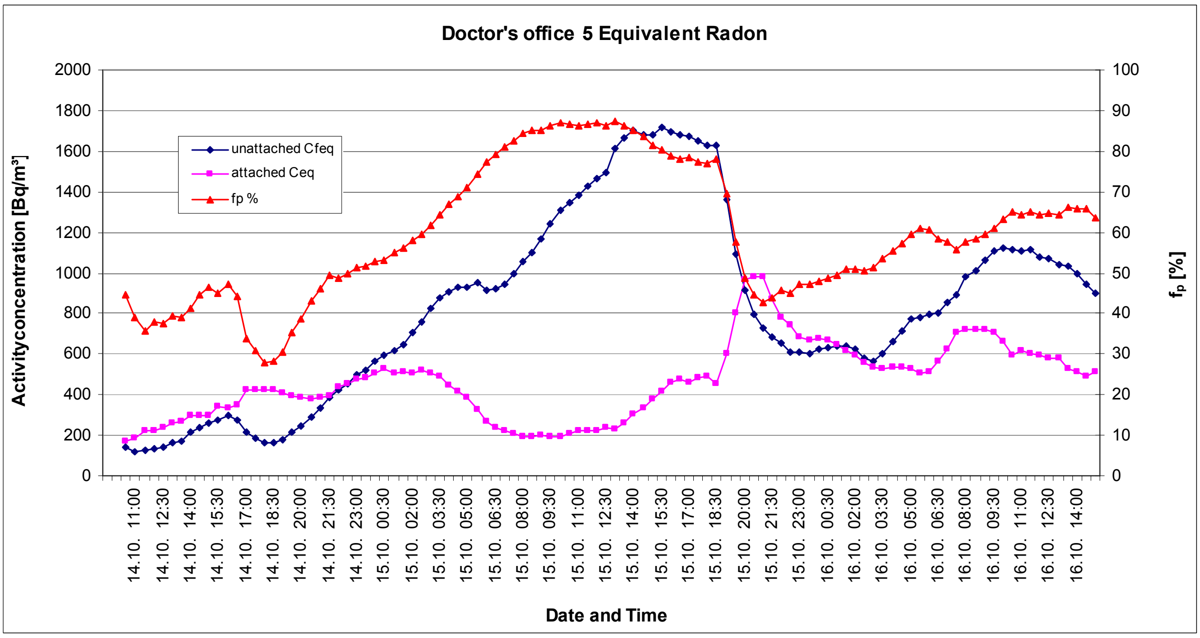

Figure 52: The activity concentrations of the attached and unattached equilibrium equivalent radon and the unattched fraction in the doctor's office 5 in October 2004.

Figure 53 shows the daily mean values of the unattached fraction and the fraction of the unattached radionuclides of the short-lived daughter products.

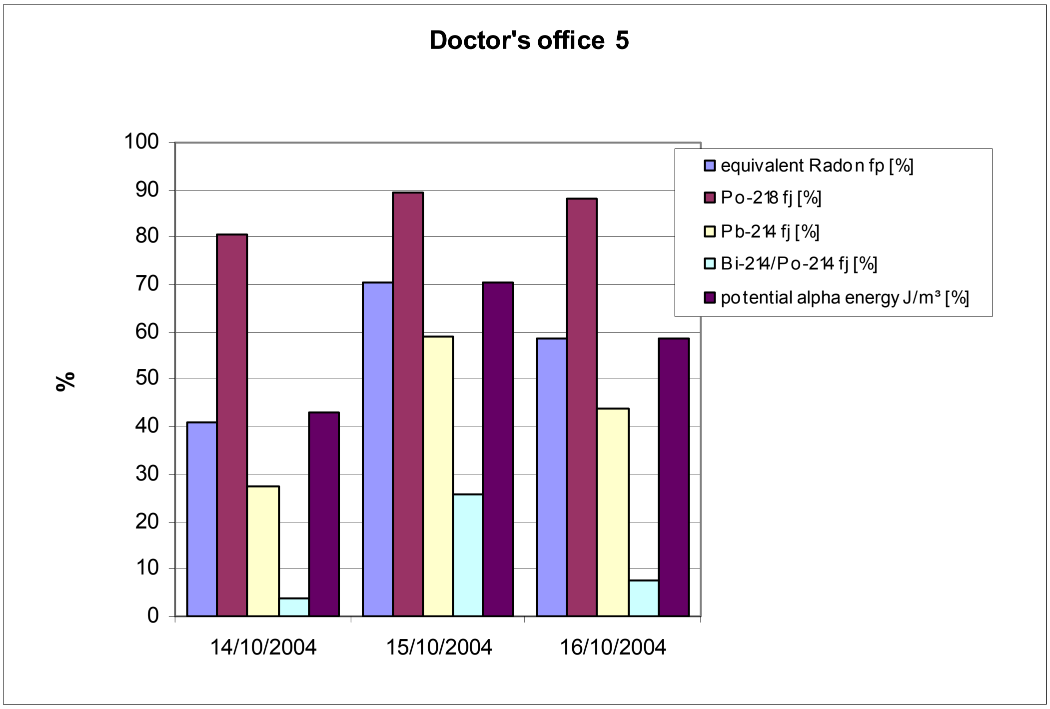

Figure 53: Mean values of the unattached fraction and the fraction of each unattached daughter product and the contribution of the unattached radionuclides to the total PAEC.

In the Doctor's office the highest unattached fraction with a mean value of 70.5 % was measured on the 15.10.2004. The highest contribution to the unattached fraction results from ^{218}Po and the lowest contribution results from ^{214}Bi and ^{214}Po like in the radon gallery and the gym. During the entire measurement period the mean contribution to the unattached fraction from ^{218}Po was 68% (maximum 78%, minimum 43%) and from ^{214}Bi just 2.1% (maximum 6.4%, minimum 1.2%). The contribution from ^{214}Pb was 30% (maximum 45%, minimum 25%). The contribution from ^{214}Po can be neglected.

Doctor's office 5 was not in use during the measurements and its windows as well as the door were closed. From 7:00 to 18:00, the equilibrium equivalent radon concentration was about 391.6 ± 4.4 Bq/m³ and the PAEC was 0.105 ± 0.001 WL. The rest of the time, the equilibrium equivalent radon concentration was 543.3 ± 1.6 Bq/m³ and the PAEC was 0.144 ± 0.002 WL. No airing occurred during the measurements but some variations during that time along with a slight increase of the equivalent equilibrium radon concentration could be observed from the beginning of the measurements to the end on the 16 October (Figure 41). Figure 45 clearly shows that the unattached radionuclides increased. With a mean value of 253.2 ± 4.2 Bq/m³, the equilibrium equivalent radon concentration increased from 14 October to a mean

value of 1,128 ± 12 Bq/m³ on 15 October. The next day, the mean value of the equilibrium equivalent radon declined to 866 ± 11 Bq/m³.
Doctor's office 5 showed the highest equilibrium equivalent radon concentrations of all three selected rooms (foyer, gym, doctor's office 5). On the one hand this can be explained by the low ventilation. Other publications such as that from Pereira et. al. showed higher concentrations in bedrooms and dining rooms compared to halls and work areas due to low ventilation and air change conditions [26].
On the other hand this can be explained by the decrease of the atmospheric pressure between 12 October and 16 October. The mean value of atmospheric pressure for the measurements in the foyer was 912 hPa, for the measurements in the gym 907 hPa and 897 hPa for the measurements in doctor's office 5. Figure 54 shows the atmospheric pressure and the PAEC in the foyer, the gym and the doctor's office. An increase of the PAEC in correlation with the decrease of the atmospheric pressure can be observed.

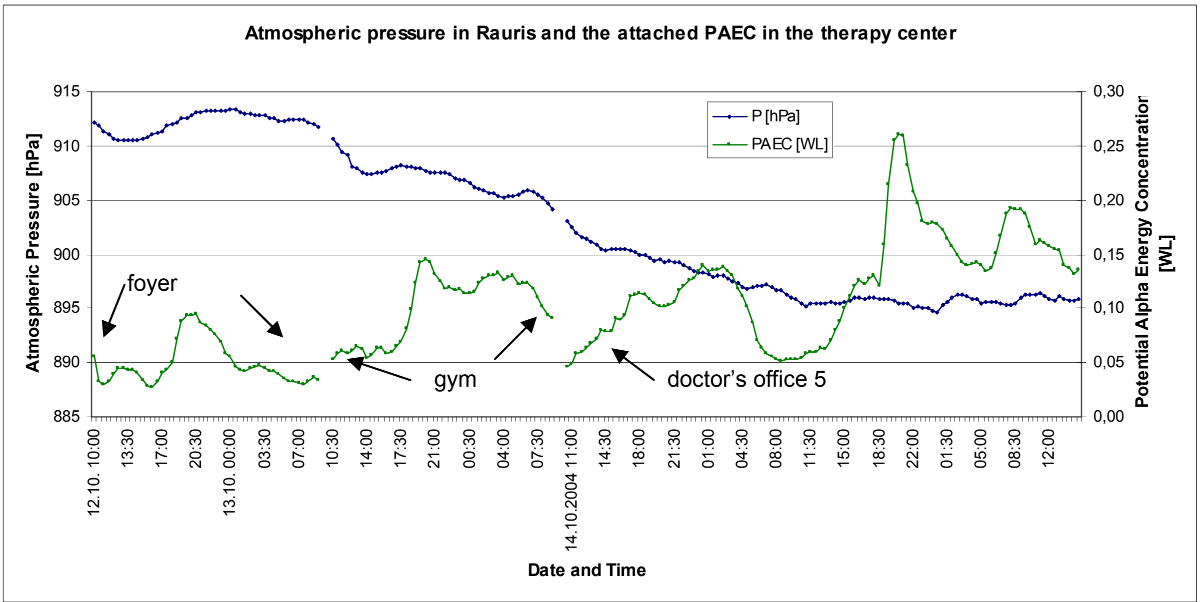

Fig: 54: The atmospheric pressure measured in Rauris and the PAEC measured in the therapy centre building.

The activity concentration of the equilibrium equivalent radon from the attached radionuclides in the foyer was 184.5 ± 2.6 Bq/m³. In the gym, measurements of the attached fraction showed an equilibrium equivalent radon of 374.8 ± 4.5 Bq/m³ and 182.0 ± 2.6 Bq/m³ for the measurements of the unattached fraction. Due to the low ventilation in the doctor's office 5, the activity concentration of the equilibrium equivalent radon from the measurements of the attached fraction was 466.0 ±

3.7 Bq/m³ and 828.7 ± 6.4 Bq/m³ when measuring the unattached fraction. The equilibrium equivalent radon concentration of the gym was lower than in the doctor's office 5, but higher than in the foyer, even though the gym is located in the second floor, whereas the other two selected rooms are on the ground floor. This shows that the equilibrium equivalent radon concentration has a higher dependence on the atmospheric pressure than on the location in the house.
The estimated activity concentration of radon in the foyer was 300 Bq/m³. In the gym, the estimated activity concentration was 390 Bq/m³ measuring the attached fraction and 3,800 Bq/m³ from the measurements of the unattached fraction. Due to low ventilation in the doctor's office 5, the estimated activity concentration in air was 840 Bq/m³ measuring the attached fraction and 22,500 Bq/m³ from the measurements of the unattached fraction.
Unfortunately, no direct measurements of the radon activity concentration in the air have been conducted. The estimation of the high activity concentration of radon in air was due to the high unattached fraction and especially the high unattached ^{218}Po activity concentration.
Measurements of radon and the short-lived decay products in more than 215 dwellings in West Germany were reported in literature [27]. The PAEC ranged from 0.3 to 29.1 mWL with a median value of 1.8 mWL. Compared with these values, the PAEC measured in the therapy centre (foyer 49 ± 0.7 mWL, the gym unattached and attached 148 ± 1 mWL, the doctor's office 5 unattached and attached 343 ± 2 mWL) are about twice as high to ten times higher than the maximum value of 29.1 mWL from West Germany. This is in agreement with the "Radon in dwellings" map of Germany [28], in which most values are below 60 Bq/m³ and the "Radon Potential" map of Austria created during the Austrian Radon Project, in which the radon potential is higher than 400 Bq/m³ in the municipality of Bad Gastein [29]. The radon potential is the annual mean radon concentration in a standard situation (living room on the ground floor of a single family house).

3.3. Influence of the aerosol particle concentration

Porstendörfer showed that the influence of ventilation on the unattached fraction f_p and the equilibrium factor F is negligible. Whereas the plate-out of the unattached fraction, the attachment rate and the aerosol particle concentration have a big

influence on the equilibrium factor F and the unattached fraction f_p [30]. The aerosol particle concentration indoors depends mainly on the particle concentration outdoors, the ventilation rate and the number of particle sources indoors. In doctor's office 5, there were no particle sources indoors and the windows were closed which provided only very low aeration. It is therefore possible that the particle concentration is very low which would explain the high unattached fraction. According to Porstendörfer poorly ventilated rooms (v=0.3 /h) have low particle concentrations [19].
As a consequence, radon exposure can be reduced by ventilation on the one hand, because of the mixing of the outdoor air, which usually has lower radon and radon daughter concentrations, with the air of the room. On the other hand, a reduction can be reached through increasing the particle concentration, which can be elevated in outdoor air if there are no other aerosol sources in the room. An increase of the particle concentration reduces the unattached fraction. When the unattached fraction decreases the effective dose also decreases. Further explanation will be given in the section "3.4. Calculation of the Effective Dose".
After the measurement period in October 2004, the aerosol particle concentration in the radon gallery was determined by weighing the aluminium foils of the cascade impactor. Assuming a density of 1.55 g/cm³ [31] and with the average aerosol diameter the aerosol particle concentration can be calculated. The values of 12 October, 13 October and 14 October are shown in Table 42.

Aerosol Diameter	12.10.2004		13.10.2004		14.10.2004	
µm	µg/m³	n/cm³	µg/m³	n/cm³	µg/m³	n/cm³
0.05 -0.12	10.2	18,506	3.8	6,980	2.6	4,821
0.12 – 0.25	12.2	3,071	6.7	1,681	4.1	1,029
0.25 – 0.5	5.8	167	3.4	97	2.0	58
0.5 – 1 µm	2.9	9.9	1.8	6.3	1.2	4.2
1 – 2 µm	5.5	2.5	4.2	1.9	2.1	0.95
2 – 4 µm	5.6	0.31	2.2	0.12	1.5	0.084
4 – 8	3.0	0.021	2.6	0.018	1.4	0.010
8 – 16	1.0	0.00094	2.5	0.0023	1.5	0.0014
Total Aerosol Concentration	46.3	21,757	27.2	8,766	16.6	5,913

Table 42: Aerosol particle concentration collected on the stages of the cascade impactor in the radon gallery.

The average aerosol particle concentration during these days was 12,145 cm^{-3} . According to Porstendörfer et al. the unattached fraction can be calculated with the following equation [32].

$$f_p = \frac{414}{Z} \qquad \text{Equation 11}$$

Z = aerosol particle concentration [n/cm³]

The unattached fraction calculated with the average aerosol concentration during the measurement period in October is 3.4 %. This corresponds to the values measured in the gallery in January, which give a mean value for the unattached fraction of 3.6 % during the whole measuring period. In numerous publications Porstendörfer et al showed that the unattached fraction is a function of the aerosol particle concentration as is the equilibrium factor F. The unattached fraction decreases with increasing aerosol particle concentration whereas the equilibrium factor increases with increasing aerosol particle concentration.

Another factor which has a big influence on the unattached fraction and the equilibrium factor is the attachment rate. The attachment rate expresses the attachment velocity. The attachment rate can be calculated by two equations

$$\overline{X} = \overline{\beta} \cdot \overline{Z}$$

$$\overline{Z} = particle\ concentration\ [cm^{-3}] \qquad \text{Equation 12}$$

$$\overline{\beta} = attachment\ coefficient\ [cm^3 / h]$$

For the calculation of the attachment rate, an average attachment coefficient of 5.2 x 10^{-3} cm³/h can be assumed [33].

The attachment rate calculated with this value and the average aerosol particle concentration of 12,145 cm^{-3} during these days is 63/h.

The attachment rate can also be calculated by assuming “steady state” conditions and the measured unattached and attached ^{218}Po activity concentrations.

$$X = \frac{C_1}{C_1^f} \cdot \lambda_1$$

$$\lambda_1 = decay\ constant\ of\ the\ {}^{218}Po = 0.00379 / \sec \qquad \text{Equation 13}$$

$$C_1 = activity\ concentration\ of\ the\ attached\ {}^{218}Po\ [Bq / cm^3]$$

$$C_1^f = activity\ concentration\ of\ the\ unattached\ {}^{218}Po\ [Bq / cm^3]$$

With this equation, the attachment rate was calculated from each point of measurement and from this values the average attachment rate is 64/h.

These values, calculated from two different independent measurements, show excellent agreement as well as agreement with the correlations from the room model from Porstendörfer [19,32,33].

This attachment rate is relatively high compared to the attachment rates of rooms with low ventilation and without additional aerosol sources which is between 20/h and 50/h.

The next figures show the equilibrium factor F and the unattached fraction f_p of the radon gallery (Figure 55), the gym (Figure 56) and the doctor's office 5 (Figure 57). The equilibrium factor F was calculated applying equation 3.

$$F = \frac{C_{eq}}{C_0} \qquad \text{Equation 3}$$

F = equilibrium factor

C_{eq} = equilibrium equivalent activity concentration of ^{222}Rn in air [Bq/m³]

C_0 = activity concentration of ^{222}Rn in air [Bq/m³]

The activity concentration of radon in air was not measured directly. It was only estimated with the LCD-BWLM-PLUS, which measures the attached radionuclides, and with the BWLM-PLUS Free Fraction Measurement System, which measures the unattached radionuclides. For this reason, the equilibrium factor can also only be estimated.

For the Figures 55 to 57 the estimated radon activity concentration in air for the unattached and the attached measurements were summed up. Additionally, the equilibrium equivalent radon activity concentration for the unattached and the attached measurements were summed up. From these values, the equilibrium factor was calculated.

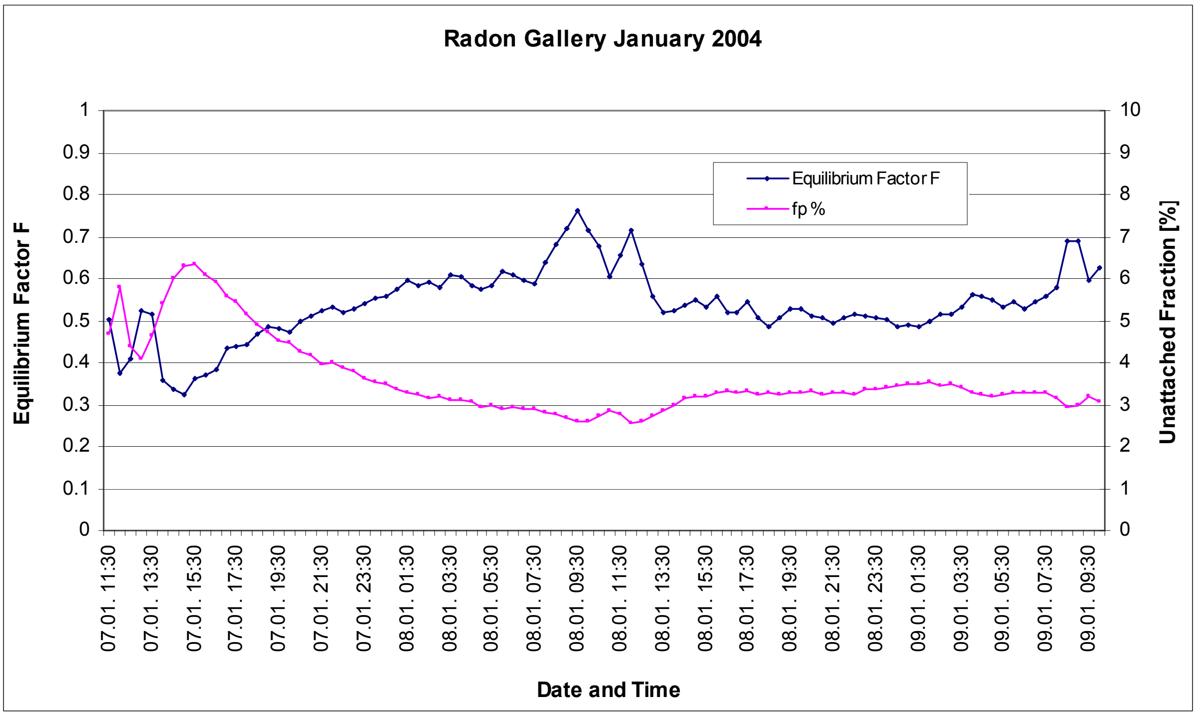

Figure 55: Typical variations of the unattached fraction and the equilibrium factor with time in the radon gallery.

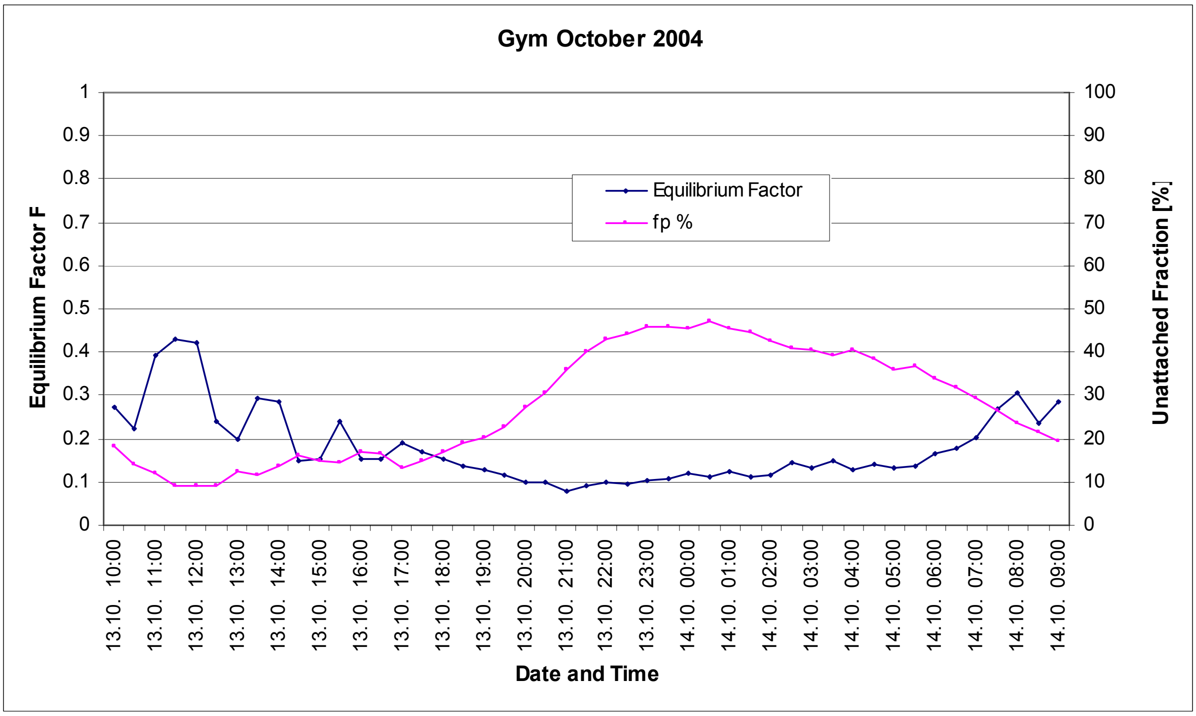

Figure 56: Variation of the unattached fraction and the equilibrium factor with time in the gym.

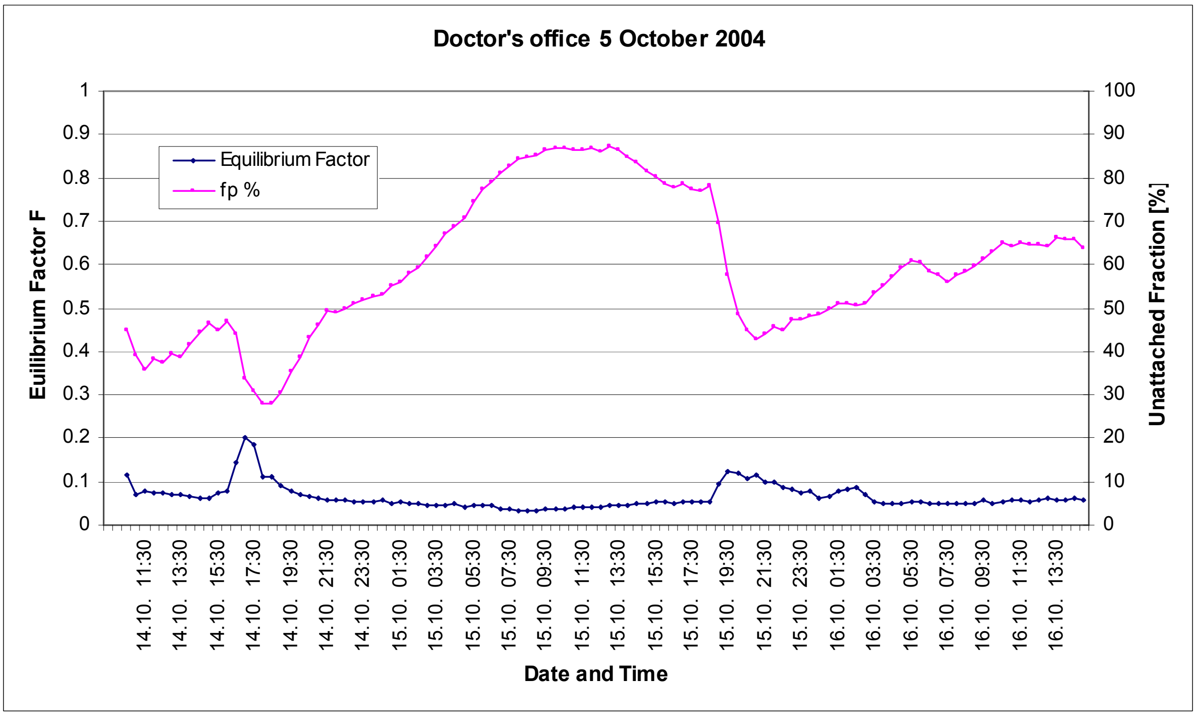

Figure 57: Variation of the unattached fraction and the equilibrium factor with time in the doctor's office.

As many other publications have shown [34], the unattached fraction and the equilibrium factor change with the aerosol concentration. If the unattached fraction increases, the equilibrium factor decreases, if the equilibrium factor increases, the unattached fraction decreases.

Table 43 shows the mean values of the measured unattached fraction and the calculated equilibrium factor at the three sampling sites. Additionally, the Table 43 shows the measured aerosol concentration in the radon gallery and the calculated aerosol concentration (equation 10) in the gym and the doctor's office.

	unattached fraction	equilibrium factor	aerosol concentration
radon gallery	3.6%	0.54	12,145
gym	27%	0.18	1,963
doctor's office	60%	0.07	751

Table 43. Mean values of the measured unattached fraction, the calculated equilibrium factor and the measured or calculated aerosol concentration.

During a study conducted in the Czech Republic, the unattached fraction and the equilibrium factor were measured in several caves. The unattached fraction was found to be relatively stable during time in the cave, but the unattached fraction varied between the different caves from 2 to 58 % [35]. Thinova et al. calculated a dependence of the unattached fraction on the equilibrium factor and received the following equation:.

$$\ln\left(\frac{1}{f_p}\right) = 1.816 \cdot \left(\ln\left(\frac{1}{F}\right)\right)^{-1.167}$$ Equation 14

F = equilibrium factor

f_p = unattached fraction

If the mean unattached fraction of 3.6% measured in the radon gallery is taken, then the equilibrium factor calculated by this equation is 0.55. This corresponds very well to the equilibrium factor calculated with the estimated radon activity concentration in air, which is 0.54.

In a paper from Nikezic et al. [36], the dependence of the unattached fraction and the equilibrium factor from the attachment rate are calculated by using the Jacobi model, which describes the dynamical behaviour of radon and radon progeny in indoor air. Figure 3 of this paper from Nikezic et al. shows this dependance. In the gym the unattached fraction was 27%, the attachment rate was about 9/h calculated with the equation 12 and the calculated equilibrium factor was about 0.18. These values are in good agreement with the Figure 3 of Nikezic's paper, in which at the attachment rate of 10/h the equilibrium factor is 0.16 and the unattached fraction is 27%. This shows that using the estimated radon activity concentration of the unattached and the attached radon daughter measurements is an appropriate way to calculate the equilibrium factor.

Jilek et al. [37] compared room conditions in towns and villages. The equilibrium factor in family houses in towns and villages was 0.40 and 0.32, respectively. The unattached fraction in towns and villages was 8.6 % and 10.7 %, respectively. The calculated attachment rate in urban houses and rural houses was 26/h and 18/h respectively. The calculated attachment rate at day was 24/h and at night 20/h. Figure 58 below shows the attachment rate in the gym calculated with equation 12. It can be clearly seen that just like in the paper from Jilek et al. the attachment rate decreases in the afternoon and raises in the morning. The attachment rate during daytime was 15/h and during night 4/h. These values are lower than in the paper of Jilek et al. as the therapy centre is not in use during night, which is not the case for family houses. A reason for lower attachment rates during daytime could be due to the therapy centre being situated on the mountain and not in a village. In their paper, from Jilek et al. present values that are lower in the villages than in towns due to the lower aerosol particle concentrations in villages. On mountains, however, lower aerosol particle concentrations than in the villages can be found due to reduced traffic.

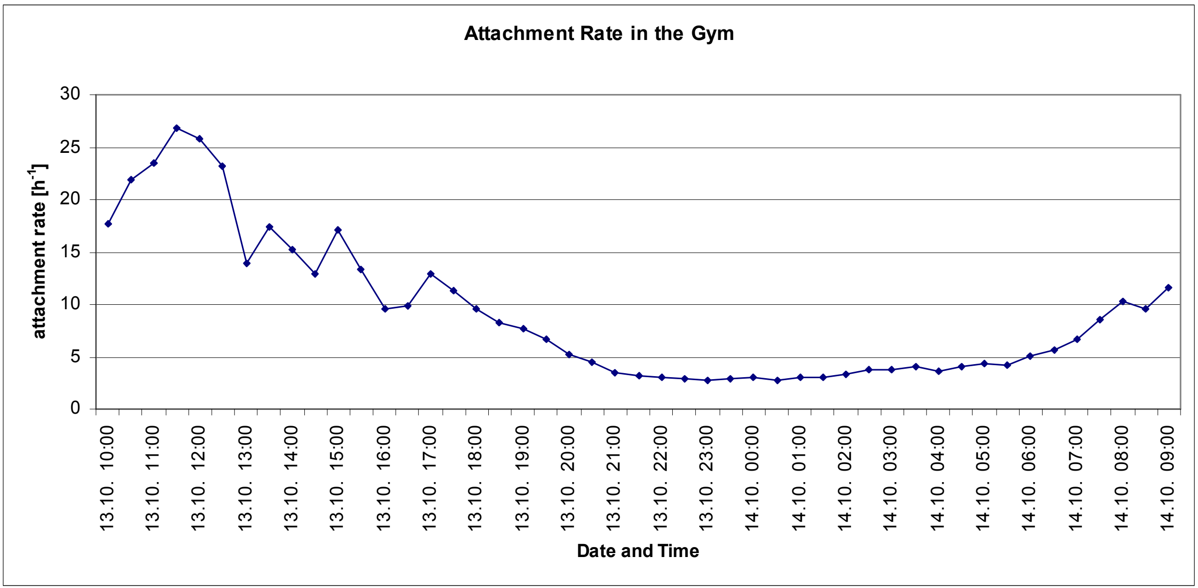

Figure 58: Attachment rate calculated with equation 13 during the measurements in the gym.

Unfortunately, the aerosol concentration was not measured in the gym or in the doctor's office 5. However, according to the data from the literature referenced, the mean aerosol particle concentration in rooms without additional aerosols from cooking or cigarette smoke varies between 500 to 6,100 cm^{-3}.

3.4. Calculation of the effective dose

Currently, different methods exist for the calculation of the effective dose.
In ICRP 65 [38], the recommended value of the dose conversion factor for the calculation of the effective dose is 1.4 Sv/Jhm^{-3} or 5 mSv/WLM at work and 1.1 Sv/Jhm^{-3} or 4 mSv/WLM at home. These values have been adopted by the European commission in the Council Directive 96/29/Euratom of 13 May 1996, laying down basic safety standards for the protection of the health of workers and the general public against the dangers arising from ionizing radiation. They also have been adopted by the Austrian Standards ÖNORM S5223-2 "Abschätzung der effektiven Dosis bei Arbeiten mit natürlichen radioaktiven Stoffen".
These dose conversion factors (DCF) were derived from epidemiological studies. These studies were mainly conducted with underground miners. This can lead to uncertainties when the DCFs are taken to calculate the dose indoors. In some studies, workers also inhaled other cancer causing substances such as arsenic.

Additionally inhaled radioactive dust and gamma radiation can cause lung cancer. The uncertainties of the studies are pointed out extensively in a paper by Puskin and James [1].

Another way to calculate the effective dose is to use DCFs derived from model calculations that are based on the human respiratory tract model (HRTM) of the ICRP 66 [2] or airway generation dosimetry models [3]. The airway generation dosimetry models, along with their sub-models, are explained in greater detail in the paper by Hofmann et al.. Additionally, this paper describes the influences of different conditions in mines and homes on the distribution of the dose within airway generations on the basis of the stochastic lung dosimetry model IDEAL-DOSE. Furthermore, the distribution among the five human pulmonary lobes is described. Unfortunately, the calculation of the DCF with an epidemiological dosimetric approach leads to different values of the DCF.

The effective dose by unit exposure resulting from the dosimetric approach is between 2 to 3 times higher than the effective dose by unit exposure resulting from the epidemiological approach. The estimates from the dosimetric approach are around 15 mSv/WLM while the estimates from the epidemiological approach are around 5 mSv/WLM [39].

To obtain an overview of the parameters which can cause these differences, Birchall et al. studied the influence of the variation of some parameters on the effective dose by unit exposure. The parameters of interest for this study were the aerosol condition (without the variation of the unattached fraction, because it is assumed that in underground mines it is only 1 %), such as the attached aerosol size, aerosol dispersion, particle density and particle shape factor as well as the degree of disequilibrium. Additionally, the influence of the variation of the breathing rate, fraction breathed through nose, deposition, clearance rates, slow cleared fraction, thickness of mucus, target cell depth and weighting of target cell doses as well as the apportionment of regional risk

$H_{TH} = H_{BB} A_{BB} + H_{bb} A_{bb} + H_{AI} A_{AI} + H_{LN_{TH}} A_{LN_{TH}}$ with

$H_{TH} = \text{detriment} - \textit{weighted equivalent dose for the thoracic regions}$
$H_i = \textit{equivalent doses for tissues}$
$A_i = \textit{factors for apportionment of radiation detriment}$
$BB = \textit{bronchial region}$
$bb = \textit{bronchiolar region}$
$AI = \textit{alveolar} - \textit{interstitial region}$
$LN_{TH} = \textit{lymphatics and lymph nodes that drain the thoracic region}$

were studied.

Yet the influences of these parameter variations could not explain the large differences between the two DCFs. For that reason, the lung weighting factor w_T and the radiation weighting factor w_α for alpha particles were studied as well. The values suggested by the ICRP in Publication 60 $w_{T\,(lung)}$ = 0,12 and $w_{R\,(\alpha)}$ = 20 could be afflicted with large uncertainties [40]. Maybe the alpha weighting factor is different for different tissues. Birchall et al showed that if these weighting factors are used for calculations it is very unlikely that the DCF is 5 mSv/WLM.

Stather [41] discussed the influence of $w_{T\,(lung)}$ and $w_{R\,(\alpha)}$ as well as uncertainties of the structure of the HRTM and stated that the ICRP 66 combined the airway generations into three defined regions instead of examining each airway generation separately. These three regions are the bronchial region (airway generations 0 to 8), the bronchiolar region (airway generations 9 to 15) and the alveolar interstitial region (airway generations >15)

An publication by Mohamed [42] furthermore considered the uncertainties of the unattached fraction. There he mentions that the particle size distribution of the attached and unattached radionuclides is an important factor as the radionuclides deposit in different airway generations, depending on their size. The parameters of interest in his study were the biological parameters breathing rate, particle transport in the respiratory tract (e.g. blood absorption) and whether secretory or basal cells were used as target cells. In addition, the aerosol parameters unattached size distribution and the attached size distribution were taken into account.

Marsh et al. calculated the dependence of different parameters on the DCF with the software package RADEP which uses the ICRP 66 HRTM model. The most important aerosol parameter which showed the highest influence on the DCF was the unattached fraction. They reached this correlation (equation 15) between the unattached fraction and the DCF by using the best estimates for a typical home atmosphere of all other parameters that can be varied [43]. The best estimates are shown in Table 44.

$$H = 11.35 + 0.43\, f_p \qquad \text{Equation 15}$$

best estimates for home condition	
unattached fraction	8 %
unattached aerosol size	0.9 nm
nucleation mode fraction	25.8 %
nucleation aerosol size	50 nm
accumulation mode fraction	64.4 %
accumulation mode aerosol size	250 nm
coarse mode fraction	1.8 %
coarse mode aerosol size	1500 nm
nose breathing rate	0.78 m³/h
equilibrium factor	0.4

Table 44: Best estimates for typical home atmosphere by Marsh et al..

Zock et al calculated a dependence of the DCF on the unattached fraction for different situations with an airway generation dosimetry model [44]. They used the ICRP 66 lung compartment model with the three defined regions (the bronchial, the bronchiolar and the alveolar interstitial region). They examined every airway generation separately and calculated the particle deposition in each generation of the respiratory tract. Zock et al. calculated 4 different situations, which are shown in Table 48.

	breathing rate	breathing through	equation (eq.)	Eq. Number
indoor	0.75 m³/h	nose	$H = f_p\ 35.9 + (1 - f_p)\,6.2$	16
indoor	0.75 m³/h	mouth	$H = f_p\ 118.5 + (1 - f_p)\,6.7$	17
mine	1.2 m³/h	nose	$H = f_p\ 50.2 + (1 - f_p)\,8.9$	18
mine	1.2 m³/h	mouth	$H = f_p\ 148.6 + (1 - f_p)\,12.3$	19

Table 48: Dependence of the DCF from the unattached fraction calculated by Zock et al..

Porstendörfer calculated a correlation with an airway generation dosimetry model and used a relative cancer sensitivity distribution of the three regions of the lung of [32]

$$w_{BB} : w_{bb} : w_{AI} = 0.80 : 0.15 : 0.05$$

instead of the recommended ICRP 66 apportionment factors of

$$w_{BB} : w_{bb} : w_{AI} = 0.333 : 0.333 : 0.333 .$$

Additionally, he took the different distributions of the basal and the secretory cells into account, as, compared to the secretory cells, a higher number of basal cells are located in the deeper epithelium tissue.

He calculated the following correlations between the unattached fraction and the DCF for different situations (Table 49)

	breathing rate	breathing through	equation (eq.)	Eq. Number
indoor	0.75 m³/h	nose	$H = 6.1 + 42\ f_p$	20
outdoor	1.2 m³/h	nose	$H = 9.1 + 64\ f_p$	21
working place (no coarse mode and no nucleation mode aerosols)	1.2 m³/h	nose	$H = 5.4 + 67\ f_p$	22
working place (no coarse mode aerosols)	1.2 m³/h	nose	$H = 8.4 + 64\ f_p$	23
working place (10% coarse mode fraction)	1.2 m³/h	nose	$H = 10.6 + 62\ f_p$	24

Table 49: Dependence of the DCF from the unattached fraction calculated by Porstendörfer.

With these equations the DCF for the unattached fraction (DCF_u) and the DCF for the attached fraction (DCF_a) can be derived [45].

$$DCF = f_p\ DCF_u + \left(1 - f_p\right) DCF_a \qquad \text{Equation 25}$$

or

$$DCF = DCF_a + \left(DCF_u - DCF_a\right) f_p \qquad \text{Equation 26}$$

3.4.1. Radon gallery Bad Gastein

If the PAEC is measured the effective dose can be calculated as follows:

$$E_{Rn} = DCF \cdot \sum_i PAEC_i \cdot T_i$$

$$PAEC_i = potential\ alpha\ energy\ concentration\ in\ mJ/m^3 \qquad \text{Equation 27}$$

$$T_i = \exp osure\ time$$

In Table 50 the effective dose of the attached radionuclides during a stay of one hour is calculated with an ICRP 65 DCF of 1.4 mSv/mJhm^{-3} and the mean PAEC within the working hours of 7:00 to 18:00 during the measurements in July.

July 2003 mean values	PAEC$_a$ [mJ/m³]	E_{Rn} [mSv]
07.07.2003 12:00 - 18:00	0.057	0.080
08.07.2003 7:00 - 18:00	0.058	0.081
09.07.2003 7:00 - 18:00	0.075	0.106
10.07.2003 7:00 - 11:30	0.095	0.133

Table 50: Effective dose in the radon gallery during a stay of one hour (attached radionuclides) calculated according to the ICRP 65, the Council Directive 96/29/Euratom of 13 May 1996 and the Austrian Standards.

During this time when the patients are in the therapy section the employees can rest in the so-called climate room with higher ventilation outside the therapy stations.
The effective dose during one year received in the therapy section would be about 20 mSv/a [46] if an employee stays for about 200 working hours in the therapy section. 20 mSv/a is the maximum permissible value for radiation exposed workers during one year.
For the patients which stay about 10 hours in the gallery during their entire treatments in one year the effective dose would be about 1 mSv/a which is the maximum permissible value for general population. This effective dose is calculated by assuming a breathing rate for workers of 1.2 m³/h. Actually the breathing rate for patients who rest in the therapy section would be lower than 1.2 m³/h which would lead to a lower effective dose than 1 mSv/a.
In Table 51 the effective dose during a stay of one hour is calculated with an ICRP 65 DCF of 1.4 mSv/mJhm^{-3} and the mean PAEC within the working hours of 7:00 to 18:00 during the measurements in January.

January 2004 mean values	PAEC$_a$ [mJ/m³]	E$_{Rn}$ [mSv]
07.01.2004 11:30 - 18:00	0.088	0.123
08.01.2004 7:00 - 18:00	0.109	0.153
09.01.2004 7:00 - 10:30	0.360	0.505

Table 51: Effective dose caused by the attached radionuclides in the radon gallery, during a stay of one hour, calculated according to the ICRP 65, the Council Directive 96/29/Euratom of 13 May 1996 and the Austrian Standards

During this time of the year the gallery is closed for repair works, cleaning and reconstruction. The ventilation system was not operating with full ventilation conditions because the reconstruction was conducted in the so-called climate room. With these effective dose values an employee can only stay about 75 hours in the gallery before he or she gets an effective dose of 20 mSv.
In Table 52, the effective dose caused by the unattached radionuclides during a stay of one hour is calculated with an ICRP 65 DCF of 1.4 mSv/mJhm^{-3} and the mean PAEC within the working hours of 7:00 to 18:00 during the measurements in January.

January 2004 mean values		$PAEC_u$ [mJ/m³]	E_{Rn} [mSv]
07.01.2004	11:30 - 18:00	0.005	0.007
08.01.2004	7:00 - 18:00	0.003	0.005
09.01.2004	7:00 - 10:30	0.012	0.016

Table 52: Effective dose caused by the unattached radionuclidesin the radon gallery, during a stay of one hour, calculated according to the ICRP 65, the Council Directive 96/29/Euratom of 13 May 1996 and the Austrian Standards.

Table 53 shows the PAEC of the attached and the unattached radionuclides and the sum of both.

mean values	$PAEC_a$ [mJ/m³]	$PAEC_u$ [mJ/m³]	total PAEC [mJ/m³]
07.01.2004	0.088	0.005	0.093
08.01.2004	0.109	0.003	0.113
09.01.2004	0.360	0.012	0.372

Table 53: PAEC in the radon gallery in January 2004.

If the different DCFs for the attached and unattached radionuclides are taken into account the equation 18 from Zock et al. and equation 23 from Porstendörfer can be taken for the calculation. The results are shown in Figure 59.

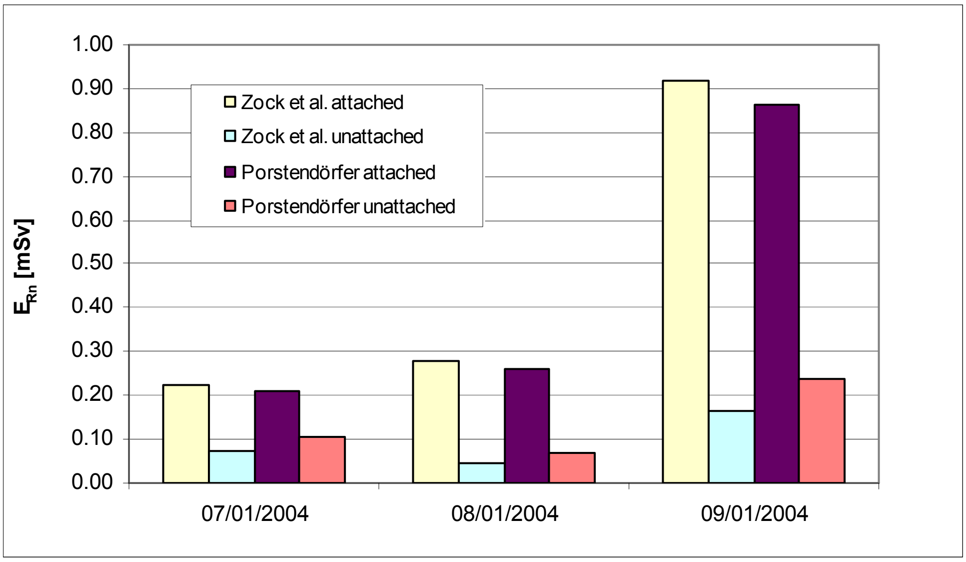

Figure 59: Effective dose of unattached and attached radionuclides calculated with the DCFs derived from model calculations by Zock et al. and Porstendörfer in the radon gallery, January 2004.

Table 54 shows the contribution of the unattached fraction to the effective dose for the two calculation methods.

mean values	Zock et al. E_{Rn} [mSv]	dose from unattached radionuclides %	Porstendörfer E_{Rn} [mSv]	dose from unattached radionuclides %
07.01.2004	0.294	24	0,313	33
08.01.2004	0.325	15	0,330	21
09.01.2004	1.079	15	1,104	22

Table 54: Contribution of the unattached fraction to the total effective dose calculated using DCFs from Zock et al.[44] and Porstendörfer [32] in the radon gallery, January 2004.

Using the model from Zock et al., the maximum contribution of the unattached radionuclides to the effective dose is 24%. For the Porstendörfer model it is 33%. Using the ICRP 65 calculation, the maximum contribution of the unattached radionuclides to the effective dose is just 5.4 %.

The mean effective dose for the stay of one hour calculated with the model calculations of Zock et al is 0.566 mSv and calculated with the model of Porstendorfer is 0.583 mSv, whereas calculated with the ICRP 65 recommended method the mean effective dose is 0.270 mSv. The calculated effective dose with the two model calculations are in good agreement, whereas the effective dose calculated according to ICRP 65 is only about the half of the effective dose from the two model calculations.

In the recent ICRP publication about lung cancer risk from radon and progeny and statement on radon from 2010 (ICRP 115), the commission recommends using the ICRP biokinetic and dosimetric models, including the HRTM and the ICRP systemic models to calculate the effective dose [4]. However, the recommendation by the ICRP of the dose coefficients per unit exposure of radon and its progeny to be used is still pending. For these dose coefficients, different reference conditions of domestic and occupational exposure with specified equilibrium factors and aerosol characteristics will be considered. The ICRP states that these dose coefficients by unit exposure to radon and its progeny will be lager, by a factor of two or more, than the previous dose coefficients. If this is taken into account, the calculated effective dose in the radon gallery in January from the three models would be in good agreement.

3.4.2. Therapy centre building

3.4.2.1. Foyer Bad Gastein, October 2004

In Table 55, the effective dose during a of stay of one hour is calculated with an ICRP 65 DCF of 1.4 $mSv/mJhm^{-3}$ and the mean PAEC within the working hours of 7:00 to 18:00 during the measurements in the foyer in October 2004.

foyer - mean values	$PAEC_a$ [mJ/m³]	E_{Rn} [mSv]
12.10.2004 10:00 – 18:00	0.0008	0.0011
13.10.2004 7:00 - 9:30	0.0007	0.0009

Table 55: Effective dose during a stay of one hour (attached radionuclides) calculated according to the ICRP 65, the Council Directive 96/29/Euratom of 13 May 1996 and the Austrian Standards.

For employees who spend about 1,810 hours in the foyer, the effective dose will be 1.9 mSv/a, which exceeds the maximum permissible value of 1 mSv/a for the general population. This exposure can be reduced by additional artificial ventilation. The importance of the ventilation rate is shown in many resent papers. Ashok et al. [47] showed that the ventilation rate had a higher influence on the radon concentration than the flooring type (granite, cement and mosaic). For this paper, the build up of radon in the room started at 18:00 and the highest concentration could be measured at 6:00. This effect can be explained by the opening of the doors and windows during the day. Sathish et al. measured 200 dwellings in ten different locations and distinguished between poorly (no or one window), moderately (two windows), well (three windows) very well (four windows) and excellently (five windows) ventilated houses. The arithmetic mean value of the radon concentration in poorly ventilated houses was ten times higher than the arithmetic mean in excellently ventilated houses [48].

3.4.2.2. Gym Bad Gastein, October 2004

In Table 56, the effective dose during a stay of one hour is calculated with an ICRP 65 DCF of 1.4 $mSv/mJhm^{-3}$ and the mean PAEC within the working hours of 7:00 to 18:00 during the measurements in the gym in October 2004.

gym - mean values	$PAEC_a$ [mJ/m³]	E_{Rn} [mSv]
13.10.2004 10:00 – 18:00	0.001	0.002
14.10.2004 7:00 - 9:00	0.002	0.003

Table 56: Effective dose during a stay of one hour (attached radionuclides) calculated according to the ICRP 65, the Council Directive 96/29/Euratom of 13 May 1996 and the Austrian Standards.

In Table 57, the effective dose of the unattached fraction during a stay of one hour is calculated with an ICRP 65 DCF of 1.4 $mSv/mJhm^{-3}$ and the mean PAEC within the working hours of 7:00 to 18:00 during the measurements in October.

gym - mean values	$PAEC_u$ [µJ/m³]	E_{Rn} [µSv]
13.10.2004 10:00 – 18:00	0.20	0.28
14.10.2004 7:00 - 9:00	0.70	0.97

Table 57: Effective dose during a stay of one hour (unattached radionuclides) calculated according to the ICRP 65, the Council Directive 96/29/Euratom of 13 May 1996 and the Austrian Standards.

Table 58 shows the PAEC of the attached and the unattached radionuclides and their sum.

mean values	$PAEC_a$ [mJ/m³]	$PAEC_u$ [µJ/m³]	total PAEC [mJ/m³]
13.10.2004	0.001	0.20	0.001
14.10.2004	0.002	0.70	0.003

Table 58: PAEC in the gym in October 2004.

For employees who spend about 1,810 hours in the gym, the effective dose will be 4.32 mSv/a from the attached and 1.14 mSv/a from the unattached radionuclides. The overall effective dose would be 5.46 mSv/a, which exceeds the maximum permissible value of 1 mSv/a for the general population. Under these circumstances an employee can only work 330 hours per year in this room to be below 1 mSv/a. It should be recommended that the duration of stay of the employees is documented and that additional ventilation is installed if necessary.

If the different DCFs of the unattached and attached radionuclides are taken into account, equation 16 from Zock et al., equation 20 from Porstendörfer as well as the equation from Marsh et al. can be used for the calculation.

The results are shown in Figure 60.

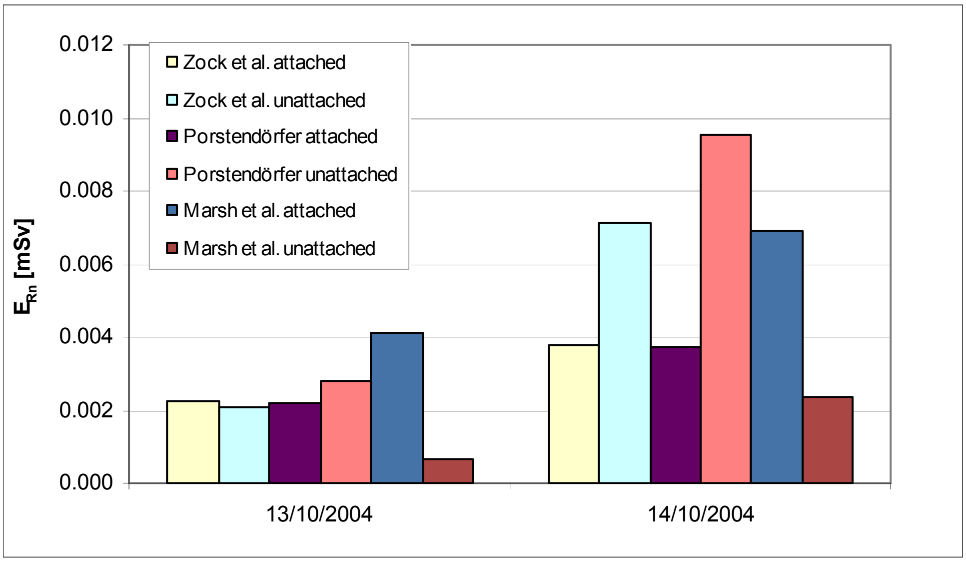

Figure 60: Effective dose of unattached and attached radionuclides calculated with the DCFs derived from model calculations by Zock et al., Porstendörfer and Marsh et al. in the gym, October 2004.

Table 59 shows the contribution of the unattached radionuclides to the effective dose for the three calculation methods.

mean values	Zock et al. E_{Rn} [mSv]	dose from unattached radionuclides %	Porstendörfer E_{Rn} [mSv]	dose from unattached radionuclides %	Marsh et al. E_{Rn} [mSv]	dose from unattached radionuclides %
13.10.2004	0.004	48	0.005	56	0.005	14
14.10.2004	0.011	65	0.013	72	0.009	25

Table 59: Contribution of the unattached fraction to the total effective dose calculated using DCFs from Zock et al.[44], Porstendörfer [32] and Marsh et al. [43] in the gym, October 2004.

Using the model from Zock et al., the maximum contribution of the unattached radionuclides to the total effective dose is 65%. For the Porstendörfer model it is 72% and for the Marsh model it is 25%. Using the ICRP 65 calculation, the maximum contribution of the unattached radionuclides is 25%. The lowest contribution of the unattached radionuclides result from the calculation from the Marsh model and the ICRP 65 model. However, in the equation of the Marsh model the DCF for the attached radionuclides is quite high with (11.35) and the DCF for the unattached radionuclides is quite low, compared to the other models. The mean effective dose calculated with the Marsh model is therefore higher than calculated with the ICRP 65-recommended method and is comparable with the mean effective dose calculated with the Zock et al model.

The mean effective dose for the stay of one hour calculated with the model calculations of Zock et al is 7.6 μSv, 9.1 μSv calculated with the model of

Porstendörfer and 7.0 μSv calculated with the equation from Marsh. If calculated with the ICRP 65-recommended method, the mean effective dose is 3.0 μSv. However, when taking the statement from ICRP 115 into account, the new DCFs should be at least twofold than the previously used ones.

3.4.2.3. Doctor's office 5 Bad Gastein, October 2004

In Table 60, the effective dose during a stay of one hour is calculated with an ICRP 65 DCF of 1.4 mSv/mJhm^{-3} and the mean PAEC within the working hours of 7:00 to 18:00 during the measurements in the doctor's office 5 in October 2004.

doctor's office 5 - mean values		$PAEC_a$ [mJ/m³]	E_{Rn} [mSv]
14.10.2004	10:30 - 18:00	0.002	0.002
15.10.2004	7:00 - 18:00	0.002	0.002
16.10.2004	7:00 - 15:00	0.003	0.005

Table 60: Effective dose during a stay of one hour (attached radionuclides) calculated according to the ICRP 65, the Council Directive 96/29/Euratom of 13 May 1996 and the Austrian Standards.

In Table 61, the effective dose of the unattached radionuclides during a stay of one hour is calculated with an ICRP 65 DCF of 1.4 mSv/mJhm^{-3} and the mean PAEC within the working hours of 7:00 to 18:00 during the measurements in October.

doctor's office 5 - mean values		$PAEC_u$ [mJ/m³]	E_{Rn} [mSv]
14.10.2004	10:30 - 18:00	0.001	0.002
15.10.2004	7:00 - 18:00	0.008	0.011
16.10.2004	7:00 - 15:00	0.006	0.008

Table 61: Effective dose caused by the unattached radionuclides in doctor's office 5, calculated according to the ICRP 65, the Council Directive 96/29/Euratom of 13 May 1996 and the Austrian Standards.

Table 62 shows the PAEC of the attached and the unattached radionuclides and the sum of both.

mean values	$PAEC_a$ [mJ/m³]	$PAEC_u$ [mJ/m³]	total PAEC [mJ/m³]
14.10.2004	0.002	0.001	0.003
15.10.2004	0.002	0.008	0.010
16.10.2004	0.003	0.006	0.009

Table 62: PAEC in doctor's office 5 in October 2004.

For employees who work about 1,810 hours in the doctor's office 5, the effective dose will be 18.1 mSv/a, which exceeds the maximum permissible value of 1 mSv/a for general population. Under these circumstances an employee can only work 100 hours per year in this room to be below 1 mSv/a. However, this effective dose results from low ventilation rates and closed windows. The measurements have to be conducted under real circumstances to calculate the effective dose for employees. If the different DCFs for the attached and unattached radionuclides are taken into account, equation 16 from Zock et al, equation 20 from Porstendörfer and equation 15 from Marsh et al. can be taken for the calculation. The results are illustrated in Figure 61.

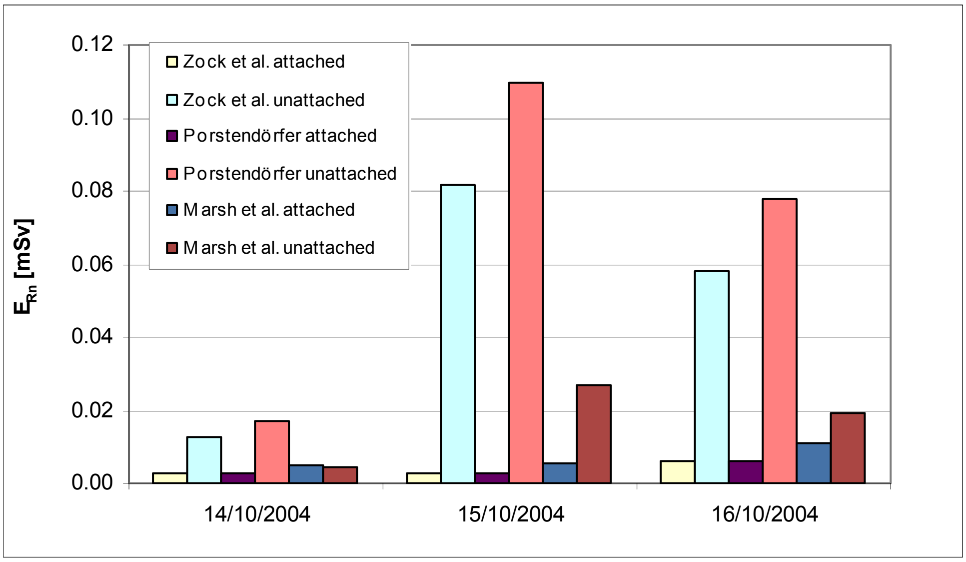

Figure 61: Effective dose of the unattached and the attached radionuclides calculated with the DCFs derived from model calculations by Zock et al., Porstendörfer and Marsh et al. in doctor's office 5, October 2004.

Table 63 shows the contribution of the unattached radionuclides to the effective dose for the three calculation methods.

mean values	Zock et al. E_{Rn} [mSv]	dose from unattached radionuclides %	Porstendörfer E_{Rn} [mSv]	dose from unattached fraction %	Marsh et al. E_{Rn} [mSv]	dose from unattached radionuclides %
14.10.2004	0.015	82	0.020	86	0.009	46
15.10.2004	0.085	97	0.113	97	0.032	84
16.10.2004	0.064	91	0.084	93	0.030	63

Table 63: Contribution of the unattached fraction to the total effective dose calculated using DCFs from Zock et al.[44], Porstendörfer [32] and Marsh et al. [43] in doctor's office 5, October 2004.

Using the model from Zock et al., the maximum contribution of the unattached radionuclides to the total effective dose is 97%. It is 97 % for the Porstendörfer model and 84% for the Marsh model. Using the ICRP 65 calculation, the maximum contribution of the unattached radionuclides to the total effective dose is 83%.

The mean effective dose for the stay of one hour calculated with the model calculations of Zock et al is 0.055 mSv, 0.072 mSv if calculated with the model of Porstendörfer and 0.024 mSv when calculated with the equation from Marsh. When calculated with the ICRP 65-recommended method, the mean effective dose is 0.010 mSv. The difference between the effective dose calculated with the model calculations of Zock et al and that of Porstendörfer is about 25 % and hence bigger than in the gym. Whereas the effective dose calculated with the model calculation of Marsh is just half of the effective dose from Zock et al.
These results indicate that the differences of the effective dose calculated from the three models are increasing with higher unattached fraction in the room. Taking into account the statement from ICRP 115, the new DCFs should be at least threefold than the previously used.
These results clearly show that the unattached fraction is very important for the calculation of the effective dose. Even if the different DCFs for the unattached and the attached radionuclides are not taken into consideration and the effective dose is calculated using only the ICRP 65 DCF, in low ventilated rooms, the contribution of the unattached fraction to the total effective dose can be 83%. Therefore it is important to measure the attached and the unattached radionuclides and measuring methods which just determine the attached radionuclides are insufficient to determine the effective dose.

3.4.3. Dose contribution of the long-lived radionuclides

For ^{210}Pb the dose conversion factor for workers h(g) for particles with 1 µm and 5 µm is $8.9 \cdot 10^{-7}$ Sv/Bq and $1.1 \cdot 10^{-6}$ Sv/Bq, respectively, according to the Council Directive 96/29/EURATOM of 13 May 1996 laying down basic safety standards for the protection of the health of workers and the general public against the dangers arising from ionizing radiation [49].
For ^{210}Bi the dose conversion factor h(g) for 1 µm and 5 µm is $8.4 \cdot 10^{-8}$ Sv/Bq and $6.0 \cdot 10^{-8}$ Sv/Bq, respectively.
For ^{210}Po the dose conversion factor h(g) for 1 µm and 5 µm is $3.0 \cdot 10^{-6}$ Sv/Bq and $2.2 \cdot 10^{-6}$ Sv/Bq, respectively.
These conversion factors have been recommended in the ICRP 68 [50]. The recommended AMAD in the ICRP 68 for the calculation of the effective dose for workers is 5 µm. The ICRP considers this AMAD as representative for workplace

aerosols, whereas 1 µm is considered to be representative for indoor or outdoor exposure of the general public (ICRP 66).
Using these conversion factors, the breathing rate for workers of 1.2 m³/h and an annual working time of 200 h (working time in the gallery), the effective dose caused by the three radionuclides can be calculated as follows:

$$E_i = h(g)_i \cdot t \cdot \nu \cdot A_i$$

$$t = working\ time\ [h]$$
$$\nu = breathing\ rate\ [m^3/h]$$
$$A = Activityconcentration\ [Bq/m^3]$$
$$i = Radionuclide$$

Equation 28

The effective dose calculated from the data of the three measurement periods is shown is table 64.

	^{210}Pb [µSv/a]	^{210}Bi [µSv/a]	^{210}Po [µSv/a]	sum [µSv/a]
July 2003	82	1.2	61	143
January 2004	314	6.7	92	412
Octobre 2004	429	6.5	169	605

Table 64: Effective dose caused by ^{210}Pb, ^{210}Bi and ^{210}Po in the radon gallery.

The effective dose of the short-lived daughter products calculated according to the ICRP 65 is about 20 mSv/a. Compared to this effective dose of 20 mSv/a the effective dose caused by ^{210}Pb, ^{210}Bi and ^{210}Po, with a maximum value of 0.605 mSv/a, is negligible.

4. Conclusion

The unattached fraction is very important for the calculation of the effective dose and should be taken into account. This is not the case in the present recommendations of the ICRP, EU or Austrian Standards. However the ICRP is reconsidering to recommend dose conversion factors according to the aerosol conditions in an indoor atmosphere.
With 33%, the maximum contribution of the unattached radionuclides to the total effective dose calculated from the attached and the unattached radionuclides is relatively low in the radon gallery compared to the other measuring sites. In the gym and in doctor's office 5, the main part of the total effective dose is caused by the unattached radionuclides. The highest contribution of the effective dose caused by

the unattached radionuclides to the total effective dose for the gym and doctor's office 5 are 72% and 97%, respectively. These high contributions of the unattached radionuclides are due to the high values of the unattached fraction in the gym and in doctor's office 5 with 27% and 60%, respectively. In addition, the dose conversion factor for the unattached radionuclides is higher than for the attached radionuclides, taking the DCFs derived from the model calculations.

DCFs were derived from an epidemiological approach and dosimetric approach, differing by a factor of 2 to 3. Many studies of the influences of different biological and aerosol parameters on the DCF showed that even with a variation of these parameters it is unlikely bring these two approaches together. Nevertheless, if the tissue-weighting factor for the lung or the radiation-weighting factor for the α-particle were varied, it would be possible to merge these two approaches.

Even if those two weighting factors change, however, the contribution of the unattached radionuclides to the effective dose calculated in the radon gallery, the gym and the doctor's office 5 will stay the same. Certainly if different weighting factors for the three lung regions, the bronchial region, the bronchiolar region and the alveolar interstitial region were recommended, a change of the contribution of the unattached fraction to the total effective dose might occur. That is due to the unattached fraction contributing more to the bronchial region while the attached radionuclides contribute to the bronchiolar region.

The results of our measurements have clearly shown how important the determination of the unattached fraction or the aerosol particle concentration is in order to assess the effective dose, especially in poorly ventilated rooms.

The effective dose from the long-lived radionuclides is negligible. The activity size distribution of the long-lived radon daughters is analysed. The activity median aerodynamic diameter (AMAD) of ^{210}Po is shifted to smaller particle sizes compared to the AMAD of ^{210}Pb and ^{210}Bi. This effect had been observed before by Wallner et al. during previous measurements and published in 2002. The reason for this is still not known and further studies on the chemical differences of the aerosols need to be conducted. Additionally, the AMAD in January 2004 is shifted to higher particle sizes compared to the AMAD in May 1999, July 2003 and October 2004. This could be due to the production of the smaller particles by friction of the train with the rail track during the opening hours of the gallery. Without these additional aerosol sources, only the aged aerosols exist. The AMAD in January was therefore between 250 nm

and 500 nm and between 125 nm and 250 nm during the other measurement periods.
The equilibrium equivalent radon activity concentration and the potential alpha energy concentration can be reduced through sufficient ventilation. This can be observed in the radon gallery during daytime, when the ventilation is turned on or in the gym and the foyer, where the equilibrium equivalent radon concentration increases during the night when all doors and windows are closed. The measurement of our results clearly showed that, in the gallery, the atmospheric pressure has a higher influence on the equilibrium equivalent concentration than the ventilation and that an increase of the ventilation rate should be considered when the atmospheric pressure drops. In January the equilibrium equivalent radon concentration in the gallery raised about threefold from 20.8 ± 1.3 kBq/m³ to 68.6 ± 4.2 kBq/m³. The atmospheric pressure declined from 910 hPa to 900 hPa during this time, whereas artificial ventilation only reduced the equilibrium equivalent radon concentration from 68.6 ± 4.2 kBq/m³ to 61.5 ± 3.8 kBq/m³. Additionally, atmospheric pressure has a higher influence on the equilibrium equivalent concentration than the location of the room in the building. Higher concentrations were measured in the gym than in the foyer, even though the gym is located on the second floor and the foyer is located on the ground floor. In the gym the equilibrium equivalent radon for the attached radionuclides was 374.8 ± 4.5 Bq/m³ and 184.5 ± 2.6 Bq/m³ in the foyer. Atmospheric pressure dropped form 912 hPa during the measurements in the foyer to 907 hPa during the measurements in the gym.
In our measurements, the correlation of the aerosol particle concentration with the attachment rate and the unattached fraction as well as the correlation of the unattached fraction with the equilibrium factor could be shown.
In the radon gallery the unattached fraction is just 3.6% due to the relatively high particle concentration of 12,000 cm^{-3}. Here the equilibrium factor was 0.54, whereas the average value of the unattached fraction is 27% and the equilibrium factor is 0.18 in the gym. In very poorly ventilated rooms without aerosol producing sources resulting in low aerosol particle concentrations, such as the doctor’s office 5, the unattached fraction can reach up to 60%. The equilibrium factor in doctor's office 5 was 0.07.

5. Appendix 1

5.1. References

[1] Puskin J., James A.C. (2006), *Radon Exposure Assessment and Dosimetry Applied to Epidemiology and Risk Estimation*; Radiat. Res. 166 pp. 193-208.

[2] ICRP, 1994. Human Respiratory Tract Model for Radiological Protection. ICRP Publication 66. Ann. ICRP 24 (1-3).

[3] Hofmann W., Winkler-Heil R. (2011), *Radon Lung Dosimetry Models*; Radiat. Prot. Dosim. 145(2-3) pp. 206-212

[4] ICRP, 2010. Lung Cancer Risk from Radon and Progeny and Statement on Radon. ICRP Publication 115, Ann. ICRP 40(1).

[5] Radioactivity and Radiation in Austria 2005 and 2006 (May 2009) Republic of Austria, BMG Sektion III, BMLFUW Sektion V (in German)

[6] Hongbing S., Furbish D.J. (1995) M*oisture content effect on radon emanation in porous media*; J. Contam. Hydrol. 18 pp. 239-255

[7] Dankelmann V., Reineking A., Porstendörfer J. (2001) *Determination of neutralisation rates of ^{218}Po ions in air*; Radiat. Prot. Dosim. 94(4) pp. 353-357

[8] Auvinen A., Mäkeläinen I., Hakama M., Castrén O., Pukkala E,Reisbacka H., Rytömaa T. (1996) *Indoor Radon Exposure and Risk of Lung Cancer: a Nested Case-Control Study in Finland* J. Natl. Cancer Inst. 88 pp. 966-972

[9] Field R.W. (1999) *IOWA Radon Lung Cancer Study*; Radiat. Res. 151 pp. 101-103

[10] Wang Z., Lubin J.H., Wnag L., Zhang A., Boice J.D., Cui H, Zhang S., Conrath S., Xia Y., Shang B., Brenner A., Lei S., Metayer C., Cao J., Chen K.W., Lei S., Kleineman R.A. (2002) *Residental Radon and Lung Cancer Risk in a High-exposure Area of Gansu Province, China*; Am.J.Epidemiol. 155(6) pp. 554-564

[11] World Health Organisation (2009) *WHO Handbook on Indoor Radon: A Public Health Perspective. WHO Press*

[12] ÖNORM S 5280-1, (2008); *Radon – Messverfahren und deren Anwendungsbereiche*

[13] Wallner G. (1997) *Simultaneous Determination of ^{210}Pb and ^{212}Pb Progenies by Liquid Scintillation Counting.* Appl. Radiat. Isot. 48(4) pp. 511-514

[14] Markl P. (1972) *Extraktion und Extraktions-Chromatographie in der anorganischen Analytik*. Methoden der Analyse in der Chemie, Bd. 13 Akad. Verlagsgesellschaft Frankfurt am Main.

[15] McDowell W.J., McDowell B.L. (1991) *Liquid scintillation alpha spectrometry: a method for today and tomorrow.* Proc. Int. Conf. on New Trends in Liquid Scintillation Counting and Organic Scintillators, 1989. Eds H. Ross, J.E. Noakes and J.D. Spaulding. Lewis, Mich.

[16] Rovenska K., Thinova L. (2010) *Seasonal variation of radon in the Bozkov cave*; Nukl. 55(4) pp. 483-489

[17] Pohl-Rüling J., Pohl E. (1969) *The Radon-222 concentration in the atmosphere of mines as a function of the barometric pressure.* Health Phys. 16 pp. 579-584

[18] Wallner G., Berner A., Irlweck K. (2002) *Aerosols: unexpected disequilibrium phenomena between airborne radio activities of lead-210 and its progeny bismuth-210 and polonium-210;* Naturwissenschaften 89 pp. 569-574

[19] Porstendörfer J. (1991) *Properties and Behaviour of Radon and Thoron and Their Decay Products in the air;* 5th International Symposium on the natural Radiation Environment; Salzburg, Austria, 22.-28. Sept.

[20] Wallner G. (2001) *Distribution of ^{212}Pb, ^{214}Pb and ^{210}Pb with its daughter products on aerosol fractions from Vienna and Badgastein (Austria)*. Radiochim. Acta 89 pp. 791-798

[21] Reineking A., Becker K.H., Porstendörfer J. (1988) *Measurements of activity size distributions of the short- lived Radon Daughters in the Indoor and Outdoor Environment;* Radiat. Prot. Dosim. 25 (1/4) pp. 245-250

[22] Butterweck G., Porstendörfer J., Reineking A., Kesten J. (1992) *Unattached fraction and the Aerosol Size Distribution of the Radon Progeny in a natural cave and mine Atmospheres.,* Radiat. Prot. Dosim. 45(1/4) pp. 167-170

[23] Wallner G., Berner A. (2005) Determination of heavy metals in aerosol fractions of different particle sizes from the healing gallery of Badgastein (Austria) Radiochim. Acta 93 pp. 637-641

[24] Bucci S., Pratesi G., Viti M. L., Pantani M., Bochicchio F., Venoso G. (2011) *Radon in Workplaces: First results of an extensive survey and comparison with radon in homes;* Radiat. Prot. Dosim. 145(2-3) pp. 202-205

[25] Poulin P., Leclerc J., Dessau J., Deck W., Gagnon F. (2012) *Radon measurement in schools located in three priority investigation areas in the province of Quebec, Canada*; Radiat. Prot. Dosim. 151(2) pp. 278-289

[26] Pereira C. E., Vaidyan V. K., Chougaonkar M. P., Mayya Y. S., Sahoo B. K., Jojo P. J. (2012) *Indoor radon and thoron levels in Neendakara and Chavara regions of southern coastal Kerala, India;* Radiat. Prot. Dosim. 150(3) pp. 385-390

[27] Keller G., Folkerts K.H. (1984) *Radon-222 Concentrations and Decay-Product Equilibrium in Dwellings and in the open air,* Health Phys. 47(3) pp. 385-398

[28] http://www.bfs.de/de/ion/radon/radon_in_haeusern.html

[29] Friedmann H. (2005) *Final results of the Austrian radon project*, Health Phys 89(4) pp. 339-348

[30] Porstendörfer J. (1984) *Behaviour of the Radon Daughter Products in indoor air*. Radiat. Prot. Dosim. 7, (1-4) pp. 107-113

[31] Kannosto J., Virtanen A., Lemmetty M., Mäkelä J.M., Keskinen J., Junninen H., Hussein T., Aalto P., Kulmala M. (2008) *Mode resolved density of atmospheric aerosol particles*; Atmos. Chem. Phys. 8 pp. 5327-5337

[32] Porstendörfer J. (2001), *Physical Parameters and Dose Factors of the Radon and Thoron Decay Products,* Radiat. Prot. Dosim. 94(4) pp. 365-373

[33] Reineking A., Porstendörfer J. (1990) *"unattached fraction" of short-lived Rn decay products in indoor and outdoor environments: an improved single-screen Method and Results*, Health Phys. 58 (6) pp. 715-727

[34] Huet C., Tymen G., Boulaud D. (1999) *Size distribution, equilibrium ratio and unattached fraction of Radon decay Products under typical Indoor Doestic Conditions* Radon in the Living Environment 19. – 23. April 1999, Athens, Greece pp. 741-750

[35] Thinova L., Rovenska K. (2011) *Radon dose calculation methodology for underground workers in the Czech Republic*, Radiat. Prot. Dosim. 145(2-3) pp. 233-237

[36] Nikezic D., Yu K.N. (2005) *Are radon gas measurements adequate for epidemiological studies and case control studies of radon-induced lung cancer*; Radiat. Prot. Dosim. 113 (2) pp. 233-235

[37] Jilek K., Thomas J., Tomášek L. (2010) *First results of measurement of equilibrium factors F and unattached fractions* f_p *of radon progeny in Czech dwellings*; Nukl., 55(4) pp. 439-444

[38] ICRP, 1993. Protection Against Radon-222 at Home and at Work. ICRP Publication 65. Ann. ICRP 23 (2).

[39] Birchall A., James A.C. (1994) *Uncertainty analysis of the effective dose per unit exposure from radon progeny and implications for ICRP risk-weighting factors.* Radiat. Prot. Dosim. 53(1-4) pp. 133-140

[40] ICRP, 1991. 1990 Recommendations of the International Commission on Radiological Protection. ICRP Publication 60. Ann. ICRP 21 (1-3).

[41] Stather J.W. (2004) *Dosimetric and epidemiological approaches to assessing radon doses – can the differences be reconciled?*; Radiat. Prot. Dosim. 112(4) pp. 487-492

[42] Mohamed A. (2005) *Influence of radioactive aerosol and biological parameters of inhaled radon progeny on human lung dose*; Radiat. Prot. Dosim. 113(1) pp. 115-122

[43] Marsh J.W., Birchall A. (2000), *Sensitivity Analysis of the Weighted Equivalent Lung Dose Per Unit Exposure from Radon Progeny,* Radiat. Prot. Dosim. 87(3) pp. 167-178

[44] Zock C., Porstendörfer J., Reineking A. (1996), *The Influence of Biological and Aerosol Parameters of Inhaled Short-Lived Radon Decay Products on Human Lung Dose;* Radiat. Prot. Dosim. 63(3) pp. 197-206

[45] Porstendorfer J., Reineking A. (1999) *Radon: Characteristics in air and dose conversion factors*; Health Phys. 76 pp. 300-310

[46] Allgemeine Strahlenschutzverordnung – AllgStrSchV BGBl. II Nr. 76/2012

[47] Ashok G.V., Nagaiah N., Shiva Prasad N.G. (2012) *Indoor radon concentration and its possible dependence on ventilation rate and flooring type*; Radiat. Prot. Dosim. 148(1) pp. 92-100

[48] Sathish L.A., Nagaraja K., Ramachandran T.V., (2012) *Indoor ^{222}Rn and ^{220}Rn concentrations and doses in Bangalore, India*; Radiat. Prot. Dosim. 151(2) pp. 344-353

[49] Council Directive 96/29/Euratom of 13 May 1996 laying down basic safety standards for the protection of the health of workers and the general public against the dangers arising from ionizing radiation

[50] ICRP, 1994. *Dose Coefficients for Intakes of Radionuclides by Workers*. ICRP Publication 68. Ann. ICRP 24

5.2. List of figures

Figure 1: Radon gallery measurement results from July 2003. The activity concentrations of the short lived radon daughter products, the equilibrium equivalent radon and the estimated radon are illustrated. 13
Figure 2: The potential alpha energy in WL and J/m³ during the radon gallery measurements in July 2003. 14
Figure 3: Mean values of the attached short-lived radon daughter products, the equilibrium equivalent radon and the estimated radon in teh radon gallery in July 2003. 15
Figure 4: Mean values of the PAEC during the sampling period in the radon gallery from 7 July to 10 July, 2003 15
Figure 5: The atmospheric pressure in Rauris and the PAEC in the radon gallery in July 2003 16
Figure 6: Activity concentration of the attached short lived radon daughter products, the equilibrium equivalent radon and the estimated radon in the radon gallery in January 2004. 17
Figure 7: Potential alpha energy concentration calculated from the attached radionuclides in the radon gallery, January 2004 17
Figure 8: The atmospheric pressure measured in Rauris and the PAEC measured in the radon gallery in January 2004 18
Figure 9: Mean values of the activity concentrations of the attached short lived radon daughter products, the equilibrium equivalent radon and the estimated radon in the radon gallery, January 2004 19
Figure 10: Daily mean values of the PAEC of the attached radionuclides in the radon gallery, January 2004 19
Figure 11: Activity concentrations of the unattached short-lived radon daughter products, the equilibrium equivalent radon and the estimated radon in the radon gallery in January 2004 21
Figure 12: The potential alpha energy concentration in the radon gallery, January 2004 22
Figure 13: Mean values of the activity concentrations of the unattached short lived radon daughter products, the equilibrium equivalent radon and the estimated radon in the radon gallery, January 2004. 23
Figure 14: Daily mean values of the PAEC of the unattached radionuclides. 23
Figure 15: Activity concentrations of the attached and unattached ^{218}Po and the fraction of the unattached ^{218}Po to the total ^{218}Po in the radon gallery, January 2004 24
Figure 16: Activity concentrations of the attached and unattached ^{214}Pb and the fraction of the unattached ^{214}Pb to the total ^{214}Pb in the radon gallery, January 2004. 25
Figure 17: Activity concentrations of the attached and unattached ^{214}Bi/^{214}Po and the fraction of the unattached ^{214}Bi/^{214}Po to the total ^{214}Bi/^{214}Po in the radon gallery, January 2004 25
Figure 18: Activity concentrations of the attached and unattached equilibrium equivalent radon concentration and the unattached fraction in the radon gallery, January 2004. 26
Figure 19: Mean values of the unattached fraction, the fraction of each unattached daughter product and the contributions of the unattached radionuclides to the total PAEC in the radon gallery, January 2004 26

Figure 20: The fraction of the activity of ^{210}Pb, ^{210}Bi and ^{210}Po collected on each stage in relation to the total activity collected by the cascade impactor in the radon gallery, May 1999. 33
Figure 21: The fraction of the activity of ^{210}Pb, ^{210}Bi and ^{210}Po collected on each stage in relation to the total activity collected by the cascade impactor in the radon gallery, July 2003. 33
Figure 22: The fraction of the activity of ^{210}Pb, ^{210}Bi and ^{210}Po collected on each stage in relation to the total activity collected by the cascade impactor in the radon gallery, January 2004. 34
Figure 23: The fraction of the activity of ^{210}Pb, ^{210}Bi and ^{210}Po collected on each stage in relation to the total activity collected by the cascade impactor in the radon gallery, October 2004. 34
Figure 24: Activity concentrations of the attached short-lived radon daughters, the equilibrium equivalent radon and the estimated radon in the foyer, October 2004. 37
Figure 25: The potential alpha energy concentration in the foyer, October 2004. 37
Figure 26: Mean values of the attached short-lived radon daughter products, the equilibrium equivalent radon and the estimated radon in the foyer, October 2004. 38
Figure 27: Daily mean values of the PAEC of the attached radionuclides in teh foyer, October 2004. 38
Figure 28: Activity concentrations of the attached short-lived radon daughters, the equilibrium equivalent radon and the estimated radon in the gym in Oct. 2004. 39
Figure 29: The potential alpha energy concentration of the attached radionuclides in the gym, October 2004. 40
Figure 30: Mean values of the attached short-lived radon daughter products, the equilibrium equivalent radon and the estimated radon in the gym, October 2004. 41
Figure 31: Daily mean values of the PAEC of the attached radionuclides in the gym, October 2004. 41
Figure 32: Activity concentrations of the unattached radon daughter products, the equilibrium equivalent radon and the estimated radon in the gym in Oct. 2004 42
Figure 33: The potential alpha energy concentration of the unattached radionuclides in the gym in October 2004. 42
Figure 34: Mean values of the unattached short-lived radon daughter products, the equilibrium equivalent radon and the estimated radon in the gym, October 2004. 43
Figure 35: Daily mean values of the PAEC of the unattached radionuclides in the gym, October 2004. 43
Figure 36: The activity concentrations of the attached and the unattached ^{218}Po and the fraction of the unattached ^{218}Po to the total ^{218}Po in the gym, October 2004. 44
Figure 37: The activity concentrations of the attached and the unattached ^{214}Pb and the fraction of the unattached ^{214}Pb to the total ^{214}Pb in the gym, October 2004. 44
Figure 38: The activity concentrations of the attached and the unattached $^{214}Bi/^{214}Po$ and the fraction of the unattached $^{214}Bi/^{214}Po$ to the total $^{214}Bi/^{214}Po$ in the gym, October 2004. 45

Figure 39: The activity concentrations of the attached and the unattached equilibrium equivalent radon and the unattached fraction in the gym, October 2004. 45
Figure 40: Mean values of the unattached fraction and the fraction of each unattached daughter product and the contribution of the unattached radionuclides to the total PAEC in the gym, October 2004. 46
Figure 41: Activity concentrations of the attached radon daughters, the equilibrium equivalent radon and the estimated radon in doctor's office 5, October 2004. 47
Figure 42: The potential alpha energy concentration of the attached radionuclides in doctor's office 5 in October 2004. This room was not in use during measurements. 47
Figure 43: Mean values of the attached short lived radon daughter products, the equilibrium equivalent radon and the estimated radon in doctor's office 5, October 2004.. 48
Figure 44: Daily mean values of the PAEC of the attached radionuclides in doctor's office 5, October 2004. 48
Figure 45: The activity concentrations of the unattached radon daughters, the equilibrium equivalent radon and the estimated radon in doctor's office 5 in October 2004. 49
Figure 46: The potential alpha energy concentration in doctor's office 5, October 2004. 49
Figure 47: Mean values of the unattached short lived radon daughter products, the equilibrium equivalent radon and the estimated radon in doctor's office 5, October 2004. 50
Figure 48: Daily mean values of the PAEC of the unattached radionuclides in doctor's office 5, October 2004. 50
Figure 49: The activity concentrations of the attached and unattached ^{218}Po and the fraction of the unattached ^{218}Po to the total ^{218}Po in doctor's office 5 in October 2004. 51
Figure 50: The activity concentrations of the attached and the unattached ^{214}Pb and the fraction of the unattached ^{214}Pb to the total ^{214}Pb in doctor's office 5 in October 2004. 51
Figure 51: The activity concentrations of the attached and unattached ^{214}Bi/^{214}Po and the fraction of the unattached ^{214}Bi/^{214}Po to the total ^{214}Bi/^{214}Po in doctor's office 5 in October 2004. 52
Figure 52: The activity concentrations of the attached and unattached equilibrium equivalent radon and the unattched fraction in doctor's office 5 in October 2004. 52
Figure 53: Mean values of the unattached fraction and the fraction of each unattached daughter product and the contribution of the unattached radionuclides to the total PAEC in doctor's office 5, October 2004. 53
Figure: 54: The atmospheric pressure measured in Rauris and the PAEC measured in the therapy centre building. 54
Figure 55: Typical variations of the unattached fraction and the equilibrium factor with time in the radon gallery. 59
Figure 56: Variation of the unattached fraction and the equilibrium factor with time in the gym. 59

Figure 57: Variation of the unattached fraction and the equilibrium factor with time in the doctor's office 5. 60
Figure 58: Attachment rate calculated with equation 13 during the measurements in the gym. 62
Figure 59: Effective dose of unattached and attached radionuclides calculated with the DCFs derived from model calculations by Zock et al. and Porstendörfer in the radon gallery, January 2004. 68
Figure 60: Effective dose of unattached and attached radionuclides calculated with the DCFs derived from model calculations by Zock et al., Porstendörfer and Marsh et al. in the gym, October 2004. 72
Figure 61: Effective dose of the unattached and the attached radionuclides calculated with the DCFs derived from model calculations by Zock et al., Porstendörfer and Marsh et al. in doctor's office 5, October 2004. 74

5.3. List of tables

Table 1: Cut off and average aerosol diameter of the collected particles on the aluminium foils of the cascade impactor 10
Table 2: List of measurements which were performed at different periods and sites. 12
Table 3: The mean, maximum and minimum values of the attached radionuclides in the radon gallery, 7 July 2003. 90
Table 4: The mean, maximum and minimum values of the attached radionuclides in the radon gallery, 8 July 2003. 91
Table 5: The mean, maximum and minimum values of the attached radionuclides in the radon gallery, 9 July 2003. 91
Table 6: The mean, maximum and minimum values of the attached radionuclides in the radon gallery, 10 July 2003. 91
Table 7: The mean, maximum and minimum values of the attached radionuclides in the radon gallery, 7 January 2004. 91
Table 8: The mean, maximum and minimum values of the attached radionuclides in the radon gallery, 8 January 2004. 91
Table 9: The mean, maximum and minimum values of the attached radionuclides in the radon gallery, 9 January 2004. 92
Table 10: The mean, maximum and minimum values of the unattached radionuclides in the radon gallery, 7 January 2004. 92
Table 11: The mean, maximum and minimum values of the unattached radionuclides in the radon gallery, 8 January 2004. 92

Table 12: The mean, maximum and minimum values of the unattached radionuclides in the radon gallery, 9 January 2004. 92
Table 13: The unattached fraction, the fraction of each unattached daughter product and the contributions of the unattached radionuclides to the total PAEC in the radon gallery, 7 January 2004. 92
Table 14: The unattached fraction, the fraction of each unattached daughter product and the contributions of the unattached radionuclides to the total PAEC in the radon gallery, 8 January 2004. 93
Table 15: The unattached fraction, the fraction of each unattached daughter product and the contributions of the unattached radionuclides to the total PAEC in the radon gallery, 9 January 2004. 93
Table 16: Activity concentration of ^{210}Pb, ^{210}Bi and ^{210}Po in mBq/m³ collected in the radon gallery with the cascade impactor, 8 July 2003. 28
Table 17: Activity concentration of ^{210}Pb, ^{210}Bi and ^{210}Po in mBq/m³ collected in the radon gallery with the cascade impactor, 9 July 2003. 29
Table 18: Activity concentration of ^{210}Pb, ^{210}Bi and ^{210}Po in mBq/m³ collected in the radon gallery with the cascade impactor, 7 January 2004. 29
Table 19: Activity concentration of ^{210}Pb, ^{210}Bi and ^{210}Po in mBq/m³ collected in the radon gallery with the cascade impactor, 8 January 2004. 30
Table 20: Activity concentration of ^{210}Pb, ^{210}Bi and ^{210}Po in mBq/m³ collected in the radon gallery with the cascade impactor, 12 October 2004 31
Table 21: Activity concentration of ^{210}Pb, ^{210}Bi and ^{210}Po in mBq/m³ collected in the radon gallery with the cascade impactor 13 October 2004 31
Table 22: Activity concentration of ^{210}Pb, ^{210}Bi and ^{210}Po in mBq/m³ collected in the radon gallery with the cascade impactor 14 October 2004 31
Table 23: Results of the measurements in the radon gallery from Wallner et. al.[18], May 1999. 32
Table 24: Total activity concentration of ^{210}Pb, ^{210}Bi and ^{210}Po during four different measurement periods collected in the radon gallery with a cascade impactor. 32
Table 25: The mean, maximum and minimum values of the attached radionuclides in the foyer, 12 October 2004. 93
Table 26: The mean, maximum and minimum values of the attached radionuclides in the foyer, 13 October 2004. 93

Table 27: The mean, maximum and minimum values of the attached radionuclides in the gym, 13 October 2004. 93

Table 28: The mean, maximum and minimum values of the attached radionuclides in the gym, 14 October 2004. 94

Table 29: The mean, maximum and minimum values of the unattached radionuclides in the gym, 13 October 2004. 94

Table 30: The mean, maximum and minimum values of the unattached radionuclides in the gym 14 October 2004. 94

Table 31: The unattached fraction, the fraction of each unattached daughter product and the contributions of the unattached radionuclides to the total PAEC in the gym, 13 October 2004. 94

Table 32: The unattached fraction, the fraction of each unattached daughter product and the contributions of the unattached radionuclides to the total PAEC in the gym, 14 October 2004. 95

Table 33: The mean, maximum and minimum values of the attached radionuclides in doctor's office 5, 14 October 2004. 95

Table 34: The mean, maximum and minimum values of the attached radionuclides in doctor's office 5, 15 October 2004. 95

Table 35: The mean, maximum and minimum values of the attached radionuclides in doctor's office 5, 16 October 2004. 95

Table 36: The mean, maximum and minimum values of the unattached radionuclides in doctor's office 5, 14 October 2004. 96

Table 37: The mean, maximum and minimum values of the unattached radionuclides in doctor's office 5, 15 October 2004. 96

Table 38: The mean, maximum and minimum values of the unattached radionuclides in doctor's office 5, 16 October 2004. 96

Table 39: The unattached fraction, the fraction of each unattached daughter product and the contributions of the unattached radionuclides to the total PAEC in doctor's office 5, 14 October 2004. 96

Table 40: The unattached fraction, the fraction of each unattached daughter product and the contributions of the unattached radionuclides to the total PAEC in doctor's office 5, 15 October 2004. 97

Table 41: The unattached fraction, the fraction of each unattached daughter product and the contributions of the unattached radionuclides to the total PAEC in doctor's office 5, 16 October 2004. 97
Table 42: Aerosol particle concentration collected on the stages of the cascade impactor in the radon gallery. 56
Table 43. Mean values of the measured unattached fraction, the calculated equilibrium factor and the measured or calculated aerosol concentration in the radon gallery, gym and doctor's office 5. 60
Table 44: Best estimates for typical home atmosphere by Marsh et al.. 65
Table 48: Dependence of the DCF from the unattached fraction calculated by Zock et al.. 65
Table 49: Dependence of the DCF from the unattached fraction calculated by Porstendörfer. 66
Table 50: Effective dose in the radon gallery during a stay of one hour (attached radionuclides) calculated according to the ICRP 65, the Council Directive 96/29/Euratom of 13 May 1996 and the Austrian Standards, July 2003. 66
Table 51: Effective dose caused by the attached radionuclides in the radon gallery, during a stay of one hour, calculated according to the ICRP 65, the Council Directive 96/29/Euratom of 13 May 1996 and the Austrian Standards, January 2004. 67
Table 52: Effective dose caused by the unattached radionuclides in the radon gallery, during a stay of one hour, calculated according to the ICRP 65, the Council Directive 96/29/Euratom of 13 May 1996 and the Austrian Standards, January 2004. 68
Table 53: PAEC in the radon gallery in January 2004. 68
Table 54: Contribution of the unattached fraction to the total effective dose calculated using DCFs from Zock et al.[44] and Porstendörfer [32] in the radon gallery, January 2004 69
Table 55: Effective dose during a stay of one hour in the foyer (attached radionuclides) calculated according to the ICRP 65, the Council Directive 96/29/Euratom of 13 May 1996 and the Austrian Standards. 70

Table 56: Effective dose during a stay of one hour in the gym (attached radionuclides) calculated according to the ICRP 65, the Council Directive 96/29/Euratom of 13 May 1996 and the Austrian Standards. 70
Table 57: Effective dose during a stay of one hour in the gym (unattached radionuclides) calculated according to the ICRP 65, the Council Directive 96/29/Euratom of 13 May 1996 and the Austrian Standards. 71
Table 58: PAEC in the gym in October 2004. 71
Table 59: Contribution of the unattached fraction to the total effective dose calculated using DCFs from Zock et al.[44], Porstendörfer [32] and Marsh et al [43] in the gym, October 2004. 72
Table 60: Effective dose during a stay of one hour in doctor's office 5 (attached radionuclides) calculated according to the ICRP 65, the Council Directive 96/29/Euratom of 13 May 1996 and the Austrian Standards. 73
Table 61: Effective dose caused by the unattached radionuclides during a stay of one hour in doctor's office 5, calculated according to the ICRP 65, the Council Directive 96/29/Euratom of 13 May 1996 and the Austrian Standards. 73
Table 62: PAEC in the doctor's office 5 in October 2004. 73
Table 63: Contribution of the unattached fraction to the total effective dose calculated using DCFs from Zock et al.[44], Porstendörfer [32] and Marsh et al. [43] in doctor's office 5, October 2004. 74
Table 64: Effective dose caused by ^{210}Pb, ^{210}Bi and ^{210}Po in the radon gallery. 76

5.4. Data tables

07.07.2003 (12:00 – 0:00)	mean value	maximum value	minimum value
equilibrium equivalent Radon [Bq/m³]	11,800	13,900	5,500
^{218}Po [Bq/m³]	16,600	70,300	9,900
^{214}Pb [Bq/m³]	11,500	13,900	3,900
^{214}Bi/^{214}Po [Bq/m³]	10,800	13,900	300
estimated Radon [Bq/m³]	34,400	291,000	9,900
PAEC [WL]	3.1	3.7	1.5

Table 3: The mean, maximum and minimum values of the attached radionuclides in the radon gallery.

08.07.2003	mean value	maximum value	minimum value
equilibrium equivalent Radon [Bq/m³]	12,200	14,400	7,200
^{218}Po [Bq/m³]	12,100	14,300	7,200
^{214}Pb [Bq/m³]	12,100	14,300	7,200
^{214}Bi/^{214}Po [Bq/m³]	12,100	14,300	7,200
estimated Radon [Bq/m³]	12,100	14,300	7,200
PAEC [WL]	3.2	3.8	1.9

Table 4: The mean, maximum and minimum values of the attached radionuclides in the radon gallery.

09.07.2003	mean value	maximum value	minimum value
equilibrium equivalent Radon [Bq/m³]	14,500	18,300	12,000
^{218}Po [Bq/m³]	14,800	26,100	11,900
^{214}Pb [Bq/m³]	14,500	18,200	11,900
^{214}Bi/^{214}Po [Bq/m³]	14,300	18,200	11,900
estimated Radon [Bq/m³]	15,000	32,600	11,900
PAEC [WL]	3.7	4.9	3.2

Table 5: The mean, maximum and minimum values of the attached radionuclides in the radon gallery.

10.07.2003 (0:00 – 11:30)	mean value	maximum value	minimum value
equilibrium equivalent Radon [Bq/m³]	17,600	18,600	15,800
^{218}Po [Bq/m³]	21,400	33,600	15,700
^{214}Pb [Bq/m³]	18,000	19,300	15,700
^{214}Bi/^{214}Po [Bq/m³]	15,700	18,600	10,100
estimated Radon [Bq/m³]	24,300	47,900	15,700
PAEC [WL]	4.7	5.0	4.2

Table 6: The mean, maximum and minimum values of the attached radionuclides in the radon gallery.

07.01.2004 (11:30 – 0:00)	mean value	maximum value	minimum value
equilibrium equivalent Radon [Bq/m³]	16,800	22,100	12,800
^{218}Po [Bq/m³]	18,300	38,300	13,000
^{214}Pb [Bq/m³]	17,000	24,000	12,800
^{214}Bi/^{214}Po [Bq/m³]	16,100	18,500	11,700
estimated Radon [Bq/m³]	19,300	50,700	13,100
PAEC [WL]	4.5	5.9	3.4

Table 7: The mean, maximum and minimum values of the attached radionuclides in the radon gallery.

08.01.2004	mean value	maximum value	minimum value
equilibrium equivalent Radon [Bq/m³]	22,500	37,800	16,100
^{218}Po [Bq/m³]	22,400	37,700	16,000
^{214}Pb [Bq/m³]	22,400	37,700	16,000
^{214}Bi/^{214}Po [Bq/m³]	22,400	37,700	16,000
estimated Radon [Bq/m³]	22,400	37,700	16,000
PAEC [WL]	6.0	10.0	4.3

Table 8: The mean, maximum and minimum values of the attached radionuclides in the radon gallery.

09.01.2004 (0:00 – 10:30)	mean value	maximum value	minimum value
equilibrium equivalent Radon [Bq/m³]	56,500	68,600	39,400
^{218}Po [Bq/m³]	56,200	68,300	39,300
^{214}Pb [Bq/m³]	56,200	68,300	39,300
^{214}Bi/^{214}Po [Bq/m³]	56,200	68,300	39,300
estimated Radon [Bq/m³]	56,200	68,300	39,300
PAEC [WL]	15.0	18.2	10.5

Table 9: The mean, maximum and minimum values of the attached radionuclides in the radon gallery.

07.01.2004 (11:30 – 0:00)	mean value	maximum value	minimum value
equilibrium equivalent Radon [Bq/m³]	860	1,400	590
^{218}Po [Bq/m³]	5,100	6,700	2,500
^{214}Pb [Bq/m³]	560	1,300	370
^{214}Bi/^{214}Po [Bq/m³]	70	340	30
estimated Radon [Bq/m³]	20,400	32,700	5,000
PAEC [WL]	0.23	0.36	0.16

Table 10: The mean, maximum and minimum values of the unattached radionuclides in the radon gallery.

08.01.2004	mean value	maximum value	minimum value
equilibrium equivalent Radon [Bq/m³]	720	1,300	430
^{218}Po [Bq/m³]	4,600	8,800	2,300
^{214}Pb [Bq/m³]	440	730	250
^{214}Bi/^{214}Po [Bq/m³]	40	80	20
estimated Radon [Bq/m³]	19,200	39,500	6,400
PAEC [WL]	0.19	0.35	0.11

Table 11: The mean, maximum and minimum values of the unattached radionuclides in the radon gallery.

09.01.2004 (0:00 – 10:00)	mean value	maximum value	minimum value
equilibrium equivalent Radon [Bq/m³]	1,900	2,300	1,400
^{218}Po [Bq/m³]	11,900	14,100	9,400
^{214}Pb [Bq/m³]	1,200	1,600	760
^{214}Bi/^{214}Po [Bq/m³]	120	240	60
estimated Radon [Bq/m³]	49,100	61,200	32,300
PAEC [WL]	0.50	0.60	0.37

Table 12: The mean, maximum and minimum values of the unattached radionuclides in the radon gallery.

07.01.2004	mean value	maximum value	minimum value
unattached fraction fp [%]	4.9	6.3	3.6
^{218}Po fj [%]	23	32	7.9
^{214}Pb fj [%]	3.2	5.3	2.3
^{214}Bi/^{214}Po fj [%]	0.5	2.2	0.2
potential alpha energy J/m³ [%]	4.9	6.4	3.6

Table 13: The unattached fraction, the fraction of each unattached daughter product and the contributions of the unattached radionuclides to the total PAEC in the radon gallery.

08.01.2004	mean value	maximum value	minimum value
unattached fraction fp [%]	3.1	3.5	2.6
^{218}Po fj [%]	17	19	11
^{214}Pb fj [%]	1.9	2.3	1.5
^{214}Bi/^{214}Po fj [%]	0.2	0.4	0.1
potential alpha energy J/m³ [%]	3.1	3.5	2.6

Table 14: The unattached fraction, the fraction of each unattached daughter product and the contributions of the unattached radionuclides to the total PAEC in the radon gallery.

09.01.2004	mean value	maximum value	minimum value
unattached fraction fp [%]	3.3	3.5	2.9
^{218}Po fj [%]	18	20	14
^{214}Pb fj [%]	2.0	2.4	1.8
^{214}Bi/^{214}Po fj [%]	0.2	0.4	0.1
potential alpha energy J/m³ [%]	3.3	3.5	2.9

Table 15: The unattached fraction, the fraction of each unattached daughter product and the contributions of the unattached radionuclides to the total PAEC in the radon gallery.

12.10.2004 (10:00 – 0:00)	mean value	maximum value	minimum value
equilibrium equivalent Radon [Bq/m³]	210	360	100
^{218}Po [Bq/m³]	300	580	110
^{214}Pb [Bq/m³]	220	380	110
^{214}Bi/^{214}Po [Bq/m³]	170	310	60
estimated Radon [Bq/m³]	370	850	110
PAEC [WL]	0.056	0.096	0.028

Table 25: The mean, maximum and minimum values of the attached radionuclides in the foyer of the therapy center building.

13.10.2004 (0:00 – 10:00)	mean value	maximum value	minimum value
equilibrium equivalent Radon [Bq/m³]	150	210	110
^{218}Po [Bq/m³]	180	250	130
^{214}Pb [Bq/m³]	150	210	110
^{214}Bi/^{214}Po [Bq/m³]	130	210	80
estimated Radon [Bq/m³]	210	350	130
PAEC [WL]	0.039	0.056	0.028

Table 26: The mean, maximum and minimum values of the attached radionuclides in the foyer of the therapy center building.

13.10.2004 (10:00 – 0:00)	mean value	maximum value	minimum value
equilibrium equivalent Radon [Bq/m³]	330	550	170
^{218}Po [Bq/m³]	340	540	210
^{214}Pb [Bq/m³]	330	540	180
^{214}Bi/^{214}Po [Bq/m³]	320	540	140
estimated Radon [Bq/m³]	350	540	210
PAEC [WL]	0.086	0.15	0.045

Table 27: The mean, maximum and minimum values of the attached radionuclides in the gym of the therapy center building.

14.10.2004 (0:00 – 9:00)	mean value	maximum value	Minimum value
equilibrium equivalent Radon [Bq/m³]	450	500	340
^{218}Po [Bq/m³]	450	500	340
^{214}Pb [Bq/m³]	450	500	340
^{214}Bi/^{214}Po [Bq/m³]	450	500	340
estimated Radon [Bq/m³]	450	500	340
PAEC [WL]	0.12	0.13	0.091

Table 28: The mean, maximum and minimum values of the attached radionuclides in the gym of the therapy center building.

13.10.2004 (10:00 – 0:00)	mean value	maximum value	minimum value
equilibrium equivalent Radon [Bq/m³]	120	380	20
^{218}Po [Bq/m³]	780	2,200	150
^{214}Pb [Bq/m³]	80	280	10
^{214}Bi/^{214}Po [Bq/m³]	8	40	1
estimated Radon [Bq/m³]	3,300	9,500	350
PAEC [WL]	0.033	0.100	0.006

Table 29: The mean, maximum and minimum values of the unattached radionuclides in the gym of the therapy center building.

14.10.2004 (0:00 – 9:00)	mean value	maximum value	minimum value
equilibrium equivalent Radon [Bq/m³]	270	380	80
^{218}Po [Bq/m³]	1,400	2,100	400
^{214}Pb [Bq/m³]	210	290	70
^{214}Bi/^{214}Po [Bq/m³]	30	40	10
estimated Radon [Bq/m³]	4,500	7,200	1,200
PAEC [WL]	0.071	0.10	0.022

Table 30: The mean, maximum and minimum values of the unattached radionuclides in the gym of the therapy center building.

13.10.2004	mean value	maximum value	minimum value
unattached fraction fp [%]	22	46	8.9
^{218}Po fj [%]	58	83	34
^{214}Pb fj [%]	15	38	4.5
^{214}Bi/^{214}Po fj [%]	2.1	7.3	0.4
potential alpha energy J/m³ [%]	22	46	8.9

Table 31: The unattached fraction, the fraction of each unattached daughter product and the contributions of the unattached radionuclides to the total PAEC in the gym of the therapy center building.

14.10.2004	mean value	maximum value	minimum value
unattached fraction fp [%]	36	47	19
^{218}Po fj [%]	73	83	54
^{214}Pb fj [%]	31	40	17
^{214}Bi/^{214}Po fj [%]	6.4	8.9	3.3
potential alpha energy J/m³ [%]	36	47	19

Table 32: The unattached fraction, the fraction of each unattached daughter product and the contributions of the unattached radionuclides to the total PAEC in the gym of the therapy center building.

14.10.2004	mean value	maximum value	minimum value
equilibrium equivalent Radon [Bq/m³]	350	480	170
^{218}Po [Bq/m³]	370	570	180
^{214}Pb [Bq/m³]	350	490	180
^{214}Bi/^{214}Po fj [%]	330	450	140
estimated Radon [Bq/m³]	390	630	180
PAEC [WL]	0.092	0.13	0.046

Table 33: The mean, maximum and minimum values of the attached radionuclides in doctor's office 5 of the therapy center building.

15.10.2004	mean value	maximum value	minimum value
equilibrium equivalent Radon [Bq/m³]	450	980	190
^{218}Po [Bq/m³]	780	1602	500
^{214}Pb [Bq/m³]	470	980	200
^{214}Bi/^{214}Po [Bq/m³]	330	980	50
estimated Radon [Bq/m³]	1,200	2,800	500
PAEC [WL]	0.12	0.26	0.052

Table 34: The mean, maximum and minimum values of the attached radionuclides in doctor's office 5 of the therapy center building.

16.10.2004	mean value	maximum value	minimum value
equilibrium equivalent Radon [Bq/m³]	600	730	490
^{218}Po [Bq/m³]	730	890	560
^{214}Pb [Bq/m³]	620	740	520
^{214}Bi/^{214}Po [Bq/m³]	530	720	350
estimated Radon [Bq/m³]	820	1,200	560
PAEC [WL]	0.16	0.19	0.13

Table 35: The mean, maximum and minimum values of the attached radionuclides in the doctor's office 5 of the therapy center building.

14.10.2004	mean value	maximum value	minimum value
equivalent Radon [Bq/m³]	250	520	119
^{218}Po [Bq/m³]	1,700	3,600	756
^{214}Pb [Bq/m³]	140	260	59
^{214}Bi/^{214}Po [Bq/m³]	10	40	4
estimated Radon [Bq/m³]	7,900	17,700	2,400
PAEC [WL]	0.067	0.14	0.032

Table 36: The mean, maximum and minimum values of the unattached radionuclides in doctor's office 5 of the therapy center building.

15.10.2004	mean value	maximum value	minimum value
equivalent Radon [Bq/m³]	1,100	1,700	560
^{218}Po [Bq/m³]	7,100	10,800	3,800
^{214}Pb [Bq/m³]	690	1,200	280
^{214}Bi/^{214}Po [Bq/m³]	70	220	20
estimated Radon [Bq/m³]	29,800	44,300	13,500
PAEC [WL]	0.30	0.46	0.15

Table 37: The mean, maximum and minimum values of the unattached radionuclides in doctor's office 5 of the therapy center building.

16.10.2004	mean value	maximum value	minimum value
equivalent Radon [Bq/m³]	870	1,100	570
^{218}Po [Bq/m³]	5,710	7,600	3,400
^{214}Pb [Bq/m³]	490	670	300
^{214}Bi/^{214}Po [Bq/m³]	40	70	20
estimated Radon [Bq/m³]	25,200	35,500	12,500
PAEC [WL]	0.23	0.30	0.15

Table 38: The mean, maximum and minimum values of the unattached radionuclides in doctor's office 5 of the therapy center building.

14.10.2004	mean value	maximum value	minimum value
unattached fraction fp [%]	41	52	28
^{218}Po fj [%]	81	87	69
^{214}Pb fj [%]	28	40	17
^{214}Bi/^{214}Po fj [%]	3.6	11	1.5
potential alpha energy J/m³ [%]	43	83	28

Table 39: The unattached fraction, the fraction of each unattached daughter product and the contributions of the unattached radionuclides to the total PAEC in doctor's office 5 of the therapy center building.

15.10.2004	mean value	maximum value	minimum value
unattached fraction fp [%]	71	87	43
^{218}Po fj [%]	89	94	80
^{214}Pb fj [%]	59	80	34
^{214}Bi/^{214}Po fj [%]	26	56	3.8
potential alpha energy J/m³ [%]	71	87	43

Table 40: The unattached fraction, the fraction of each unattached daughter product and the contributions of the unattached radionuclides to the total PAEC in doctor’s office 5 of the therapy center building.

16.10.2004	mean value	maximum value	minimum value
unattached fraction fp [%]	59	66	48
^{218}Po fj [%]	88	91	84
^{214}Pb fj [%]	44	54	33
^{214}Bi/^{214}Po fj [%]	7.7	13	4.0
potential alpha energy J/m³ [%]	59	66	48

Table 41: The unattached fraction, the fraction of each unattached daughter product and the contributions of the unattached radionuclides to the total PAEC in doctor’s office 5 of the therapy center building.

6. Appendix 2

Radon gallery							Potential Alpha Energy	
Date	Time	Equivalent Radon [Bq/m³]	Po-218 [Bq/m³]	Pb-214 [Bq/m³]	Bi-214/Po-214 [Bq/m³]	Estimated Radon [Bq/m³]	[J/m³]	[WL]
07.07.03	12:00	10797 +- 879	16150	11526	8226	19772	5.96E-05 +- 4.85E-06	2.87 +- 0.23
	12:30	11000 +- 834	70320	6592	618	291007	6.08E-05 +- 4.85E-06	2.92 +- 0.22
	13:00	7836 +- 642	54771	3873	274	268446	4.33E-05 +- 4.85E-06	2.08 +- 0.17
	13:30	5507 +- 435	11051	6003	3261	15937	3.04E-05 +- 4.85E-06	1.46 +- 0.12
	14:00	8495 +- 569	11839	8986	6820	13969	4.69E-05 +- 4.85E-06	2.26 +- 0.15
	14:30	10490 +- 680	10854	10530	10215	11054	5.79E-05 +- 4.85E-06	2.79 +- 0.18
	15:00	11265 +- 723	11215	11215	11215	11215	6.22E-05 +- 4.85E-06	2.99 +- 0.19
	15:30	10787 +- 691	10739	10739	10739	10739	5.96E-05 +- 4.85E-06	2.86 +- 0.18
	16:00	9980 +- 639	9936	9936	9936	9936	5.51E-05 +- 4.85E-06	2.65 +- 0.17
	16:30	10573 +- 676	10526	10526	10526	10526	5.84E-05 +- 4.85E-06	2.81 +- 0.18
	17:00	11398 +- 726	11347	11347	11347	11347	6.30E-05 +- 4.85E-06	3.03 +- 0.19
	17:30	12464 +- 792	12409	12409	12409	12409	6.88E-05 +- 4.85E-06	3.31 +- 0.21
	18:00	13297 +- 844	13238	13238	13238	13238	7.34E-05 +- 4.85E-06	3.53 +- 0.22
	18:30	13708 +- 869	13647	13647	13647	13647	7.57E-05 +- 4.85E-06	3.64 +- 0.23
	19:00	13916 +- 882	13854	13854	13854	13854	7.69E-05 +- 4.85E-06	3.70 +- 0.23
	19:30	13852 +- 878	13791	13791	13791	13791	7.65E-05 +- 4.85E-06	3.68 +- 0.23
	20:00	13656 +- 866	13595	13595	13595	13595	7.54E-05 +- 4.85E-06	3.63 +- 0.23
	20:30	13394 +- 850	13334	13334	13334	13334	7.40E-05 +- 4.85E-06	3.56 +- 0.23
	21:00	13374 +- 848	13314	13314	13314	13314	7.39E-05 +- 4.85E-06	3.55 +- 0.23
	21:30	13208 +- 838	13149	13149	13149	13149	7.29E-05 +- 4.85E-06	3.51 +- 0.22
	22:00	13115 +- 832	13056	13056	13056	13056	7.24E-05 +- 4.85E-06	3.48 +- 0.22
	22:30	13049 +- 828	12991	12991	12991	12991	7.21E-05 +- 4.85E-06	3.46 +- 0.22
	23:00	13023 +- 827	12965	12965	12965	12965	7.19E-05 +- 4.85E-06	3.46 +- 0.22
	23:30	13257 +- 841	13198	13198	13198	13198	7.32E-05 +- 4.85E-06	3.52 +- 0.22
08.07.2003	00:00	13217 +- 839	13158	13158	13158	13158	7.30E-05 +- 4.85E-06	3.51 +- 0.22
	00:30	13345 +- 847	13286	13286	13286	13286	7.37E-05 +- 4.85E-06	3.54 +- 0.22
	01:00	13386 +- 849	13326	13326	13326	13326	7.39E-05 +- 4.85E-06	3.55 +- 0.23
	01:30	13608 +- 863	13547	13547	13547	13547	7.52E-05 +- 4.85E-06	3.61 +- 0.23
	02:00	13581 +- 861	13521	13521	13521	13521	7.50E-05 +- 4.85E-06	3.61 +- 0.23
	02:30	13771 +- 873	13709	13709	13709	13709	7.61E-05 +- 4.85E-06	3.66 +- 0.23
	03:00	13951 +- 884	13889	13889	13889	13889	7.71E-05 +- 4.85E-06	3.70 +- 0.23
	03:30	14289 +- 905	14226	14226	14226	14226	7.89E-05 +- 4.85E-06	3.79 +- 0.24
	04:00	14371 +- 910	14307	14307	14307	14307	7.94E-05 +- 4.85E-06	3.82 +- 0.24
	04:30	14203 +- 900	14139	14139	14139	14139	7.84E-05 +- 4.97E-06	3.77 +- 0.24
	05:00	14097 +- 893	14034	14034	14034	14034	7.79E-05 +- 4.97E-06	3.74 +- 0.24
	05:30	14009 +- 888	13947	13947	13947	13947	7.74E-05 +- 4.97E-06	3.72 +- 0.24

Radon gallery		Equivalent Radon [Bq/m^3]			Po-218 [Bq/m^3]	Pb-214 [Bq/m^3]	Bi-214/Po-214 [Bq/m^3]	Estimated Radon [Bq/m^3]	Potential Alpha Energy [J/m^3]			[WL]		
Date	Time													
08.07.2003	06:00	13648	+-	866	13587	13587	13587	13587	7.54E-05	+-	4.97E-06	3.62	+-	0.23
	06:30	13356	+-	848	13296	13296	13296	13296	7.38E-05	+-	4.97E-06	3.55	+-	0.23
	07:00	13287	+-	843	13228	13228	13228	13228	7.34E-05	+-	4.97E-06	3.53	+-	0.22
	07:30	13487	+-	856	13427	13427	13427	13427	7.45E-05	+-	4.97E-06	3.58	+-	0.23
	08:00	13326	+-	846	13267	13267	13267	13267	7.36E-05	+-	4.97E-06	3.54	+-	0.22
	08:30	12830	+-	815	12773	12773	12773	12773	7.09E-05	+-	4.97E-06	3.41	+-	0.22
	09:00	11580	+-	738	11528	11528	11528	11528	6.40E-05	+-	4.97E-06	3.07	+-	0.20
	09:30	10288	+-	658	10242	10242	10242	10242	5.68E-05	+-	4.97E-06	2.73	+-	0.17
	10:00	9134	+-	586	9093	9093	9093	9093	5.04E-05	+-	4.97E-06	2.43	+-	0.16
	10:27	9141	+-	589	9101	9101	9101	9101	5.05E-05	+-	4.97E-06	2.43	+-	0.16
	11:00	7211	+-	502	7179	7179	7179	7179	3.98E-05	+-	4.97E-06	1.91	+-	0.13
	11:30	7236	+-	479	7204	7204	7204	7204	3.10E-05	+-	4.97E-06	1.92	+-	0.13
	12:00	7377	+-	482	7345	7345	7345	7345	4.07E-05	+-	4.97E-06	1.96	+-	0.13
	12:30	8129	+-	526	8093	8093	8093	8093	4.49E-05	+-	4.97E-06	2.16	+-	0.14
	13:00	9189	+-	591	9148	9148	9148	9148	5.08E-05	+-	4.97E-06	2.44	+-	0.16
	13:30	10111	+-	647	10066	10066	10066	10066	5.58E-05	+-	4.97E-06	2.68	+-	0.17
	14:00	10331	+-	661	10285	10285	10285	10285	5.71E-05	+-	4.97E-06	2.74	+-	0.18
	14:30	10591	+-	677	10544	10544	10544	10544	5.85E-05	+-	4.97E-06	2.81	+-	0.18
	15:00	10883	+-	695	10834	10834	10834	10834	6.01E-05	+-	4.97E-06	2.89	+-	0.18
	15:30	10820	+-	691	10772	10772	10772	10772	5.98E-05	+-	4.97E-06	2.87	+-	0.18
	16:00	11180	+-	713	11130	11130	11130	11130	6.17E-05	+-	4.97E-06	2.97	+-	0.19
	16:30	11407	+-	727	11356	11356	11356	11356	6.30E-05	+-	4.97E-06	3.03	+-	0.19
	17:00	11325	+-	722	11274	11274	11274	11274	6.25E-05	+-	4.97E-06	3.01	+-	0.19
	17:30	11350	+-	723	11299	11299	11299	11299	6.27E-05	+-	4.97E-06	3.01	+-	0.19
	18:00	11922	+-	759	11869	11869	11869	11869	6.58E-05	+-	4.97E-06	3.17	+-	0.20
	18:30	12673	+-	805	12616	12616	12616	12616	6.10E-05	+-	4.97E-06	3.37	+-	0.21
	19:00	13237	+-	840	13178	13178	13178	13178	7.31E-05	+-	4.97E-06	3.51	+-	0.22
	19:30	13705	+-	869	13644	13644	13644	13644	7.57E-05	+-	4.97E-06	3.64	+-	0.23
	20:00	13793	+-	874	13732	13732	13732	13732	7.62E-05	+-	4.97E-06	3.66	+-	0.23
	20:30	13827	+-	876	13765	13765	13765	13765	7.64E-05	+-	4.97E-06	3.67	+-	0.23
	21:00	13825	+-	876	13763	13763	13763	13763	7.64E-05	+-	4.84E-06	3.67	+-	0.23
	21:30	13768	+-	873	13707	13707	13707	13707	7.60E-05	+-	4.82E-06	3.66	+-	0.23
	22:00	13686	+-	868	13625	13625	13625	13625	7.56E-05	+-	4.79E-06	3.63	+-	0.23
	22:30	13624	+-	864	13563	13563	13563	13563	7.52E-05	+-	4.77E-06	3.62	+-	0.23
	23:00	13516	+-	857	13456	13456	13456	13456	7.46E-05	+-	4.73E-06	3.59	+-	0.23
	23:30	13383	+-	849	13323	13323	13323	13323	7.39E-05	+-	4.69E-06	3.55	+-	0.23
09.07.2003	00:00	13334	+-	846	13274	13274	13274	13274	7.36E-05	+-	4.67E-06	3.54	+-	0.22
	00:30	13285	+-	843	13225	13225	13225	13225	7.34E-05	+-	4.66E-06	3.53	+-	0.22
	01:00	13276	+-	843	13217	13217	13217	13217	7.33E-05	+-	4.65E-06	3.53	+-	0.22
	01:30	13297	+-	844	13238	13238	13238	13238	7.34E-05	+-	4.66E-06	3.53	+-	0.22
	02:00	13400	+-	850	13340	13340	13340	13340	7.40E-05	+-	4.69E-06	3.56	+-	0.23
	02:30	13634	+-	865	13573	13573	13573	13573	7.53E-05	+-	4.77E-06	3.62	+-	0.23
	03:00	13667	+-	867	13606	13606	13606	13606	7.55E-05	+-	4.79E-06	3.63	+-	0.23
	03:30	13913	+-	882	13851	13851	13851	13851	7.68E-05	+-	4.87E-06	3.69	+-	0.23
	04:00	13950	+-	884	13888	13888	13888	13888	7.70E-05	+-	4.88E-06	3.70	+-	0.23
	04:30	13890	+-	880	13829	13829	13829	13829	7.67E-05	+-	4.86E-06	3.69	+-	0.23
	05:00	13927	+-	883	13865	13865	13865	13865	7.69E-05	+-	4.87E-06	3.70	+-	0.23
	05:30	13950	+-	884	13888	13888	13888	13888	7.70E-05	+-	4.88E-06	3.70	+-	0.23
	06:00	13895	+-	881	13833	13833	13833	13833	7.67E-05	+-	4.86E-06	3.69	+-	0.23
	06:30	14222	+-	901	14159	14159	14159	14159	7.86E-05	+-	4.98E-06	3.78	+-	0.24
	07:00	14558	+-	922	14493	14493	14493	14493	8.04E-05	+-	5.09E-06	3.87	+-	0.24
	07:30	15018	+-	950	14952	14952	14952	14952	8.29E-05	+-	5.25E-06	3.99	+-	0.25
	08:00	15354	+-	971	15286	15286	15286	15286	8.48E-05	+-	5.36E-06	4.08	+-	0.26
	08:30	15672	+-	990	15603	15603	15603	15603	8.66E-05	+-	5.47E-06	4.16	+-	0.26
	09:00	15198	+-	961	15131	15131	15131	15131	8.39E-05	+-	5.31E-06	4.04	+-	0.26
	09:30	14402	+-	912	14338	14338	14338	14338	7.95E-05	+-	5.04E-06	3.82	+-	0.24
	10:00	13214	+-	839	13155	13155	13155	13155	7.30E-05	+-	4.63E-06	3.51	+-	0.22
	10:30	13194	+-	837	13135	13135	13135	13135	7.29E-05	+-	4.62E-06	3.50	+-	0.22
	11:00	12753	+-	810	12696	12696	12696	12696	7.04E-05	+-	4.47E-06	3.39	+-	0.22
	11:21	12556	+-	807	12501	12501	12501	12501	6.94E-05	+-	4.46E-06	3.33	+-	0.21
	11:30	10991	+-	1081	10942	10942	10942	10942	6.07E-05	+-	5.97E-06	2.92	+-	0.29
	12:00	11960	+-	798	11907	11907	11907	11907	6.61E-05	+-	4.41E-06	3.18	+-	0.21
	12:30	12710	+-	821	12653	12653	12653	12653	7.02E-05	+-	4.53E-06	3.37	+-	0.22
	13:00	12867	+-	823	12810	12810	12810	12810	7.11E-05	+-	4.55E-06	3.42	+-	0.22
	13:30	12656	+-	807	12599	12599	12599	12599	6.99E-05	+-	4.46E-06	3.36	+-	0.21
	14:00	12344	+-	786	12289	12289	12289	12289	6.82E-05	+-	4.34E-06	3.28	+-	0.21
	14:30	12630	+-	803	12573	12573	12573	12573	6.98E-05	+-	4.44E-06	3.35	+-	0.21
	15:00	13011	+-	827	12953	12953	12953	12953	7.19E-05	+-	4.56E-06	3.45	+-	0.22
	15:30	13103	+-	832	13045	13045	13045	13045	7.24E-05	+-	4.60E-06	3.48	+-	0.22
	16:00	12808	+-	814	12751	12751	12751	12751	7.07E-05	+-	4.49E-06	3.40	+-	0.22
	16:30	13368	+-	848	13308	13308	13308	13308	7.38E-05	+-	4.69E-06	3.55	+-	0.23
	17:00	14266	+-	904	14202	14202	14202	14202	7.88E-05	+-	4.99E-06	3.79	+-	0.24
	17:30	14928	+-	945	14862	14862	14862	14862	8.25E-05	+-	5.22E-06	3.96	+-	0.25
	18:00	15487	+-	979	15418	15418	15418	15418	8.55E-05	+-	5.41E-06	4.11	+-	0.26
	18:30	15901	+-	1005	15830	15830	15830	15830	8.78E-05	+-	5.55E-06	4.22	+-	0.27
	19:00	16270	+-	1027	16198	16198	16198	16198	8.99E-05	+-	5.67E-06	4.32	+-	0.27

Radon gallery Date	Time	Equivalent Radon [Bq/m^3]			Po-218 [Bq/m^3]	Pb-214 [Bq/m^3]	Bi-214/Po-214 [Bq/m^3]	Estimated Radon [Bq/m^3]	Potential Alpha Energy [J/m^3]			Potential Alpha Energy [WL]		
09.07.2003	19:30	16698	+-	1054	16623	16623	16623	16623	9.22E-05	+-	5.82E-06	4.43	+-	0.28
	20:00	17043	+-	1075	16967	16967	16967	16967	9.41E-05	+-	5.94E-06	4.53	+-	0.29
	20:30	17392	+-	1096	17314	17314	17314	17314	9.61E-05	+-	6.05E-06	4.62	+-	0.29
	21:00	17726	+-	1117	17647	17647	17647	17647	9.79E-05	+-	6.17E-06	4.71	+-	0.30
	21:30	18124	+-	1141	18044	18044	18044	18044	1.00E-04	+-	6.30E-06	4.81	+-	0.30
	22:00	18280	+-	1151	18199	18199	18199	18199	1.01E-04	+-	6.36E-06	4.85	+-	0.31
	22:30	17973	+-	1132	17893	17893	17893	17893	9.93E-05	+-	6.25E-06	4.77	+-	0.30
	23:00	17167	+-	1083	17811	17242	16691	18161	9.48E-05	+-	5.98E-06	4.56	+-	0.29
	23:30	16770	+-	1058	22519	17644	13825	26069	9.26E-05	+-	5.84E-06	4.45	+-	0.28
10.07.2003	00:00	16770	+-	1058	26065	17981	12404	32569	9.26E-05	+-	5.84E-06	4.45	+-	0.28
	00:30	16736	+-	1056	29130	18128	11281	38720	9.24E-05	+-	5.83E-06	4.44	+-	0.28
	01:00	16481	+-	1040	31829	17948	10121	44885	9.10E-05	+-	5.74E-06	4.38	+-	0.28
	01:30	17090	+-	1077	33602	18621	10319	47883	9.44E-05	+-	5.95E-06	4.54	+-	0.29
	02:00	17730	+-	1117	29917	19159	12270	39088	9.79E-05	+-	6.17E-06	4.71	+-	0.30
	02:30	18325	+-	1154	24429	19260	15185	28175	1.01E-04	+-	6.37E-06	4.87	+-	0.31
	03:00	18372	+-	1157	18864	18412	17971	19140	1.01E-04	+-	6.39E-06	4.88	+-	0.31
	03:30	18634	+-	1173	18551	18551	18551	18551	1.03E-04	+-	6.48E-06	4.95	+-	0.31
	04:00	18392	+-	1158	18310	18310	18310	18310	1.02E-04	+-	6.39E-06	4.88	+-	0.31
	04:30	18496	+-	1164	18580	18450	18320	18658	1.02E-04	+-	6.43E-06	4.91	+-	0.31
	05:00	18374	+-	1157	20848	18787	16929	22192	1.01E-04	+-	6.39E-06	4.88	+-	0.31
	05:30	18415	+-	1159	20767	18806	17031	22040	1.02E-04	+-	6.40E-06	4.89	+-	0.31
	06:00	17942	+-	1130	21018	18454	16203	22724	9.91E-05	+-	6.24E-06	4.76	+-	0.30
	06:30	17882	+-	1126	21018	18403	16114	22761	9.88E-05	+-	6.22E-06	4.75	+-	0.30
	07:00	18118	+-	1141	19774	18385	17094	20657	1.00E-04	+-	6.30E-06	4.81	+-	0.30
	07:30	18384	+-	1157	19931	18631	17415	20754	1.02E-04	+-	6.39E-06	4.88	+-	0.31
	08:00	18475	+-	1163	18519	18420	18322	18578	1.02E-04	+-	6.42E-06	4.91	+-	0.31
	08:30	18359	+-	1156	21492	18880	16586	23230	1.01E-04	+-	6.38E-06	4.87	+-	0.31
	09:00	17910	+-	1128	21285	18469	16026	23177	9.89E-05	+-	6.23E-06	4.76	+-	0.30
	09:30	17015	+-	1073	16939	16939	16939	16939	9.40E-05	+-	5.93E-06	4.52	+-	0.28
	10:00	15925	+-	1006	15854	15854	15854	15854	8.80E-05	+-	5.56E-06	4.23	+-	0.27
	10:30	15831	+-	1000	15760	15760	15760	15760	8.74E-05	+-	5.52E-06	4.20	+-	0.27
	11:00	15948	+-	1007	15877	15877	15877	15877	8.81E-05	+-	5.56E-06	4.23	+-	0.27
	11:30	15775	+-	1003	15704	15704	15704	15704	8.71E-05	+-	5.54E-06	4.19	+-	0.27

Radon gallery attached radionuclides		Equivalent Radon [Bq/m^3]			Po-218 [Bq/m^3]	Pb-214 [Bq/m^3]	Bi-214/Po-214 [Bq/m^3]	Estimated Radon [Bq/m^3]	Potential Alpha Energy [WL]		
07.01.2004	11:30	18663	+-	1277	22859	19348	16376	25264	4.96	+-	0.34
	12:00	22137	+-	1436	38292	23967	15002	50721	5.88	+-	0.38
	12:30	17299	+-	1108	29734	18721	11787	39248	4.59	+-	0.29
	13:00	13917	+-	889	18295	14596	11645	20950	3.70	+-	0.24
	13:30	12818	+-	817	12992	12810	12632	13102	3.40	+-	0.22
	14:00	13146	+-	835	13088	13088	13088	13088	3.49	+-	0.22
	14:30	13612	+-	863	13551	13551	13551	13551	3.61	+-	0.23
	15:00	14171	+-	897	14108	14108	14108	14108	3.76	+-	0.24
	15:30	14792	+-	936	14726	14726	14726	14726	3.93	+-	0.25
	16:00	15425	+-	975	15356	15356	15356	15356	4.10	+-	0.26
	16:30	15969	+-	1008	15898	15898	15898	15898	4.24	+-	0.27
	17:00	16405	+-	1035	16332	16332	16332	16332	4.36	+-	0.27
	17:30	16853	+-	1063	16778	16778	16778	16778	4.47	+-	0.28
	18:00	17092	+-	1078	17016	17016	17016	17016	4.54	+-	0.29
	18:30	17348	+-	1093	17271	17271	17271	17271	4.61	+-	0.29
	19:00	17562	+-	1107	17484	17484	17484	17484	4.66	+-	0.29
	19:30	17693	+-	1115	17614	17614	17614	17614	4.70	+-	0.30
	20:00	17828	+-	1123	17748	17748	17748	17748	4.73	+-	0.30
	20:30	18007	+-	1134	17927	17927	17927	17927	4.78	+-	0.30
	21:00	18092	+-	1139	18011	18011	18011	18011	4.80	+-	0.30
	21:30	18160	+-	1143	18080	18080	18080	18080	4.82	+-	0.30
	22:00	18206	+-	1146	18125	18125	18125	18125	4.83	+-	0.30
	22:30	18451	+-	1161	18369	18369	18369	18369	4.90	+-	0.31
	23:00	18382	+-	1157	18301	18301	18301	18301	4.88	+-	0.31
	23:30	18602	+-	1171	18519	18519	18519	18519	4.94	+-	0.31
08.01.2004	00:00	18954	+-	1192	18869	18869	18869	18869	5.03	+-	0.32
	00:30	19300	+-	1214	19214	19214	19214	19214	5.12	+-	0.32
	01:00	19617	+-	1233	19530	19530	19530	19530	5.21	+-	0.33
	01:30	19793	+-	1244	19705	19705	19705	19705	5.26	+-	0.33
	02:00	19962	+-	1254	19873	19873	19873	19873	5.30	+-	0.33
	02:30	19990	+-	1256	19901	19901	19901	19901	5.31	+-	0.33
	03:00	19981	+-	1256	19892	19892	19892	19892	5.31	+-	0.33
	03:30	20018	+-	1258	19929	19929	19929	19929	5.32	+-	0.33
	04:00	20161	+-	1267	20071	20071	20071	20071	5.35	+-	0.34
	04:30	20332	+-	1277	20242	20242	20242	20242	5.40	+-	0.34
	05:00	20499	+-	1287	20407	20407	20407	20407	5.44	+-	0.34
	05:30	20611	+-	1294	20520	20520	20520	20520	5.47	+-	0.34

Radon gallery		Equivalent Radon [Bq/m³]			Po-218 [Bq/m³]	Pb-214 [Bq/m³]	Bi-214/Po-214 [Bq/m³]	Estimated Radon [Bq/m³]	Potential Alpha Energy [WL]		
attached radionuclides											
08.01.2004	06:00	20756	+-	1303	20664	20664	20664	20664	5.51	+-	0.35
	06:30	20830	+-	1308	20737	20737	20737	20737	5.53	+-	0.35
	07:00	20892	+-	1312	20799	20799	20799	20799	5.55	+-	0.35
	07:30	21037	+-	1321	20943	20943	20943	20943	5.59	+-	0.35
	08:00	21080	+-	1323	20986	20986	20986	20986	5.60	+-	0.35
	08:30	20809	+-	1307	20716	20716	20716	20716	5.53	+-	0.35
	09:00	19583	+-	1231	19495	19495	19495	19495	5.20	+-	0.33
	09:30	18340	+-	1155	18258	18258	18258	18258	4.87	+-	0.31
	10:00	17377	+-	1096	17299	17299	17299	17299	4.61	+-	0.29
	10:30	16346	+-	1032	16273	16273	16273	16273	4.34	+-	0.27
	11:00	16195	+-	1023	16123	16123	16123	16123	4.30	+-	0.27
	11:30	16621	+-	1049	16547	16547	16547	16547	4.41	+-	0.28
	12:00	16533	+-	1044	16459	16459	16459	16459	4.39	+-	0.28
	12:30	16064	+-	1015	15992	15992	15992	15992	4.27	+-	0.27
	13:00	16275	+-	1028	16202	16202	16202	16202	4.32	+-	0.27
	13:30	17303	+-	1091	17226	17226	17226	17226	4.59	+-	0.29
	14:00	18496	+-	1165	18413	18413	18413	18413	4.91	+-	0.31
	14:30	19583	+-	1231	19496	19496	19496	19496	5.20	+-	0.33
	15:00	20804	+-	1307	20712	20712	20712	20712	5.52	+-	0.35
	15:30	21847	+-	1371	21750	21750	21750	21750	5.80	+-	0.36
	16:00	22823	+-	1430	22722	22722	22722	22722	6.06	+-	0.38
	16:30	23513	+-	1473	23409	23409	23409	23409	6.24	+-	0.39
	17:00	24150	+-	1512	24042	24042	24042	24042	6.41	+-	0.40
	17:30	24639	+-	1542	24529	24529	24529	24529	6.54	+-	0.41
	18:00	25276	+-	1581	25163	25163	25163	25163	6.71	+-	0.42
	18:30	25967	+-	1623	25852	25852	25852	25852	6.90	+-	0.43
	19:00	26831	+-	1676	26712	26712	26712	26712	7.12	+-	0.45
	19:30	27684	+-	1728	27561	27561	27561	27561	7.35	+-	0.46
	20:00	28741	+-	1793	28613	28613	28613	28613	7.63	+-	0.48
	20:30	29791	+-	1857	29658	29658	29658	29658	7.91	+-	0.49
	21:00	30990	+-	1931	30852	30852	30852	30852	8.23	+-	0.51
	21:30	32312	+-	2012	32168	32168	32168	32168	8.58	+-	0.53
	22:00	33617	+-	2091	33467	33467	33467	33467	8.93	+-	0.56
	22:30	34947	+-	2173	34792	34792	34792	34792	9.28	+-	0.58
	23:00	36355	+-	2259	36193	36193	36193	36193	9.65	+-	0.60
	23:30	37822	+-	2348	37654	37654	37654	37654	10.04	+-	0.62
09.01.2004	00:00	39437	+-	2447	39261	39261	39261	39261	10.47	+-	0.65
	00:30	41221	+-	2556	41038	41038	41038	41038	10.95	+-	0.68
	01:00	42860	+-	2656	42669	42669	42669	42669	11.38	+-	0.71
	01:30	44742	+-	2770	44543	44543	44543	44543	11.88	+-	0.74
	02:00	46649	+-	2887	46442	46442	46442	46442	12.39	+-	0.77
	02:30	48587	+-	3005	48371	48371	48371	48371	12.90	+-	0.80
	03:00	50328	+-	3111	50104	50104	50104	50104	13.36	+-	0.83
	03:30	52299	+-	3231	52066	52066	52066	52066	13.89	+-	0.86
	04:00	54493	+-	3365	54251	54251	54251	54251	14.47	+-	0.89
	04:30	56518	+-	3488	56267	56267	56267	56267	15.01	+-	0.93
	05:00	58162	+-	3588	57903	57903	57903	57903	15.44	+-	0.95
	05:30	59887	+-	3693	59621	59621	59621	59621	15.90	+-	0.98
	06:00	61448	+-	3788	61175	61175	61175	61175	16.32	+-	1.01
	06:30	63110	+-	3889	62829	62829	62829	62829	16.76	+-	1.03
	07:00	64541	+-	3976	64254	64254	64254	64254	17.14	+-	1.06
	07:30	66296	+-	4083	66001	66001	66001	66001	17.60	+-	1.08
	08:00	68033	+-	4188	67730	67730	67730	67730	18.07	+-	1.11
	08:30	68584	+-	4222	68279	68279	68279	68279	18.21	+-	1.12
	09:00	64568	+-	3977	64281	64281	64281	64281	17.14	+-	1.06
	09:30	61508	+-	3791	61235	61235	61235	61235	16.33	+-	1.01
	10:00	62534	+-	3854	62256	62256	62256	62256	16.60	+-	1.02
	10:30	66775	+-	4112	66478	66478	66478	66478	17.73	+-	1.09

Radon gallery		Equivalent Radon [Bq/m³]			Po-218 [Bq/m³]	Pb-214 [Bq/m³]	Bi-214/Po-214 [Bq/m³]	Estimated Radon [Bq/m³]	Potential Alpha Energy [WL]		
unattached radionuclides											
07.01.2004	11:30	916	+-	82.4	4611	748	121	13727	0.2431	+-	0.0219
	12:00	1364	+-	103.9	5205	1332	341	11788	0.3621	+-	0.0276
	12:30	789	+-	66.3	2541	818	263	5017	0.2095	+-	0.0176
	13:00	593	+-	46.4	2636	533	108	6878	0.1573	+-	0.0123
	13:30	621	+-	46.6	3634	428	51	13103	0.1649	+-	0.0124
	14:00	749	+-	54.5	5236	370	26	25662	0.1989	+-	0.0145
	14:30	866	+-	61.9	6054	428	30	29674	0.2300	+-	0.0164
	15:00	956	+-	67.6	6680	472	33	32742	0.2538	+-	0.0179
	15:30	1002	+-	70.5	6603	567	49	28801	0.2662	+-	0.0187
	16:00	1003	+-	70.5	6639	561	47	29231	0.2663	+-	0.0187
	16:30	1003	+-	70.4	6577	572	50	28478	0.2662	+-	0.0187

Radon gallery									Potential Alpha Energy		
unattached radionuclides		Equivalent Radon [Bq/m³]			Po-218 [Bq/m³]	Pb-214 [Bq/m³]	Bi-214/Po-214 [Bq/m³]	Estimated Radon [Bq/m³]	[WL]		
07.01.2004	17:00	965	+-	68	6005	607	61	23757	0.2563	+-	0.0181
	17:30	969	+-	68.2	6022	610	62	23791	0.2573	+-	0.0181
	18:00	929	+-	65.6	5854	571	56	23659	0.2466	+-	0.0174
	18:30	896	+-	63.4	5546	567	58	21777	0.2378	+-	0.0168
	19:00	872	+-	61.9	5328	565	60	20474	0.2317	+-	0.0164
	19:30	835	+-	59.4	5235	517	51	20994	0.2216	+-	0.0158
	20:00	834	+-	59.4	5298	506	48	21686	0.2215	+-	0.0158
	20:30	799	+-	57.1	5001	496	49	19999	0.2121	+-	0.0152
	21:00	785	+-	56.2	4842	501	52	18886	0.2085	+-	0.0149
	21:30	751	+-	54	4639	478	49	18133	0.1995	+-	0.0143
	22:00	758	+-	54.4	4604	494	53	17563	0.2011	+-	0.0144
	22:30	739	+-	53.2	4638	458	45	18610	0.1962	+-	0.0141
	23:00	723	+-	52.1	4512	452	45	17941	0.1920	+-	0.0138
	23:30	702	+-	50.7	4353	444	45	17131	0.1864	+-	0.0135
08.01.2004	00:00	695	+-	50.2	4290	442	45	16784	0.1844	+-	0.0133
	00:30	695	+-	50.2	4268	446	47	16550	0.1845	+-	0.0133
	01:00	680	+-	49.3	4131	445	48	15728	0.1807	+-	0.0131
	01:30	672	+-	48.7	3992	453	51	14726	0.1783	+-	0.0129
	02:00	665	+-	48.3	4051	432	46	15520	0.1765	+-	0.0128
	02:30	649	+-	47.2	3948	423	45	15082	0.1723	+-	0.0125
	03:00	658	+-	47.8	4065	419	43	15886	0.1748	+-	0.0127
	03:30	640	+-	46.6	3808	431	49	14081	0.1699	+-	0.0124
	04:00	649	+-	47.3	3863	438	50	14268	0.1724	+-	0.0125
	04:30	645	+-	46.9	4001	407	41	15778	0.1711	+-	0.0125
	05:00	624	+-	45.6	3967	378	36	16254	0.1658	+-	0.0121
	05:30	631	+-	46	3968	389	38	15977	0.1675	+-	0.0122
	06:00	621	+-	45.3	3719	414	46	13884	0.1648	+-	0.012
	06:30	632	+-	46.1	3837	412	44	14627	0.1677	+-	0.0122
	07:00	625	+-	45.6	3874	395	40	15244	0.1659	+-	0.0121
	07:30	626	+-	45.7	3948	384	37	15973	0.1662	+-	0.0121
	08:00	608	+-	44.5	3585	415	48	13065	0.1615	+-	0.0118
	08:30	589	+-	43.3	3226	442	61	10630	0.1564	+-	0.0115
	09:00	542	+-	40.1	2794	433	67	8549	0.1439	+-	0.0107
	09:30	487	+-	36.5	2303	420	76	6397	0.1294	+-	0.0097
	10:00	462	+-	34.8	2437	362	54	7653	0.1228	+-	0.0092
	10:30	456	+-	34.3	2536	335	44	8537	0.1210	+-	0.0091
	11:00	476	+-	35.6	2945	301	31	11559	0.1263	+-	0.0095
	11:30	475	+-	35.6	2726	336	41	9574	0.1260	+-	0.0094
	12:00	433	+-	32.8	2288	337	50	7214	0.1149	+-	0.0087
	12:30	431	+-	32.6	2615	282	30	9956	0.1144	+-	0.0087
	13:00	452	+-	34	3034	246	20	13713	0.1200	+-	0.009
	13:30	511	+-	38	3551	256	18	17201	0.1356	+-	0.0101
	14:00	566	+-	41.6	3864	295	23	18077	0.1502	+-	0.0111
	14:30	637	+-	46.4	4177	363	32	18097	0.1690	+-	0.0123
	15:00	688	+-	49.8	4413	410	38	18349	0.1828	+-	0.0132
	15:30	717	+-	51.7	4728	405	35	20638	0.1905	+-	0.0137
	16:00	776	+-	55.6	4881	479	47	19650	0.2061	+-	0.0148
	16:30	806	+-	57.6	5339	451	38	23537	0.2140	+-	0.0153
	17:00	815	+-	58.1	5430	450	37	24208	0.2163	+-	0.0154
	17:30	841	+-	59.9	5371	505	47	22199	0.2233	+-	0.0159
	18:00	843	+-	60	5716	449	35	26314	0.2239	+-	0.0159
	18:30	880	+-	62.4	6093	445	33	29289	0.2336	+-	0.0166
	19:00	891	+-	63.2	6052	472	37	27982	0.2366	+-	0.0168
	19:30	935	+-	66.1	6148	531	46	26724	0.2483	+-	0.0175
	20:00	971	+-	68.4	6389	550	47	27829	0.2577	+-	0.0182
	20:30	1023	+-	71.8	6836	561	46	30639	0.2716	+-	0.0191
	21:00	1038	+-	72.8	7039	552	43	32418	0.2757	+-	0.0193
	21:30	1095	+-	76.4	7532	562	42	35724	0.2907	+-	0.0203
	22:00	1141	+-	79.4	7692	614	49	35050	0.3029	+-	0.0211
	22:30	1175	+-	81.6	7843	646	53	35085	0.3119	+-	0.0217
	23:00	1262	+-	87.3	8432	692	57	37780	0.3350	+-	0.0232
	23:30	1320	+-	91	8820	725	60	39489	0.3506	+-	0.0242
09.01.2004	00:00	1396	+-	95.9	9354	762	62	42110	0.3707	+-	0.0255
	00:30	1464	+-	100.3	10041	758	57	47318	0.3888	+-	0.0266
	01:00	1545	+-	105.5	10464	822	65	48129	0.4101	+-	0.028
	01:30	1616	+-	110	10982	855	67	50811	0.4292	+-	0.0292
	02:00	1703	+-	115.6	11369	937	77	50835	0.4522	+-	0.0307
	02:30	1736	+-	117.7	11424	984	85	49748	0.4610	+-	0.0313
	03:00	1816	+-	122.9	11895	1040	91	51343	0.4823	+-	0.0326
	03:30	1834	+-	124	11830	1080	99	49731	0.4869	+-	0.0329
	04:00	1841	+-	124.5	11508	1148	114	45883	0.4888	+-	0.033
	04:30	1889	+-	127.5	11971	1151	111	48801	0.5017	+-	0.0339
	05:00	1914	+-	129.1	12326	1132	104	51656	0.5083	+-	0.0343
	05:30	2011	+-	135.3	13139	1157	102	56460	0.5341	+-	0.0359
	06:00	2079	+-	139.6	13337	1238	115	55531	0.5520	+-	0.0371

Radon gallery unattached radionuclides		Equivalent Radon [Bq/m^3]			Po-218 [Bq/m^3]	Pb-214 [Bq/m^3]	Bi-214/Po-214 [Bq/m^3]	Estimated Radon [Bq/m^3]	Potential Alpha Energy [WL]		
09.01.2004	06:30	2151	+-	144.2	14124	1225	106	61249	0.5712	+-	0.0383
	07:00	2191	+-	146.7	14025	1310	122	58171	0.5817	+-	0.039
	07:30	2250	+-	150.4	14134	1390	137	56827	0.5973	+-	0.0399
	08:00	2225	+-	148.9	13765	1411	145	53991	0.5907	+-	0.0395
	08:30	2073	+-	139.3	10901	1625	242	34150	0.5504	+-	0.037
	09:00	1978	+-	133.2	10365	1556	234	32339	0.5251	+-	0.0354
	09:30	2019	+-	135.8	12156	1338	147	45691	0.5362	+-	0.0361
	10:00	1990	+-	133.9	11553	1388	167	41199	0.5283	+-	0.0356

Foyer attached radionuclides		Equivalent Radon [Bq/m^3]			Po-218 [Bq/m^3]	Pb-214 [Bq/m^3]	Bi-214/Po-214 [Bq/m^3]	Estimated Radon [Bq/m^3]	Potential Alpha Energy [WL]		
12.10.2004	10:00	210	+-	38	321	224	157	397	0.056	+-	0.010
	10:30	123	+-	15	212	133	83	281	0.033	+-	0.004
	11:00	111	+-	12	225	121	65	326	0.029	+-	0.003
	11:30	123	+-	12	233	134	77	326	0.033	+-	0.003
	12:00	150	+-	14	284	163	94	395	0.040	+-	0.004
	12:30	168	+-	15	362	183	93	544	0.045	+-	0.004
	13:00	170	+-	15	169	169	169	169	0.045	+-	0.004
	13:30	163	+-	15	178	165	153	186	0.043	+-	0.004
	14:00	164	+-	15	272	177	115	352	0.043	+-	0.004
	14:30	155	+-	14	155	155	155	155	0.041	+-	0.004
	15:00	126	+-	12	126	126	126	126	0.034	+-	0.003
	15:30	109	+-	11	108	108	108	108	0.029	+-	0.003
	16:00	104	+-	10	231	113	56	354	0.028	+-	0.003
	16:30	125	+-	12	171	132	101	201	0.033	+-	0.003
	17:00	154	+-	14	354	167	79	556	0.041	+-	0.004
	17:30	165	+-	15	351	179	92	525	0.044	+-	0.004
	18:00	190	+-	17	375	207	114	536	0.051	+-	0.004
	18:30	272	+-	23	575	297	153	854	0.072	+-	0.006
	19:00	331	+-	27	482	353	258	582	0.088	+-	0.007
	19:30	354	+-	28	467	372	296	535	0.094	+-	0.008
	20:00	352	+-	28	488	372	283	575	0.093	+-	0.008
	20:30	361	+-	29	447	375	314	497	0.096	+-	0.008
	21:00	328	+-	27	392	339	292	428	0.087	+-	0.007
	21:30	319	+-	26	378	329	286	411	0.085	+-	0.007
	22:00	300	+-	25	299	299	299	299	0.080	+-	0.007
	22:30	287	+-	24	286	286	286	286	0.076	+-	0.006
	23:00	259	+-	22	258	258	258	258	0.069	+-	0.006
	23:30	219	+-	19	218	218	218	218	0.058	+-	0.005
13.10.2004	00:00	210	+-	18	209	209	209	209	0.056	+-	0.005
	00:30	172	+-	15	182	173	165	188	0.046	+-	0.004
	01:00	162	+-	15	193	167	145	210	0.043	+-	0.004
	01:30	157	+-	14	254	169	113	325	0.042	+-	0.004
	02:00	169	+-	15	230	178	138	268	0.045	+-	0.004
	02:30	174	+-	15	215	181	152	238	0.046	+-	0.004
	03:00	177	+-	16	231	185	149	263	0.047	+-	0.004
	03:30	171	+-	15	231	180	140	269	0.045	+-	0.004
	04:00	161	+-	15	160	160	160	160	0.043	+-	0.004
	04:30	158	+-	14	205	165	133	233	0.042	+-	0.004
	05:00	147	+-	13	172	151	133	186	0.039	+-	0.004
	05:30	133	+-	12	134	133	132	135	0.035	+-	0.003
	06:00	121	+-	11	167	128	98	195	0.032	+-	0.003
	06:30	121	+-	12	126	122	118	129	0.032	+-	0.003
	07:00	120	+-	11	147	125	106	162	0.032	+-	0.003
	07:30	114	+-	11	157	121	93	184	0.030	+-	0.003
	08:00	125	+-	12	248	136	75	354	0.033	+-	0.003
	08:30	141	+-	13	150	142	134	155	0.037	+-	0.003
	09:00	126	+-	12	125	125	125	125	0.033	+-	0.003
	09:30	107	+-	10	135	111	92	152	0.028	+-	0.003

Gym attached radionuclides		Equivalent Radon [Bq/m^3]			Po-218 [Bq/m^3]	Pb-214 [Bq/m^3]	Bi-214/Po-214 [Bq/m^3]	Estimated Radon [Bq/m^3]	Potential Alpha Energy [WL]		
13.10.2004	10:00	171	+-	26	231	180	140	269	0.045	+-	0.007
	10:30	199	+-	20	301	213	150	372	0.053	+-	0.005
	11:00	217	+-	20	237	220	205	247	0.058	+-	0.005
	11:30	229	+-	20	228	228	228	228	0.061	+-	0.005
	12:00	218	+-	19	217	217	217	217	0.058	+-	0.005
	12:30	228	+-	20	266	234	207	287	0.061	+-	0.005
	13:00	247	+-	21	246	246	246	246	0.065	+-	0.006
	13:30	235	+-	20	234	234	234	234	0.062	+-	0.005
	14:00	207	+-	18	206	206	206	206	0.055	+-	0.005

Gym		Equivalent Radon			Po-218	Pb-214	Bi-214/Po-214 [Bq/m³]	Estimated Radon [Bq/m³]	Potential Alpha Energy		
attached radionuclides		[Bq/m³]			[Bq/m³]	[Bq/m³]			[WL]		
13.10.2004	14:30	216	+-	19	271	225	186	304	0.057	+-	0.005
	15:00	242	+-	20	369	258	181	457	0.064	+-	0.005
	15:30	241	+-	20	240	240	240	240	0.064	+-	0.005
	16:00	220	+-	19	219	219	219	219	0.058	+-	0.005
	16:30	225	+-	19	224	224	224	224	0.060	+-	0.005
	17:00	245	+-	21	244	244	244	244	0.065	+-	0.006
	17:30	261	+-	22	260	260	260	260	0.069	+-	0.006
	18:00	309	+-	25	307	307	307	307	0.082	+-	0.007
	18:30	373	+-	30	371	371	371	371	0.099	+-	0.008
	19:00	463	+-	36	461	461	461	461	0.123	+-	0.010
	19:30	539	+-	41	537	537	537	537	0.143	+-	0.011
	20:00	545	+-	42	543	543	543	543	0.145	+-	0.011
	20:30	538	+-	41	535	535	535	535	0.143	+-	0.011
	21:00	495	+-	38	493	493	493	493	0.131	+-	0.010
	21:30	472	+-	37	470	470	470	470	0.125	+-	0.010
	22:00	446	+-	35	444	444	444	444	0.118	+-	0.009
	22:30	450	+-	35	448	448	448	448	0.120	+-	0.009
	23:00	438	+-	34	436	436	436	436	0.116	+-	0.009
	23:30	446	+-	35	444	444	444	444	0.118	+-	0.009
14.10.2004	00:00	431	+-	34	429	429	429	429	0.115	+-	0.009
	00:30	429	+-	34	427	427	427	427	0.114	+-	0.009
	01:00	434	+-	34	432	432	432	432	0.115	+-	0.009
	01:30	465	+-	36	463	463	463	463	0.123	+-	0.010
	02:00	481	+-	37	479	479	479	479	0.128	+-	0.010
	02:30	490	+-	38	488	488	488	488	0.130	+-	0.010
	03:00	493	+-	38	491	491	491	491	0.131	+-	0.010
	03:30	500	+-	38	498	498	498	498	0.133	+-	0.010
	04:00	475	+-	37	473	473	473	473	0.126	+-	0.010
	04:30	485	+-	37	483	483	483	483	0.129	+-	0.010
	05:00	489	+-	38	487	487	487	487	0.130	+-	0.010
	05:30	462	+-	36	460	460	460	460	0.123	+-	0.010
	06:00	467	+-	36	465	465	465	465	0.124	+-	0.010
	06:30	466	+-	36	463	463	463	463	0.124	+-	0.010
	07:00	443	+-	35	441	441	441	441	0.118	+-	0.009
	07:30	416	+-	33	414	414	414	414	0.110	+-	0.009
	08:00	382	+-	30	380	380	380	380	0.101	+-	0.008
	08:30	353	+-	28	351	351	351	351	0.094	+-	0.008
	09:00	344	+-	28	342	342	342	342	0.091	+-	0.007

Gym		Equivalent Radon			Po-218	Pb-214	Bi-214/Po-214	Estimated Radon [Bq/m³]	Potential Alpha Energy		
unattached radionuclides		[Bq/m³]			[Bq/m³]	[Bq/m³]	[Bq/m³]		[WL]		
13.10.2004	10:00	38	+-	7	178	32	6	498	0.0100	+-	0.0019
	10:30	32	+-	5	187	23	3	664	0.0086	+-	0.0012
	11:00	29	+-	4	138	25	5	382	0.0077	+-	0.001
	11:30	23	+-	3	116	18	3	357	0.0060	+-	0.0008
	12:00	22	+-	3	115	17	3	354	0.0059	+-	0.0008
	12:30	22	+-	3	156	11	1	767	0.0059	+-	0.0008
	13:00	35	+-	4	241	17	1	1182	0.0092	+-	0.0011
	13:30	31	+-	4	183	21	2	676	0.0081	+-	0.001
	14:00	33	+-	4	185	24	3	630	0.0088	+-	0.001
	14:30	41	+-	5	288	20	1	1411	0.0109	+-	0.0012
	15:00	43	+-	5	293	22	2	1393	0.0113	+-	0.0013
	15:30	41	+-	5	246	27	3	930	0.0108	+-	0.0012
	16:00	45	+-	5	312	22	2	1531	0.0119	+-	0.0013
	16:30	45	+-	5	311	22	2	1525	0.0118	+-	0.0013
	17:00	37	+-	4	259	19	1	1257	0.0099	+-	0.0011
	17:30	45	+-	5	315	22	2	1544	0.0120	+-	0.0013
	18:00	63	+-	6	437	31	2	2143	0.0166	+-	0.0017
	18:30	88	+-	8	617	44	3	3022	0.0234	+-	0.0022
	19:00	118	+-	11	824	58	4	4039	0.0313	+-	0.0028
	19:30	159	+-	14	1108	78	6	5430	0.0421	+-	0.0036
	20:00	204	+-	17	1422	101	7	6970	0.0540	+-	0.0045
	20:30	238	+-	19	1607	127	10	7372	0.0631	+-	0.0052
	21:00	276	+-	22	1929	136	10	9453	0.0733	+-	0.0059
	21:30	317	+-	25	2002	193	19	8137	0.0841	+-	0.0066
	22:00	334	+-	26	2001	223	25	7466	0.0887	+-	0.007
	22:30	356	+-	28	2158	234	25	8190	0.0946	+-	0.0074
	23:00	371	+-	29	2115	265	33	7354	0.0985	+-	0.0076
	23:30	376	+-	29	2121	273	35	7255	0.0999	+-	0.0077
14.10.2004	00:00	358	+-	28	1919	275	39	6162	0.0950	+-	0.0074
	00:30	381	+-	30	2074	288	40	6775	0.1013	+-	0.0078
	01:00	365	+-	28	1933	284	42	6107	0.0969	+-	0.0075
	01:30	378	+-	29	2115	276	36	7173	0.1003	+-	0.0078
	02:00	357	+-	28	1990	262	34	6717	0.0947	+-	0.0074

Gym unattached radionuclides		Equivalent Radon [Bq/m³]			Po-218 [Bq/m³]	Pb-214 [Bq/m³]	Bi-214/Po-214 [Bq/m³]	Estimated Radon [Bq/m³]	Potential Alpha Energy [WL]		
14.10.2004	02:30	341	+-	27	1741	275	43	5273	0.0905	+-	0.0071
	03:00	334	+-	26	1793	256	37	5763	0.0887	+-	0.007
	03:30	324	+-	26	1668	260	40	5091	0.0861	+-	0.0068
	04:00	321	+-	25	1758	241	33	5792	0.0852	+-	0.0067
	04:30	304	+-	24	1607	238	35	5060	0.0808	+-	0.0064
	05:00	276	+-	22	1551	200	26	5299	0.0732	+-	0.0059
	05:30	269	+-	22	1469	202	28	4835	0.0713	+-	0.0057
	06:00	240	+-	20	1245	190	29	3843	0.0636	+-	0.0052
	06:30	217	+-	18	1115	174	27	3404	0.0575	+-	0.0048
	07:00	184	+-	16	911	153	26	2657	0.0489	+-	0.0042
	07:30	149	+-	13	656	135	28	1698	0.0395	+-	0.0035
	08:00	118	+-	11	502	109	24	1254	0.0313	+-	0.0029
	08:30	96	+-	9	501	76	12	1550	0.0256	+-	0.0024
	09:00	83	+-	8	403	70	12	1158	0.0220	+-	0.0021

Doctor's office 5 attached radionuclides		Equivalent Radon [Bq/m³]			Po-218 [Bq/m³]	Pb-214 [Bq/m³]	Bi-214/Po-214 [Bq/m³]	Estimated Radon [Bq/m³]	Potential Alpha Energy [WL]		
14.10.2004	10:30	174	+-	17	232	183	144	268	0.046	+-	0.004
	11:00	185	+-	17	184	184	184	184	0.049	+-	0.005
	11:30	222	+-	19	221	221	221	221	0.059	+-	0.005
	12:00	223	+-	19	235	225	215	242	0.059	+-	0.005
	12:30	238	+-	20	237	237	237	237	0.063	+-	0.005
	13:00	257	+-	22	256	256	256	256	0.068	+-	0.006
	13:30	270	+-	22	268	268	268	268	0.072	+-	0.006
	14:00	301	+-	25	299	299	299	299	0.080	+-	0.007
	14:30	297	+-	24	321	301	282	333	0.079	+-	0.007
	15:00	297	+-	24	296	296	296	296	0.079	+-	0.007
	15:30	341	+-	27	339	339	339	339	0.090	+-	0.007
	16:00	337	+-	27	335	335	335	335	0.090	+-	0.007
	16:30	352	+-	28	377	356	337	390	0.094	+-	0.008
	17:00	420	+-	33	418	418	418	418	0.112	+-	0.009
	17:30	422	+-	33	420	420	420	420	0.112	+-	0.009
	18:00	428	+-	34	426	426	426	426	0.113	+-	0.009
	18:30	424	+-	33	422	422	422	422	0.112	+-	0.009
	19:00	408	+-	32	406	406	406	406	0.108	+-	0.009
	19:30	391	+-	31	390	390	390	390	0.104	+-	0.008
	20:00	386	+-	31	396	387	377	402	0.102	+-	0.008
	20:30	382	+-	30	426	389	356	449	0.101	+-	0.008
	21:00	389	+-	31	473	403	344	520	0.103	+-	0.008
	21:30	398	+-	31	513	416	337	582	0.105	+-	0.008
	22:00	442	+-	34	539	458	389	594	0.117	+-	0.009
	22:30	455	+-	35	565	472	395	628	0.121	+-	0.009
	23:00	475	+-	37	547	487	433	587	0.126	+-	0.010
	23:30	483	+-	37	544	493	447	576	0.128	+-	0.010
15.10.2004	00:00	504	+-	39	502	502	502	502	0.134	+-	0.010
	00:30	526	+-	40	598	538	485	637	0.140	+-	0.011
	01:00	505	+-	39	617	523	443	681	0.134	+-	0.010
	01:30	510	+-	39	680	536	423	785	0.135	+-	0.010
	02:00	509	+-	39	730	541	400	875	0.135	+-	0.010
	02:30	519	+-	40	784	555	393	964	0.138	+-	0.011
	03:00	508	+-	39	779	543	379	967	0.135	+-	0.010
	03:30	491	+-	38	767	527	362	960	0.130	+-	0.010
	04:00	447	+-	35	807	486	292	1095	0.119	+-	0.009
	04:30	419	+-	33	634	448	317	780	0.111	+-	0.009
	05:00	383	+-	30	645	414	266	841	0.102	+-	0.008
	05:30	327	+-	27	681	357	187	1003	0.087	+-	0.007
	06:00	266	+-	22	571	290	147	859	0.071	+-	0.006
	06:30	241	+-	20	607	261	112	1007	0.064	+-	0.005
	07:00	222	+-	19	520	241	112	825	0.059	+-	0.005
	07:30	209	+-	18	509	227	101	826	0.056	+-	0.005
	08:00	197	+-	17	594	207	72	1118	0.052	+-	0.005
	08:30	194	+-	17	617	201	66	1207	0.052	+-	0.005
	09:00	201	+-	17	698	204	60	1459	0.054	+-	0.005
	09:30	197	+-	17	707	197	55	1522	0.052	+-	0.005
	10:00	197	+-	17	643	203	64	1282	0.052	+-	0.005
	10:30	206	+-	18	661	214	69	1301	0.055	+-	0.005
	11:00	221	+-	19	720	228	72	1434	0.059	+-	0.005
	11:30	224	+-	19	811	224	62	1755	0.060	+-	0.005
	12:00	223	+-	19	649	236	86	1190	0.059	+-	0.005
	12:30	241	+-	20	744	253	86	1423	0.064	+-	0.005
	13:00	234	+-	20	734	244	81	1420	0.062	+-	0.005
	13:30	264	+-	22	904	268	80	1874	0.070	+-	0.006
	14:00	302	+-	25	871	321	118	1585	0.080	+-	0.007
	14:30	331	+-	27	844	358	152	1412	0.088	+-	0.007

Doctor's office 5		Equivalent Radon			Po-218	Pb-214	Bi-214/Po-	Estimated	Potential Alpha Energy		
attached radionuclides		[Bq/m³]			[Bq/m³]	[Bq/m³]	214 [Bq/m³]	Radon [Bq/m³]	[WL]		
15.10.2004	15:00	381	+-	30	1073	406	153	1924	0.101	+-	0.008
	15:30	420	+-	33	855	458	245	1244	0.111	+-	0.009
	16:00	457	+-	36	791	495	310	1048	0.121	+-	0.009
	16:30	474	+-	37	995	517	269	1473	0.126	+-	0.010
	17:00	458	+-	36	873	499	285	1221	0.122	+-	0.009
	17:30	481	+-	37	823	520	329	1083	0.128	+-	0.010
	18:00	489	+-	38	818	528	341	1064	0.130	+-	0.010
	18:30	457	+-	36	911	498	273	1308	0.121	+-	0.009
	19:00	600	+-	45	1602	645	259	2766	0.159	+-	0.012
	19:30	806	+-	59	1291	867	582	1640	0.214	+-	0.016
	20:00	963	+-	70	977	963	948	986	0.256	+-	0.019
	20:30	984	+-	71	980	980	980	980	0.261	+-	0.019
	21:00	979	+-	71	975	975	975	975	0.260	+-	0.019
	21:30	873	+-	64	869	869	869	869	0.232	+-	0.017
	22:00	782	+-	58	778	778	778	778	0.208	+-	0.015
	22:30	743	+-	55	740	740	740	740	0.197	+-	0.015
	23:00	680	+-	51	677	677	677	677	0.181	+-	0.014
	23:30	670	+-	50	710	676	644	731	0.178	+-	0.013
16.10.2004	00:00	675	+-	50	732	684	640	762	0.179	+-	0.013
	00:30	667	+-	50	755	682	616	802	0.177	+-	0.013
	01:00	649	+-	49	721	661	605	761	0.172	+-	0.013
	01:30	617	+-	46	614	614	614	614	0.164	+-	0.012
	02:00	594	+-	45	592	592	592	592	0.158	+-	0.012
	02:30	561	+-	43	559	559	559	559	0.149	+-	0.011
	03:00	538	+-	41	597	548	503	628	0.143	+-	0.011
	03:30	524	+-	40	630	542	466	690	0.139	+-	0.011
	04:00	532	+-	41	706	559	443	812	0.141	+-	0.011
	04:30	536	+-	41	703	562	448	805	0.142	+-	0.011
	05:00	526	+-	40	673	549	448	761	0.140	+-	0.011
	05:30	504	+-	39	828	543	356	1067	0.134	+-	0.010
	06:00	516	+-	40	889	559	351	1175	0.137	+-	0.011
	06:30	569	+-	43	888	610	419	1112	0.151	+-	0.011
	07:00	627	+-	47	835	659	520	963	0.167	+-	0.013
	07:30	704	+-	52	833	725	632	905	0.187	+-	0.014
	08:00	725	+-	54	730	723	716	734	0.192	+-	0.014
	08:30	722	+-	54	724	720	716	726	0.192	+-	0.014
	09:00	723	+-	54	809	737	672	855	0.192	+-	0.014
	09:30	704	+-	52	766	714	665	799	0.187	+-	0.014
	10:00	660	+-	49	716	669	625	746	0.175	+-	0.013
	10:30	598	+-	45	764	624	510	862	0.159	+-	0.012
	11:00	615	+-	46	677	625	578	709	0.163	+-	0.012
	11:30	601	+-	45	769	628	513	868	0.160	+-	0.012
	12:00	594	+-	45	833	629	475	986	0.158	+-	0.012
	12:30	582	+-	44	731	606	502	819	0.154	+-	0.012
	13:00	577	+-	44	762	606	482	874	0.153	+-	0.012
	13:30	527	+-	40	660	548	455	739	0.140	+-	0.011
	14:00	514	+-	39	682	540	428	784	0.137	+-	0.011
	14:30	494	+-	38	659	519	409	760	0.131	+-	0.010
	15:00	512	+-	39	805	549	375	1013	0.136	+-	0.010

Doctor's office 5		Equivalent Radon			Po-218	Pb-214	Bi-214/Po-	Estimated	Potential Alpha Energy		
unattached radionuclides		[Bq/m³]			[Bq/m³]	[Bq/m³]	214 [Bq/m³]	Radon [Bq/m³]	[WL]		
14.10.2004	10:30	140	+-	13	756	107	15	2443	0.037	+-	0.004
	11:00	119	+-	11	834	59	4	4088	0.032	+-	0.003
	11:30	124	+-	11	865	61	4	4240	0.033	+-	0.003
	12:00	137	+-	12	960	68	5	4704	0.036	+-	0.003
	12:30	142	+-	13	995	70	5	4875	0.038	+-	0.003
	13:00	167	+-	14	1166	82	6	5711	0.044	+-	0.004
	13:30	171	+-	15	1198	85	6	5873	0.045	+-	0.004
	14:00	213	+-	18	1485	105	7	7279	0.056	+-	0.005
	14:30	238	+-	19	1662	118	8	8146	0.063	+-	0.005
	15:00	257	+-	21	1795	127	9	8796	0.068	+-	0.006
	15:30	279	+-	22	1827	159	14	7907	0.074	+-	0.006
	16:00	300	+-	24	1919	179	17	7968	0.080	+-	0.006
	16:30	278	+-	22	1364	232	40	3944	0.074	+-	0.006
	17:00	216	+-	18	1008	188	35	2760	0.057	+-	0.005
	17:30	188	+-	16	954	152	24	2873	0.050	+-	0.004
	18:00	166	+-	14	1109	90	7	4990	0.044	+-	0.004
	18:30	166	+-	14	1107	92	8	4937	0.044	+-	0.004
	19:00	180	+-	15	1257	90	6	6131	0.048	+-	0.004
	19:30	214	+-	18	1495	106	7	7328	0.057	+-	0.005
	20:00	244	+-	20	1705	121	9	8356	0.065	+-	0.005
	20:30	291	+-	23	2033	144	10	9966	0.077	+-	0.006
	21:00	335	+-	26	2339	165	12	11466	0.089	+-	0.007
	21:30	387	+-	30	2705	191	14	13256	0.103	+-	0.008

Doctor's office 5		Equivalent Radon			Po-218	Pb-214	Bi-214/Po-	Estimated	Potential Alpha Energy		
unattached radionuclides		[Bq/m³]			[Bq/m³]	[Bq/m³]	214 [Bq/m³]	Radon [Bq/m³]	[WL]		
14.10.2004	22:00	421	+-	32	2945	208	15	14436	0.112	+-	0.009
	22:30	452	+-	34	3156	223	16	15471	0.120	+-	0.009
	23:00	499	+-	37	3476	248	18	16958	0.132	+-	0.010
	23:30	517	+-	39	3615	256	18	17718	0.137	+-	0.010
15.10.2004	00:00	562	+-	42	3926	278	20	19245	0.149	+-	0.011
	00:30	594	+-	44	4054	312	24	18901	0.158	+-	0.012
	01:00	620	+-	46	4335	307	22	21248	0.165	+-	0.012
	01:30	649	+-	48	4484	331	24	21434	0.172	+-	0.013
	02:00	707	+-	51	4940	349	25	24212	0.188	+-	0.014
	02:30	759	+-	55	5302	375	27	25986	0.201	+-	0.015
	03:00	822	+-	59	5746	406	29	28161	0.218	+-	0.016
	03:30	880	+-	63	6152	435	31	30154	0.234	+-	0.017
	04:00	906	+-	65	6198	473	36	29030	0.241	+-	0.017
	04:30	926	+-	66	6170	511	42	27507	0.246	+-	0.018
	05:00	933	+-	66	6419	479	36	30466	0.248	+-	0.018
	05:30	950	+-	67	6190	548	49	26502	0.252	+-	0.018
	06:00	916	+-	65	6037	517	44	26377	0.243	+-	0.017
	06:30	920	+-	65	5985	533	47	25539	0.244	+-	0.017
	07:00	941	+-	67	6452	488	37	30368	0.250	+-	0.018
	07:30	995	+-	70	6775	524	41	31466	0.264	+-	0.019
	08:00	1058	+-	75	7397	523	37	36253	0.281	+-	0.020
	08:30	1097	+-	77	7595	555	40	36520	0.291	+-	0.020
	09:00	1168	+-	82	8085	591	43	38841	0.310	+-	0.022
	09:30	1239	+-	86	8221	691	58	36323	0.329	+-	0.023
	10:00	1307	+-	91	8747	715	59	39287	0.347	+-	0.024
	10:30	1348	+-	93	9012	739	61	40417	0.358	+-	0.025
	11:00	1384	+-	96	9079	789	69	39318	0.368	+-	0.025
	11:30	1431	+-	99	9330	826	73	39955	0.380	+-	0.026
	12:00	1466	+-	101	9501	856	77	40266	0.389	+-	0.027
	12:30	1497	+-	103	9742	868	77	41568	0.398	+-	0.027
	13:00	1613	+-	110	10153	994	97	40940	0.428	+-	0.029
	13:30	1664	+-	114	10431	1032	102	41789	0.442	+-	0.030
	14:00	1705	+-	116	10820	1035	99	44253	0.453	+-	0.031
	14:30	1680	+-	115	10376	1068	110	40597	0.446	+-	0.030
	15:00	1680	+-	115	10248	1090	116	39319	0.446	+-	0.030
	15:30	1719	+-	117	10327	1142	126	38712	0.456	+-	0.031
	16:00	1697	+-	116	10231	1122	123	38543	0.451	+-	0.031
	16:30	1677	+-	115	10365	1066	110	40574	0.445	+-	0.030
	17:00	1671	+-	114	10084	1103	121	38050	0.444	+-	0.030
	17:30	1653	+-	113	9990	1088	119	37778	0.439	+-	0.030
	18:00	1631	+-	112	10123	1029	105	39906	0.433	+-	0.030
	18:30	1632	+-	112	9819	1082	119	36885	0.433	+-	0.030
	19:00	1363	+-	94	6391	1181	218	17602	0.362	+-	0.025
	19:30	1094	+-	77	5024	963	185	13537	0.290	+-	0.020
	20:00	916	+-	65	4759	727	111	14692	0.243	+-	0.017
	20:30	796	+-	57	4541	569	71	15790	0.211	+-	0.015
	21:00	729	+-	53	4061	535	71	13700	0.193	+-	0.014
	21:30	686	+-	50	4038	469	55	14687	0.182	+-	0.013
	22:00	656	+-	48	3819	456	54	13673	0.174	+-	0.013
	22:30	609	+-	45	3808	380	38	15175	0.162	+-	0.012
	23:00	612	+-	45	3833	381	38	15312	0.163	+-	0.012
	23:30	601	+-	44	3917	347	31	16769	0.160	+-	0.012
16.10.2004	00:00	622	+-	46	3950	377	36	16161	0.165	+-	0.012
	00:30	631	+-	46	4281	334	26	19767	0.167	+-	0.012
	01:00	639	+-	47	4201	363	31	18267	0.170	+-	0.012
	01:30	638	+-	47	3963	402	41	15653	0.169	+-	0.012
	02:00	621	+-	46	3732	412	46	14000	0.165	+-	0.012
	02:30	578	+-	43	3419	392	45	12536	0.153	+-	0.011
	03:00	565	+-	42	3610	339	32	14922	0.150	+-	0.011
	03:30	602	+-	44	4211	298	21	20637	0.160	+-	0.012
	04:00	658	+-	48	4601	325	23	22549	0.175	+-	0.013
	04:30	716	+-	52	5001	354	25	24512	0.190	+-	0.014
	05:00	770	+-	56	5380	380	27	26368	0.204	+-	0.015
	05:30	782	+-	56	5240	426	35	23611	0.208	+-	0.015
	06:00	794	+-	57	5220	451	39	22678	0.211	+-	0.015
	06:30	801	+-	58	5586	398	28	27242	0.213	+-	0.015
	07:00	855	+-	61	5972	422	30	29272	0.227	+-	0.016
	07:30	892	+-	64	6234	441	31	30554	0.237	+-	0.017
	08:00	978	+-	69	6838	484	34	33514	0.260	+-	0.018
	08:30	1010	+-	71	7058	499	35	34592	0.268	+-	0.019
	09:00	1062	+-	75	7364	535	39	35519	0.282	+-	0.020
	09:30	1106	+-	78	7271	628	54	31600	0.294	+-	0.021
	10:00	1125	+-	79	7590	605	48	34628	0.299	+-	0.021
	10:30	1113	+-	78	7354	625	53	32289	0.295	+-	0.021
	11:00	1108	+-	78	7138	655	60	29934	0.294	+-	0.021
	11:30	1116	+-	78	7148	667	62	29672	0.296	+-	0.021

Doctor's office 5		Equivalent Radon			Po-218	Pb-214	Bi-214/Po-214 [Bq/m³]	Estimated Radon [Bq/m³]	Potential Alpha Energy		
unattached radionuclides		[Bq/m³]			[Bq/m³]	[Bq/m³]			[WL]		
16.10.2004	12:00	1077	+-	76	6984	628	57	29622	0.286	+-	0.020
	12:30	1072	+-	75	6765	657	64	27408	0.285	+-	0.020
	13:00	1041	+-	73	6502	650	65	25887	0.276	+-	0.020
	13:30	1037	+-	73	6543	636	62	26497	0.275	+-	0.019
	14:00	996	+-	70	6254	615	61	25141	0.264	+-	0.019
	14:30	944	+-	67	5871	593	60	23233	0.251	+-	0.018
	15:00	897	+-	64	5685	545	52	23201	0.238	+-	0.017

Zusammenfassung

Im Rahmen dieser Dissertation wurden Aktivitätskonzentrationen der Folgeprodukte des Radons im Bad Gasteiner Heilstollen und in der Kuranstalt am Eingang des Heilstollens gemessen. Die Messungen wurden im Auftrag der AUVA durchgeführt um die effektive Dosis der Arbeiter und Angestellten zu bestimmen. Die Berechnung der Dosis wird zurzeit mit einem Dosiskonversionsfaktor (DCF) durchgeführt, der von epidemiologischen Studien abgeleitet wurde. Er wird in der ICRP 65 empfohlen und wurde so auch in die Richtlinie 96/29/Euratom des Rates vom 13. Mai 1996 und in die ÖNORM S5223-2 übernommen.
Allerdings können DCFs auch durch Modellrechnungen bestimmt werden. Diese Modellrechnungen verwenden als Grundlage das Lungenmodell der ICRP 66, oder andere Modelle, die die einzelnen Atemwegsgenerationen des Bronchialbaumes in Betracht ziehen. In dieser Dissertation wird die effektive Dosis mittels verschiedener DCFs von verschiedenen Modellen berechnet.
Diese DCFs sind von verschiedenen Parametern abhängig. Einen sehr großen Einfluss übt die nicht an den Aerosolen angelagerte Fraktion (unattached fraction) der Radontöchter aus. Deswegen wurden sowohl die an den Aerosolen angelagerten Radontöchter, als auch die nicht an den Aerosolen angelagerten Radontöchter bestimmt. Die unattached fraction, wird wiederum von der Aerosolpartikelkonzentration in der Luft und der Anlagerungsrate bestimmt. Die Radonaktivitätskonzentration in der Luft wird hingegen von dem Luftdruck und den Lüftungsbedingungen beeinflusst. Da die effektive Dosis also abhängig ist von der Radonaktivitätskonzentration in der Luft und der nicht an den Aerosolen angelagerten Fraktion der Radontöchter werden die Parameter Luftdruck, Lüftungsbedingungen, Aerosolpartikelkonzentration und Anlagerungsrate diskutiert. Zusätzlich wurde noch die Verteilung der langlebigen Folgeprodukte des Radon auf Aerosolpartikel verschiedener Größe bestimmt. Dafür wurden Aerosole zwischen 0,05 – 16 µm mittels eines Kaskadenimpaktors gesammelt. ^{210}Pb, ^{210}Bi and ^{210}Po wurden mittels Flüssigszintillation gemessen und auch hier wurde die Dosis berechnet.

Lebenslauf

Persönliche Daten:

Name: Claudia Landstetter

Berufserfahrung:

- Seit Jänner 2005: Radiochemikerin bei der Österreichischen Agentur für Gesundheit und Ernährungssicherheit GmbH
- April 2003 – Dez. 2004: Wissenschaftliche Mitarbeiterin an der Universität Wien; Projektmitarbeit im AUVA-Projekt „Strahlenschutz im Bergbau“

Ausbildung:

- März 2003: Beginn des Doktoratstudiums mit dem Dissertationsgebiet Chemie; Thema: „Radon exposure and the influence of aerosol dust concentration and ventilation conditions“
- Dez. 2002: Beendigung des Studiums der Chemie mit der 2. Diplomprüfung (mit Auszeichnung bestanden)
- Okt. 2002: Beginn des Studiums der Astronomie
- März 2002: Beginn der Diplomarbeit: „Bestimmung von Radiostrontium (^{90}Sr) in Rehknochen“
- Okt. 2000 – Jän. 2001: Auslandsaufenthalt in England an der University of Warwick im Rahmen des Sokrates - Erasmus Austauschprogrammes Thema: „Developing of high-loading scavenger resins for combinatorial chemistry“
- Okt. 1996: Beginn des Studiums der Chemie an der Universität Wien
- Juni 1996: Abschluß des Realgymnasiums durch die Reifeprüfung mit gutem Erfolg
- 1988 – 1996: Besuch des Bundesgymnasiums und Bundesrealgymnasiums Rosasgasse, 1120 Wien

Praktika:

- Sept. 2001: Ferialpraktikum bei Austria Tabak, Abteilung Forschung und Qualitätssicherung
- Sept. 1998: Ferialpraktikum bei der Österreichischen Unilever Ges.m.b.H., Kuner Nahrungsmittel